AD-A250 418

UMENTATION PAGE

Form Approved
OMB No. 0704-0188

2. REPORT DATE	3. REPORT TYPE AND DATES COVERED
1991	THESIS/DISSERTATION

4. TITLE AND SUBTITLE
Cloud-To-Ground Lightning Characteristics in Mesoscale Convective Systems, April-September 1986

5. FUNDING NUMBERS

6. AUTHOR(S)
Carolyn D. Morgenstern, Captain

7. PERFORMING ORGANIZATION NAME(S) AND ADDRESS(ES)
AFIT Student Attending: University of Oklahoma

8. PERFORMING ORGANIZATION REPORT NUMBER
AFIT/CI/CIA-91-120

9. SPONSORING/MONITORING AGENCY NAME(S) AND ADDRESS(ES)
AFIT/CI
Wright-Patterson AFB OH 45433-6583

10. SPONSORING/MONITORING AGENCY REPORT NUMBER

11. SUPPLEMENTARY NOTES

12a. DISTRIBUTION/AVAILABILITY STATEMENT
Approved for Public Release IAW 190-1
Distributed Unlimited
ERNEST A. HAYGOOD, Captain, USAF
Executive Officer

12b. DISTRIBUTION CODE

13. ABSTRACT (*Maximum 200 words*)

14. SUBJECT TERMS	15. NUMBER OF PAGES: 109
	16. PRICE CODE

17. SECURITY CLASSIFICATION OF REPORT	18. SECURITY CLASSIFICATION OF THIS PAGE	19. SECURITY CLASSIFICATION OF ABSTRACT	20. LIMITATION OF ABSTRACT

DISCLAIMER NOTICE

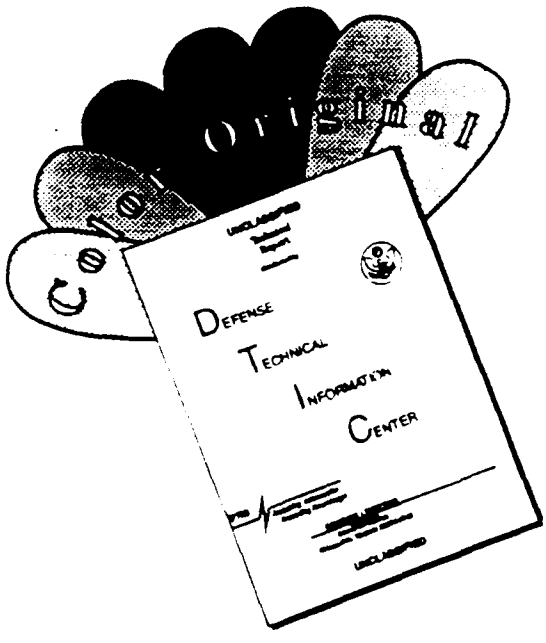

THIS DOCUMENT IS BEST QUALITY AVAILABLE. THE COPY FURNISHED TO DTIC CONTAINED A SIGNIFICANT NUMBER OF COLOR PAGES WHICH DO NOT REPRODUCE LEGIBLY ON BLACK AND WHITE MICROFICHE.

THE UNIVERSITY OF OKLAHOMA

GRADUATE COLLEGE

CLOUD-TO-GROUND LIGHTNING CHARACTERISTICS IN MESOSCALE CONVECTIVE SYSTEMS, APRIL-SEPTEMBER 1986

A THESIS

SUBMITTED TO THE GRADUATE FACULTY

in partial fulfillment of the requirements for the

degree of

MASTER OF SCIENCE IN METEOROLOGY

By

CAROLYN DIANE MORGENSTERN

Norman, Oklahoma

1991

CLOUD-TO-GROUND LIGHTNING CHARACTERISTICS

IN MESOSCALE CONVECTIVE SYSTEMS,

APRIL-SEPTEMBER 1986

A THESIS

APPROVED FOR THE SCHOOL OF METEOROLOGY

BY

Donald R MacGorman

Howard B. Bluestein

Donald W Burgess

William H. Beasley

Charles A. Doswell III

In memory of my good friend

Mary Jo "Jodi" Coulter

who was killed June, 1989
in a weather related accident

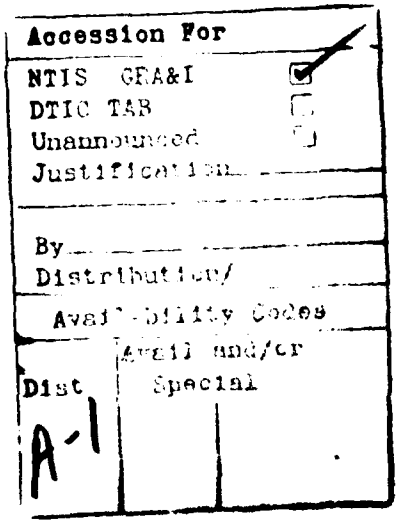

ACKNOWLEDGEMENTS

I am grateful for the help, ideas, and encouragement given to me by my committee chairman, Dr. Donald MacGorman, as well as for the comments and suggestions from the other members of my committee.

John Augustine provided the initial data set of storm systems documented in 1986 that got this research started. I owe him thanks for allowing me to use his MCS documentation software as well as for the instruction he provided to teach me to use it. John and Dave Stensrud were the most help in my struggle to get the software running here in Norman. For other programming assistance, I also must thank Kurt Nielsen, Doug Rhue, Lin Lee and Dave Keller.

The completion of this thesis would not have been possible without the tremendous amount of support from my husband, Kurt, and the many hours he spent with our daughter, Ashley, while I was studying or working. Ashley deserves credit for keeping my mind off "school" whenever I was home.

Thanks also are due to the National Severe Storms Laboratory for the use of their facilities during this research project and to the US Air Force for allowing me the opportunity to complete this degree.

TABLE OF CONTENTS

LIST OF TABLES

LIST OF ILLUSTRATIONS

ABSTRACT

Cloud-to-ground (CG) lightning characteristics were examined in 25 Mesoscale Convective Systems (MCSs) that occurred during the warm season of 1986. Lightning strike locations were superimposed on infrared (IR) satellite imagery to examine lightning ground strike patterns relative to cold cloud-tops of MCSs. Lightning strikes frequently indicated thunderstorms more than 1 h before cold clouds were apparent on IR satellite imagery. Time series of the area within various temperature contours were compared to time series of positive and negative flash rates. The patterns of variations in negative cloud-to-ground flash rates appeared most similar to variations in the area within temperatures of -60°C to -70°C on satellite imagery.

Positive flashes occurred in two different modes, a *stratiform/dissipating* mode and a *convective* mode. In the stratiform/dissipating mode, positive flashes occurred during the mature and dissipating stages of an MCS and peaked near or after the peak in negative flash rates. Ground strike locations were generally dispersed across a large area and were usually associated with either a dissipating convective region or a stratiform region on radar and with decaying and warming cloud-top temperatures on satellite imagery. The stratiform/dissipating mode appeared during all months of the warm season. In the convective mode, positive flashes occurred in the early, formation stages of an MCS and peaked an average of 3.5 h before the peak in negative flash rates. Ground strike locations were generally clustered within or near cold cloud-tops on satellite imagery and within convective regions on radar.

The convective mode tended to occur more often in the spring and early summer. Variations in positive flash rates appeared most similar to the area within the colder cloud shield temperatures (usually less than -70°C) when the convective mode of positive flashes occurred and to the area within warmer cloud-top temperatures (about -52°C) when the stratiform/dissipating mode occurred.

The amplitude distributions of signals from positive flashes varied considerably from one MCS to another and at different times in a single MCS, while the amplitudes of negative flashes were more constant. The amplitude distribution of all positive flashes in a single MCS tended to occur in one of three categories: (1) severe skew toward small amplitudes, (2) many small amplitudes with a slow decrease in numbers with high amplitudes, and (3) few flashes with small amplitudes and many with large amplitudes. The first category tended to occur in the cooler months of the warm season; the second category tended to occur in the hot months of the warm season; and the third category occurred during all months of the warm season.

CLOUD-TO-GROUND LIGHTNING CHARACTERISTICS IN MESOSCALE CONVECTIVE SYSTEMS, APRIL-SEPTEMBER 1986

CHAPTER I

INTRODUCTION

The national lightning ground strike detection network now in place across the United States provides a relatively new source of information for meteorological research. Some research with the network has focused on determining relationships between lightning and other meteorological parameters in an attempt to understand the dynamical and microphysical processes within thunderstorms and to uncover practical information that can be used by operational forecasters.

This research project focused on the cloud-to-ground lightning characteristics of mesoscale convective systems (MCSs) and the relationships between these characteristics and satellite determined cloud-top temperatures. We also examined the relationships between some lightning characteristics and the synoptic environments in which they occurred.

1.1 Background Information

A grossly simplified picture of the charge distribution within a thunderstorm is presented in Figure 1.1. The main negative charge region is inside the cloud in an altitude layer bounded by the 0°C and -25°C isotherms. The main positive charge is generally more diffuse and is found at colder temperatures above the main negative charge. Regions of localized positive charge are found beneath the main negative charge and are known as lower positive charge centers (LPCCs) (Krehbiel, 1986). The main negative and positive regions are often referred to together as the thunderstorm dipole. When the LPCC also exists, the total distribution is sometimes

Figure 1.1. An isolated thundercloud over Langmuir Laboratory in Central New Mexico and a rudimentary picture of how electric charge appears to be distributed inside and around the thundercloud, as inferred from in-cloud and remote observations. (From Krehbiel, 1986)

referred to as a tripole.

Convective growth is important to the electrification of a storm. Strong electrification is usually not observed in storms until they reach a height of 8 km above mean sea level (MSL) in the summer, which corresponds to a temperature of about -20°C (Krehbiel, 1986). The electrification of the thunderstorm at a given time is the net result of processes that place charge of one sign on some class of particles and of processes that move those charged particles. Many of the mechanisms that have been hypothesized to place charge on particles involve collisions between drops. During collisions, according to most hypotheses, positive charge is usually placed on smaller cloud droplets and ice crystals, and negative charge is usually placed on larger drops and graupel. The smaller, positively charged particles are carried to the top of the cloud by the updraft, while the larger, negatively charged particles remain in the lower portions of the cloud. Because updrafts are not uniform horizontally, and particles are also subjected to horizontal advection, turbulence, diffusion, and evaporation, thunderstorm charge distributions differ substantially from a simple dipole, even before the first lightning flash occurs. Lightning can redistribute a significant fraction of the charge in thunderstorms and further complicate the charge distribution. Processes that are hypothesized to contribute to formation of LPCCs include melting ice particles, breaking drops, lightning, positive ion generation from corona discharges, and a reversal of the polarity of charge transferred to ice crystals at warmer temperatures (Williams, 1989).

Lightning flashes are commonly divided into two categories: intracloud (IC) and cloud-to-ground (CG) lightning. Intracloud lightning is all lightning that has no channel to ground, including in-cloud lightning, cloud-to-cloud lightning and cloud-to-air flashes. Cloud-to-ground flashes usually originate in the cloud and form a channel to ground, through which they lower charge to ground. Most CG flashes lower negative charge to ground and are, therefore, called negative CG flashes. Flashes that lower positive charge to ground are called positive CG flashes.

Cloud-to-ground lightning begins with a process within the cloud called preliminary breakdown. Following this, a discharge, called a stepped leader, propagates toward the ground in discrete steps. As it nears the earth's surface, a discharge begins at the ground and propagates upward to meet the leader. When contact occurs, the first return stroke is initiated. The return stroke is an intense wave of ionization that propagates up the channel formed by the stepped leader and greatly increases its luminosity, creating a brightly illuminated channel. After a pause of 20-150 ms, another leader (called the dart leader) can propagate quickly back down the ionized channel to initiate an additional return stroke (Krider, 1986). A lightning flash is the term used to refer to all of the processes (including return strokes) in a connected network of lightning channels. A lightning stroke refers to only one of the leader/return stroke pairs in a lightning flash.

1.2 Previous Research

In a study of CG lightning in ten MCCs, Goodman and MacGorman (1986)

found that the total CG lightning activity and maximum flashing rate do not appear to be directly related to the area of the cloud shield colder than -32°C or to the duration of the MCC. Goodman et al. (1988) also list various references suggesting that the total amount of lightning and peak flash rates in a thunderstorm are a nonlinear function of storm height, size, duration, and environment. However, Goodman and MacGorman (1986) found that flash rates did increase when the -52°C cloud shield area was rapidly expanding. Lightning flash rates in their study peaked about 2.6 h prior to the maximum area of the cloud shield colder than -32°C, at approximately the same time as the minimum cloud-top temperature. The MCCs in their study typically produced more than 1000 CG flashes per hour for nine consecutive hours, and composites of the lightning activity showed an exponential increase to a peak in flash rates, followed by an exponential decrease. In the first hour of the development of the MCC, multiple stroke flashes were less common than during the mature phase, when flash rates were still increasing. They also found that lightning characteristics could evolve very differently from one storm to another in similar synoptic environments.

Goodman and MacGorman (1986) also found that the overall shape and centroid of the contours of lightning strike density and heavy rainfall rates were similar. Additional evidence for a relationship between rainfall and lightning strikes in MCSs was presented in a case study by Rutledge and MacGorman (1988): They found that negative flash rates appeared correlated with rainfall rates in the convective line, while maximum positive flash rates occurred near the time of

maximum stratiform rainfall.

Lhermitte and Krehbiel (1979) found intense electrification to be closely related to vertical development of the cloud and the presence of substantial radar reflectivity. Reap and MacGorman (1989) observed a good correspondence between lightning frequency and radar reflectivity from manually digitized radar data within 48 x 48 km grid blocks.

In a study using lightning and satellite data, Goodman et al. (1988) observed that trends in lightning flash rates can provide information on thunderstorm growth and decay that often cannot be inferred from satellite cloud-top infrared imagery. The combination of satellite and lightning data was found to be more useful than satellite imagery alone. Lightning strike data provide information on the location, growth and decay of electrical activity in thunderstorms. Dense clusters of lightning strikes occur in the vicinity of relatively strong convective cells. This is especially useful to a forecaster when convection is obscured by a higher cloud shield as often occurs in an MCS.

The bipolar pattern of lighting ground strike locations, in which negative flashes are spatially separated from positive flashes, has been observed in many MCSs (Orville et al., 1988; Rutledge and MacGorman, 1988; Engholm et al., 1990; Stolzenburg, 1990). The length of the bipole varies considerably, from a few tens of kilometers to more than 100 km. The density of positive lightning strike points in the bipole is usually much less than the density of negative lightning strike points. Orville et al. (1988) for example, reported that the ratio of positive to negative flash

densities was typically .05 to .2. The density ratio is small both because there are relatively few positive flashes and because positive flashes are spread over a larger region than negative flashes. In these reports, positive flashes were found in shallower clouds downshear of the negative flashes, such that the bipole was roughly aligned with the geostrophic wind at upper levels (Engholm et al., 1990; Stolzenburg, 1990).

In a climatological study of CG flashes that occurred in the warm season (April through September) of 1985 and 1986, Reap and MacGorman (1989) found that only 4.33% of the flashes were of positive polarity, and of these, 78.03% were single return stroke flashes. (31.20% of negative flashes had only one return stroke.) The percentage of flashes that were positive was greatest in April, decreased to a minimum in August, and increased again in September.

Positive flashes often occur late in the mature and dissipating stages of thunderstorms (Fuquay, 1982; Orville et al., 1983; Rust, 1986). Although the reasons why storms produce positive flashes are not understood very well, two mechanisms have been suggested and are discussed by Krehbiel, 1986: The first is that in the early stages of a thunderstorm, the positive charge is shielded from the ground by the negative charge region below it and therefore flashes to ground cannot occur easily. However, as the thunderstorm matures and its downdraft becomes more predominant, the positive charge region moves closer to the ground, allowing positive CG flashes to occur more easily. The second explanation is that the negative charge region is thought to be depleted by the negative flashes that occur when the

thunderstorm is in its mature stage, thereby leaving a surplus of positive charge that causes positive flashes during the dissipating stage.

Positive flashes also have been observed in mature thunderstorms (Brook et al., 1982; Rust et al., 1985; Orville et al., 1988). Brook et al. (1982) suggested that these may occur if the wind shear is great enough to tilt the thunderstorm dipole. In this case, the positive charge region is not shielded from the ground by the negative charge region, so positive flashes can occur more easily. Reap and MacGorman (1989) and Curran and Rust (1991) found that wind shear was commonly strong during thunderstorms on the Great Plains, even when positive flashes did not occur. Therefore, they hypothesized that wind shear may be a necessary, but not a sufficient, condition for the occurrence of positive flashes.

Positive flashes also have been observed in the stratiform regions of MCSs (Rutledge and MacGorman, 1988; Engholm et al., 1990; Rutledge et al., 1990). Similarly, Rust et al. (1981a) observed positive flashes in the thunderstorm anvil and to the rear of the main thunderstorm cell. One possible source of charge for these positive flashes is the advection of positive charge downwind from the upper part of convective cells of the storm system, but charge also may be generated by stratiform precipitation processes (Rutledge and MacGorman, 1988; Engholm et al., 1990; Rutledge et al., 1990).

There also have been observations of positive flashes in other storm situations. Rust et al. (1985), Curran and Rust (1991), and Stolzenburg (personal communication, 1991) have observed storms in which positive flashes dominated

lightning strike activity early in the storm's lifetime. Rust et al. (1985) discuss a set of storms on May 13, 1983 that all produced severe weather (hail and tornadoes) and had high percentages of flashes that were positive. These storms had high densities of positive flashes that occurred either early or throughout most of the lifetime of the storms. Curran and Rust (1991) found that positive flashes dominated near regions of high reflectivity as long as storms were low precipitation storms, but the dominant polarity changed to negative when the storms moved into moister regions. Stolzenburg (personal communication, 1991) observed 23 storms in the Great Plains states that were all characterized by positive flashes with high flash rates, high spatial densities, and large ratios of positive flashes to total flashes near the beginning of the mature stage of the storms. Rust et al. (1981b) found positive flashes in regions of strong updraft in mesocyclones and with other severe storms. Reap and MacGorman (1989) found significant correlations between the occurrence of severe weather (especially hail) and a high density and rate of positive flashes (30 or more per hour in 48 x 48 km grid blocks) (Figure 1.2).

MacGorman and Taylor (1989) examined the records from 340 positive CG flashes detected by an automatic lightning strike mapping system to determine if the waveforms were characteristic of positive CG flashes. They found that false detection of positive CG flashes was negligible for flashes with range-normalized amplitudes of at least 50 LLP units (the arbitrary units recorded by the detection system produced by Lightning Location and Protection, Inc. (LLP)) and that no more than about 15% of the flashes at smaller amplitudes were false detections.

Similarly, Brook et al. (1989) examined the electric field waveforms from positive CG flashes detected by an LLP lightning strike mapping system at the State University of New York, Albany (SUNYA). They found that the waveforms appeared to be from cloud-to-ground flashes, and therefore, the system appeared to identify positive CG flashes correctly. Beasley (1985) reviews other research on positive cloud-to-ground lightning.

There have been several studies in which MCSs were classified according to radar reflectivities or the synoptic conditions in which they occurred. Houze et al. (1990) defined three classes of MCS structure according to radar reflectivity: chaotically organized MCSs, and symmetric and assymmetric MCSs. The symmetric and assymetric classes both included systems with a leading convective line and a trailing stratiform region. The symmetry referred to whether the stratiform region was centered on the line or offset to the north. Blanchard (1990) also used radar

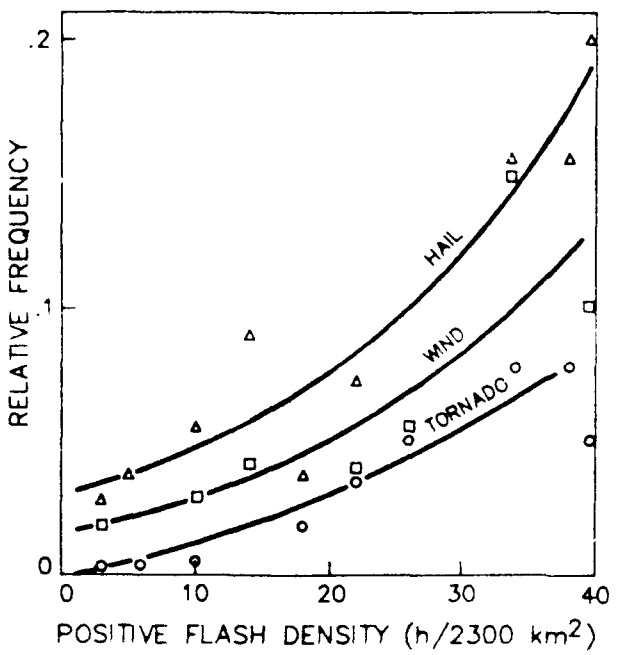

Figure 1.2. Fraction of grid blocks (relative frequency) containing large hail, damaging winds, or tornadoes as a function of postiive flash density. Flash density is the number of flashes per hour in each 48-km grid block whose area is approximately 2300 km^2. (From Reap and MacGorman, 1989)

reflectivity to classify MCSs into linear, occluding and chaotic mesoscale patterns and then compared the differences in the synoptic environments of these classes. Kane et al. (1987) compared precipitation characteristics of MCCs that had been classified according to synoptic conditions into four classes: mesohigh, frontal, synoptic and extreme-right-moving.

1.3 Goals of this Research

The purpose of the research project reported in this thesis was to learn more about the characteristics of cloud-to-ground lightning in mesoscale convective systems, to determine the relationships between lightning and cloud-top temperatures in these systems, and to determine if any lightning characteristic could be related to the synoptic environment.

Because of apparent correlations between radar reflectivity and lightning frequency, lightning data in this study was used to determine if lightning patterns could be classified and related to the synoptic environment, similar to the studies by Kane et al., (1987) and Blanchard (1990), which related classes of convective structure to synoptic features. One advantage of lightning data is that it can be readily examined over the large regions needed for examining MCSs. MCSs are often too large to be examined by a single radar, and compositing radar images is relatively difficult in real time. Satellite imagery also has the advantage of a wider region of coverage and was also available in digital form, well suited for overlaying lightning ground strike locations.

We studied 25 MCSs throughout their lifetimes to examine lightning characteristics, the spatial patterns of lightning relative to the MCS cloud shield, and the relationships between the frequency of negative and positive flashes and the areas within various temperature contours on satellite imagery. We also examined how the synoptic environments of the MCSs differed as their lightning characteristics differed. One final goal, met only partially, was to find how lightning data could help an operational forecaster in diagnosing and monitoring storm systems.

CHAPTER II

DATA AND METHODOLOGY

This chapter includes a discussion of the data used and the methods employed to analyze the data. There are two sections: (1) The data sources section describes characteristics of the lightning detection network, the satellite imagery, and synoptic data used in this study. (2) The methodology section discusses the criteria for selecting the storms in this study and describes the techniques we used to analyze and compare lightning, satellite and synoptic data.

2.1 Data Sources

2.1.1 Lightning Data

The lightning data used in this study were obtained from the National Severe Storms Laboratory's (NSSL's) lightning strike detection network. This detection network consists of seven magnetic direction-finder stations manufactured by Lightning Location and Protection, Inc. (LLP) (Krider et al., 1980). A map of NSSL's stations is shown in Figure 2.1.

At each of the seven stations there is a crossed-loop antenna and a flat-plate, electric-field antenna. The crossed-loop antenna consists of two orthogonally

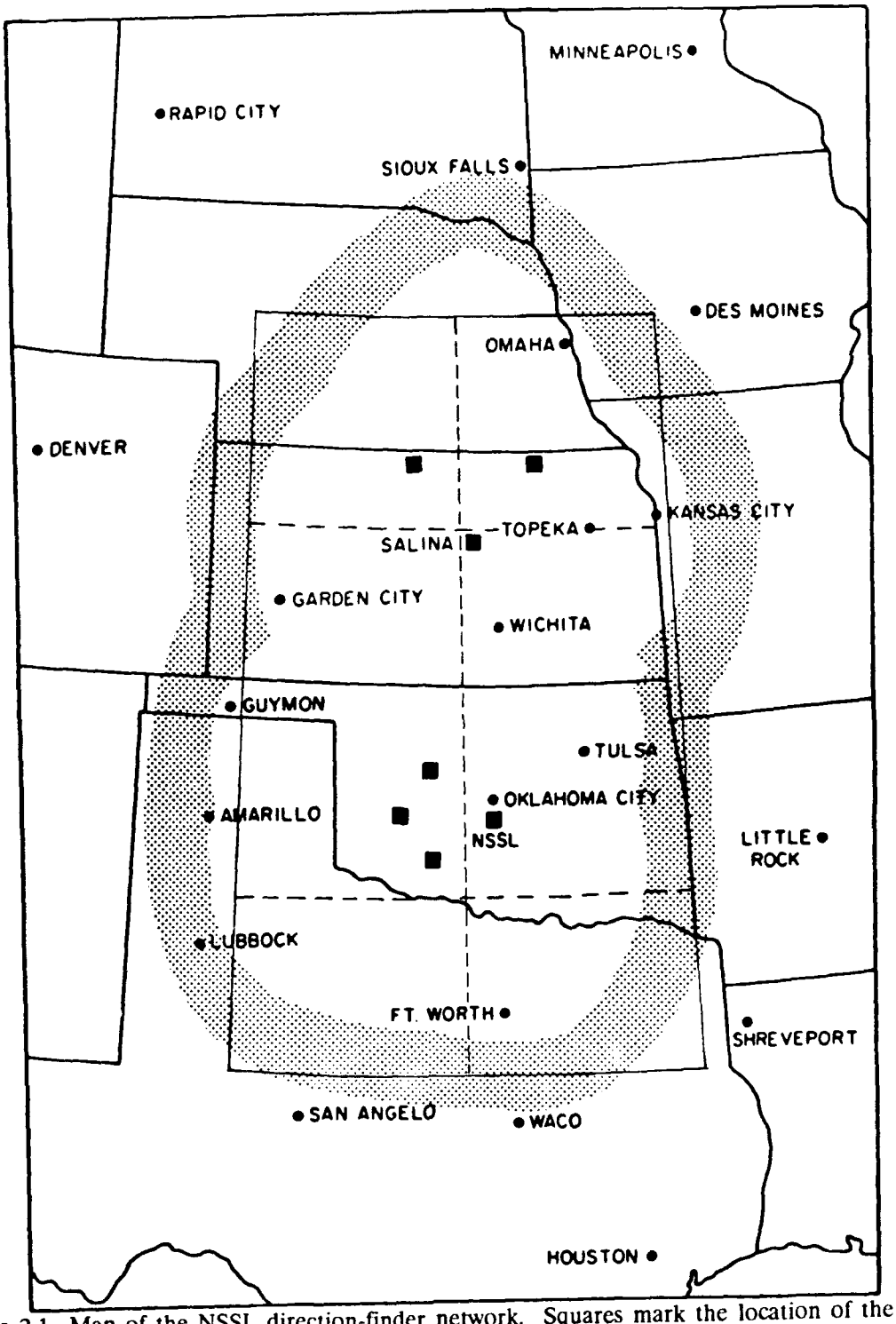

Figure 2.1 Map of the NSSL direction-finder network. Squares mark the location of the seven direction-finder stations. The inner border of the shading encloses the region within 300 km of at least two stations; the outer border encloses the region within 400 km, the nominal area of coverage of the network. The solid box is the region of analysis for this study and the dashed lines indicate the standard latitudes and longitude used in the Lambert conformal projections. (Adapted from MacGorman and Nielsen, 1991).

mounted loop antennas and determines the azimuth to a lightning strike by detecting the magnetic field change produced by the current surge in a return stroke. The received signal is proportional to the cosine of the angle between the plane of the loop and the bearing to the lightning channel. If the antenna loops are aligned N-S and E-W, the ratio of the signal received by the E-W loop to that received by the N-S loop is proportional to tan θ, where θ is the azimuth to the flash. The flat-plate antenna measures the polarity of charge lowered to ground and thus removes the 180° azimuthal ambiguity that exists if the crossed-loop antenna is used alone. Additional information about the lightning detection network can be found in Mach et al. (1986).

Data from lightning flashes detected by each station include time of occurrence, azimuth to the point where the lightning channel strikes ground, total number of return strokes in the flash, and the amplitude and polarity of the signal received from the first return stroke. LLP direction-finder stations can detect no more than 14 return strokes for a single ground flash. If more than 14 return strokes are detected, those beyond 14 are recorded as a separate flash. Flashes with more than 14 return strokes occur relatively infrequently. For the lightning data in this study, an exponential curve fit to the number of flashes versus the number of return strokes per flash suggests that less than .07% of the flashes have more than 14 return strokes. Therefore, no attempt was made to correct for those flashes incorrectly recorded separately.

Azimuths measured by each station have both random and systematic errors.

Work by several, including Krider et al. (1976) and Lopez and Passi (1991), suggests that the random error has a standard deviation of 1° or less. The largest source of systematic errors in the present system is objects that reradiate the lightning signal in the vicinity of the station. Systematic site errors have been determined for each station, as described by Mach et al. (1986) and MacGorman and Nielsen (1991), and correction factors are automatically applied to the data.

Direction finder data are sent over telephone lines to a central position analyzer located at NSSL in Norman, where they are recorded. The strike locations used in this analysis were determined by post-processing; solutions calculated by the position analyzer in real time were ignored. The post-processing algorithm checks for flashes that were detected by more than one station within a 20 ms time window and, if this occurs, assumes the data were from a single ground strike. If the flash was detected by two stations, a strike location is then computed by triangulation. If three or more stations detected the flash, the strike location is computed using an iterative, non-linear, least-squares optimization technique (MacGorman and Nielsen, 1991).

Since the received signal amplitude is inversely proportional to the range from the flash, the computed strike location is used to calculate the signal amplitude that would be received by a station 100 km from the flash. These range-normalized amplitudes are recorded in arbitrary units, which will be designated LLP units in this study. The data in final form, including the latitude and longitude of the optimum strike location, the time of the first stroke, the number of return strokes, and the

polarity and normalized amplitude of the first return stroke, are archived at NSSL.

The lightning detection system does not detect every cloud-to-ground flash that occurs. Some flashes either have too small a signal or fail waveform acceptance criteria of the system. Mach et al. (1986) and MacGorman and Rust (1988) found that the NSSL system detects about 70% of the flashes that occur, out to a range of 300 km. The 300 km range of NSSL's system is indicated by the inner border of the shading in Figure 2.1. Strikes occurring at a longer range are more likely to be undetected since the received amplitude will be smaller. Errors in the measured bearings to flashes will cause errors in a calculated location that depend on its relative orientation and distance to the network. As mentioned previously, systematic bearing errors that can be identified are subtracted. MacGorman and Rust (1988) estimate that remaining errors are around 2 km within the Oklahoma cluster of stations, 3 km within the Kansas cluster and up to 10-20 km near the edges of the area of coverage of the network.

2.1.2 Satellite Imagery

Hourly digital satellite imagery was obtained from data archived at NSSL in Boulder and were used to follow storm development and evolution. These enhanced infrared images from GOES-West have an 8-km resolution. The color enhancement shown in Figure 2.2 was used to easily determine and follow the growth of cloud shield areas having temperatures colder than -52°C, -58°C, -64°C, -70°C, and -76°C.

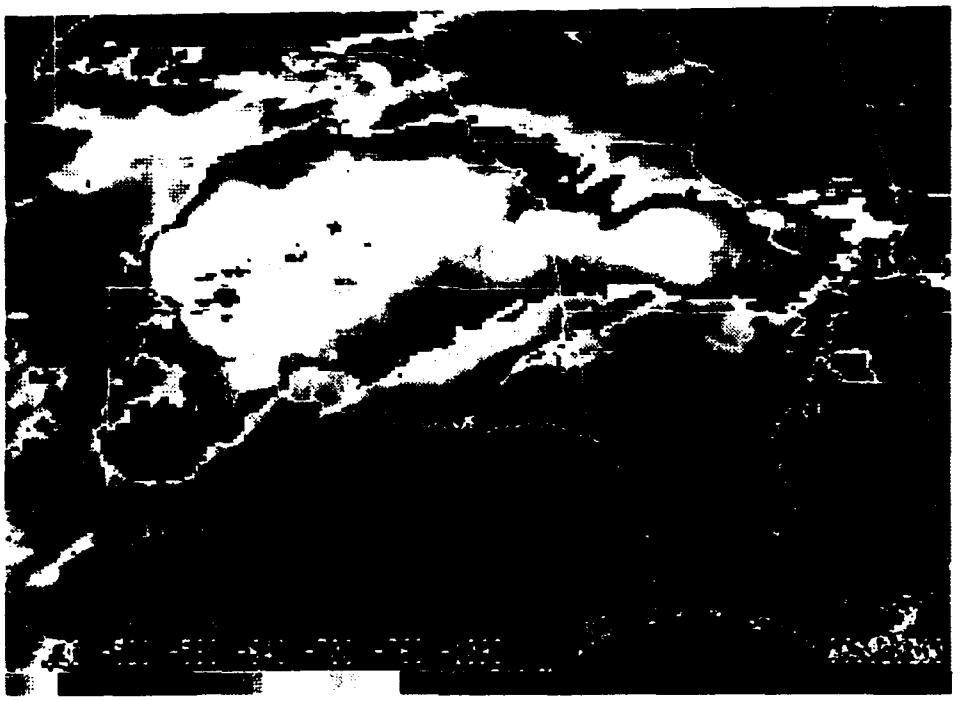

Figure 2.2. An example of the color enhancement used on the infrared satellite imagery.

2.1.3 Synoptic Data

Synoptic data, including surface, 850 mb, 700 mb, 500 mb and 300 mb charts, were obtained from microfilm archived at NSSL. Rawinsonde data used in this study were usually from standard NWS sounding locations but some special NSSL soundings were used.

2.2 Methodology

2.2.1 Selection of the MCSs for this Study

In order to choose storms with mesoscale organization, the criteria used in previous studies to define MCCs and MCSs (Maddox, 1980; Bartels et al., 1984;

Kane et al., 1987; Augustine and Howard, 1988; Watson et al., 1988; Houze et al., 1990) were reviewed and modified to establish the criteria used in this analysis. We required the storm systems we selected to have the following characteristics:

1. The -52°C cloud shield must have a major axis greater than or equal to 100 km for 6 h or more.

2. The -52°C cloud shield must have an area greater than or equal to 50,000 km^2 for 3 h or more.

An additional practical requirement was that each storm system had to be within the region of coverage of NSSL's lightning strike mapping system for at least 75% of its lifetime. These criteria include MCCs as well as large systems that do not meet the MCC definition. The time and size criteria insure that the storms chosen have mesoscale organization, although we recognize that some storms excluded from our study also could have mesoscale organization.

The storms used in this analysis were chosen by applying the above size and time criteria to storms occurring in the warm season (April through September) of 1986. These storms were documented by Augustine et al. (1988) using the MCS documentation program (Augustine, 1985). Data on duration, size, eccentricity and location of the centroid of the -52°C cloud shield were available. The length of the major axis of an elliptical fit to the -52°C cloud shield was calculated using this information. There were over 1000 storms documented across the United States in 1986. We checked only the 452 storms whose maximum spatial extent was within the region enclosed by 31° N, 43° N, -90° W and -104° W for inclusion in our study.

Those storms that met the above criteria and had -52°C centroids within the area enclosed by 32° N, 41.5° N, -94.5° W and -101.5° W (shown by the solid box in Figure 2.1) for at least 75% of the storm system's lifetime were chosen. Thirty-three MCSs met these criteria, which placed no restrictions on the shape or complexity of the storms. Five of these storms remained at the edge of coverage of the lightning detection network, where errors were large and detection efficiency was small, so these storms were omitted from our study. Lightning ground strike data were missing for significant periods of two systems, and satellite data were missing for significant periods of one system, so these were also omitted. Therefore, twenty-five MCSs were included in our analysis.

2.2.2 *Satellite Imagery with Superimposed Strike Locations*

Color thermal prints of lightning strike locations superimposed on enhanced, infrared satellite imagery were used to analyze the storms for this study. Both the satellite images and lightning strike locations were remapped to Lambert conformal projections for these plots.

A Lambert conformal projection was used because it minimizes distortion (Deetz, 1945). This projection is obtained by mapping the earth's surface on a secant cone that intersects the earth at two latitudes, as shown in Figure 2.3. These two latitudes are called the standard latitudes; scaled distance along standard latitudes on the map equals distance on the earth. Between the standard latitudes, measurements of distance on the map scale will be too small, and beyond them, too large. For this project, the standard latitudes were 34° N and 39° N. The standard

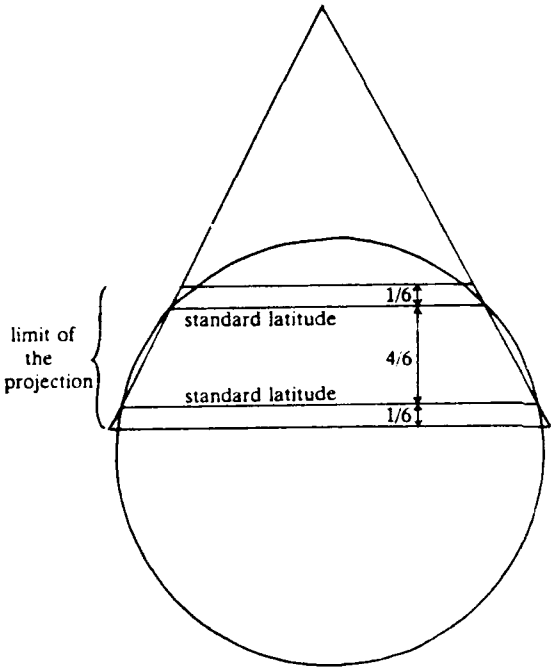

Figure 2.3. Diagram illustrating the intersection of a cone and a sphere along two standard latitudes for a Lambert conformal conic projection.

longitude, which is usually the central meridian of the area to be mapped, was 98°W The standard latitudes and longitude for this study are shown by the dashed lines in Figure 2.1.

For a symmetric distribution of error on a Lambert conformal projection, the distance of the standard latitudes from the top and bottom of the map should be one-sixth of the total distance along the central longitude of the area to be projected (Deetz, 1945). Our choice of standard latitudes was close to these values for the boxed area in Figure 2.1.

Although the mapped area was different for each system, depending on its location and movement, the same standard latitudes and longitude were used for all MCSs. To check for spatial distortion when a different region was plotted, an area

between 28°N and 38°N was projected using both the chosen standards (34°N and 39°N) and the standards using the one-sixth rule (29.67°N and 36.33°N). Satellite images and lightning on the two plots were indistinguishable at first glance. Minute differences were seen upon close scrutiny. It was, therefore, determined that using the same standards for remapping different regions did not introduce any significant error to the analysis. Distortion errors from the projection are largest at the latitudes farthest north and south of the standard latitudes, but these errors are much smaller than the errors in optimized strike locations at the boundaries of the region that we analyzed.

We made two plots of each hourly infrared satellite image, one with the half hour of lightning before the time of the image superimposed on it and one with the half hour of lightning after the time of the image. (Occasionally a quarter hour or hour of strike locations were plotted, depending on the flash density.) From the plots we determined which lightning ground strikes were associated with the storm system of interest. Determining if a particular cold cloud shield or lightning strike cluster was a part of the MCS of interest was often a challenge. The following basic rules were used:

1. If a separate cloud shield or cluster of lightning strikes merged with an existing MCS so that they could no longer be distinguished, it was included with that MCS.

2. If separate cloud shields or lightning strike clusters grew together to form the MCS, they were all included.

3. If the MCS split into two separate entities, both continued to be included.

4. Cold cloud shields whose -58°C contours did not merge for more than 2 hours and whose regions of lightning activity remained separate, were analyzed separately.

5. Clusters of lightning strikes that appeared to be associated with distant storms that were hidden by the cloud shield and never penetrated it and appeared to be unrelated to the MCS, were not included with the MCS.

6. The MCS had to be within the area covered by NSSL's lightning strike mapping network for at least 75% of its lifetime.

In several cases where the MCS had components that could be clearly separated in both the satellite imagery and ground strike regions, the lightning ground strikes were further subdivided into those belonging to each component. The MCS could then be analyzed both as a whole and by its component parts. For large systems with many components, only those components remaining within the bounds of the lightning detection network for at least 75% of their lifetimes were included.

2.2.3 MCS Documentation Program

The cloud shield areas within various temperature contours were determined by using a modified version of the MCS documentation program described by Augustine (1985). A flow chart of the program is shown in Figure 2.4. Data were collected for 15 temperature levels, at 2°C intervals from -52°C to -80°C. Once we selected the MCS or MCSs of interest on an infrared satellite image, the

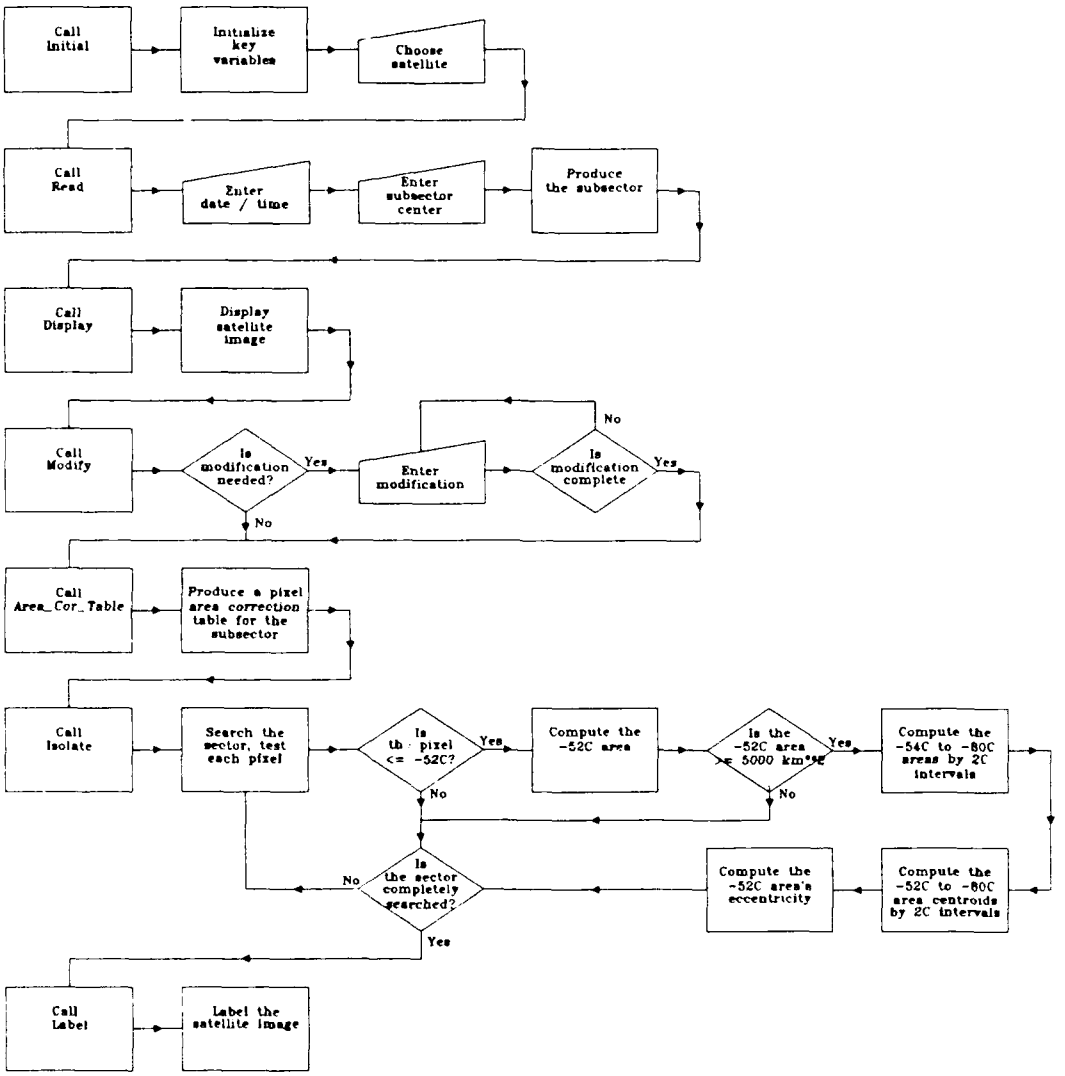

Figure 2.4. Simplified flow chart for the modified version of the MCS documentation software. The seven calls of the main program are in the left column. (Adapted from Augustine, 1985).

documentation program measured cloud shield areas by counting the number of pixels colder than each of 15 temperature levels. If the -52°C area was greater than or equal to 5000 km^2 the information about that system was written to a file. The program also fits an ellipse to the cloud shield within the -52°C contour. The documentation file includes the eccentricity and the lengths of the major and minor axes for the ellipse, along with the areas and centroids of the region within the 15 temperature levels.

The program has the capability to document parts of a continuous -52°C cloud shield separately and to document separate -52°C cloud canopies together. This capability was used to analyze systems that merged or split. After running the documentation program, it still was necessary to identify the same storm system in all images in which it appeared and to collect data from the storm's entire lifetime together. Time series plots of the area within each of the temperature levels were then made for the lifetime of that storm system.

2.2.4 Lightning Strikes Relative to Satellite Imagery and Synoptic Patterns

Lightning strikes identified from the plots as belonging to a particular MCS were collected together in half hour intervals centered on the hour and half hour for the MCSs entire lifetime. For each half hour, the number of positive and negative cloud-to-ground strikes and various other lightning parameters were tabulated, and the quartile values of the distributions of signal amplitudes were calculated. Each parameter was then plotted as a time series for the lifetime of the MCS, for comparison with the time series plots of the area of the cloud shield within various

temperature levels.

The thermal prints of lightning ground strike locations overlaid on satellite imagery were examined for various lightning characteristics. We examined the location of strikes relative to the satellite cloud-top temperatures, the density of the flashes, and the difference in the strike locations of positive and negative flashes and the relative times of occurrence of positive and negative flashes. We then used the occurrence of some of these patterns to categorize the storm systems and look for similarities in the synoptic environment of similar systems. This will be discussed further in sections 3.4 and 3.5.

CHAPTER III

RESULTS AND DISCUSSION

3.1 Lightning Characteristics

Table 1 is a summary of size, duration and time of occurrence for the MCSs in this study, along with some of their lightning characteristics. The table shows that the time of first lightning strike was usually in the afternoon or early evening, a common time for thunderstorms in the analysis region. When the time of the first strike occurred in the morning hours, strong synoptic forcing was present. Table 2 summarizes the average and range of some of the characteristics in Table 1. As might be expected (Figure 3.1a), there is a general trend for the largest number of flashes to be produced by storm systems having a larger area within -52°C contours, although MCSs of any size can produce a small number of flashes. There appears to be a more linear relationship between the number of flashes and the area within the -64°C contour of the MCS (Figure 3.1b). Table 1 shows that the dependence on size has a seasonal modulation, with MCSs in July through mid-August tending to produce larger numbers of flashes. This relationship between MCS size and number of flashes is in agreement with the observations of MCCs by Goodman and MacGorman (1986) and MCSs by Goodman et al. (1988).

TABLE 1 MCS and Cloud-to-ground Lightning Characteristics

DATE (1986)	TIME OF FIRST-LAST STRIKE (CST)	STRIKE DURATION (hrs)	TOTAL # FLASHES	MAXIMUM -52° AREA (km^2)	TOTAL # POS FLASHES	PERCENT POSITIVE	MAX # POS IN 0.5 HR/% OF TOTAL #
31 March-1 April	14:35-07:18	16.72	5993	186,312	964	16.1	74 / 54.4
26-27 April (1)	14:30-00:12	9.70	2895	72,895	460	15.9	117 / 29.3
26-27 April (2)	15:33-01:29	9.93	4063	63,727	163	4.0	28 / 5.3
26-27 April (3)	21.18-08:42	11.40	3612	117,704	426	11.8	69 / 13.6
30 April	15:06-23:00	7.90	4222	67,191	164	3.9	28 / 4.8
8-9 May (1)	08:26-02:47	18.35	9044	174,495	1368	15.1	152 / 48.1
8-9 May (2)	11:51-04:15	16.40	3978	154,369	332	8.3	47 / 20.2
8-9 May (3)	11:57-02:11	14.23	9021	80,887	2762	30.6	645 / 46.1
13-14 June	17:15-02:17	9.03	5623	107,619	376	6.7	52 / 6.5
19-20 June	14:54-06:49	15.92	3164	134,710	137	4.3	20 / 55.6
21-22 June	20:09-05:24	9.25	2690	73,677	225	8.4	35 / 44.3
23 June	15:47-22:56	7.15	775	81,078	764	98.6	201 / 100.
30 June-1 July	13:34-12:15	22.68	40,888	253,636	1825	4.5	190 / 9.4
5-6 July	14:27-08:00	17.55	20,563	199,262	686	3.3	70 / 30.3
6-7 July	12:30-00:24	11.90	14,729	111,769	677	4.6	85 / 6.0
12-13 July	15:38-13:33	21.92	27,184	184,321	402	1.5	32 / 21.5
8-9 August	19:33-12:59	17.43	8450	81,005	506	6.0	53 / 22.7
11-12 August	23:19-12:56	13.62	8613	66,933	223	2.6	25 / 4.8
13-14 August	14:26-10:30	20.07	22,964	114,297	802	3.5	54 / 53.5
14 August	11:32-22:01	10.48	8704	99,297	615	7.1	78 / 9.3
14-15 August	15:31-03:15	11.73	7963	102,424	214	2.7	36 / 8.7
20-21 August	13:17-23:04	9.78	12,883	75,471	466	3.6	93 / 5.2
26 August	12:38-21:50	9.20	5636	141,260	234	4.2	45 / 19.3
28-29 September (1)	15:03-00:19	9.27	6789	65,283	659	9.7	149 / 15.6
28-29 September (2)	22:38-10:55	12.28	5996	159,523	801	13.4	107 / 15.6

TABLE 2 Average and Range of MCS and Cloud-to-ground Lightning Characteristics

Characteristic	Minimum/ Earliest	Maximum/ Latest	Average
Time of First Strike (CST)	08:26	23:19	15:25
Lightning Duration (hrs)	7.15	22.68	13.4
-52° Area (km^2)	63,727	253,636	118,766
Total Number of Flashes	775	40,888	9858
Total Number of Negative Flashes	11	39,063	9208
Total Number of Positive Flashes	137	2762	650
Percent Positive	1.5	98.6	6.6
Maximum Number of Positives in Half Hour During Lifetime	20	645	99

The number of positive flashes in each storm varied considerably, with a low of 137, a high of 2762, and an average of 650 per MCS. The percentage of ground flashes that were positive varied across almost the whole range of possibilities, from 1.5% for the July 12-13 case to the unusual June 23 system with 98.6%. In his review of positive cloud-to-ground lightning, Beasley (1985) found that published reports of the percentage of positive flashes varied from 0% to 100%. The May 8-9 (3) case also seemed to produce an unusually large number of positive flashes (it produced 685 positive flashes in one 30 minute period, the most of any MCS), as well as a higher than normal ratio of positive to total flashes (30.6%). If these two cases with high percentages are omitted, the percentage for remaining cases was no more than 16.1%. The average percentage was 6.6% for all storms and was only 5.4% when the two cases with high percentages were omitted. These values are slightly higher than the 4.3% of positive flashes reported by Reap and MacGorman

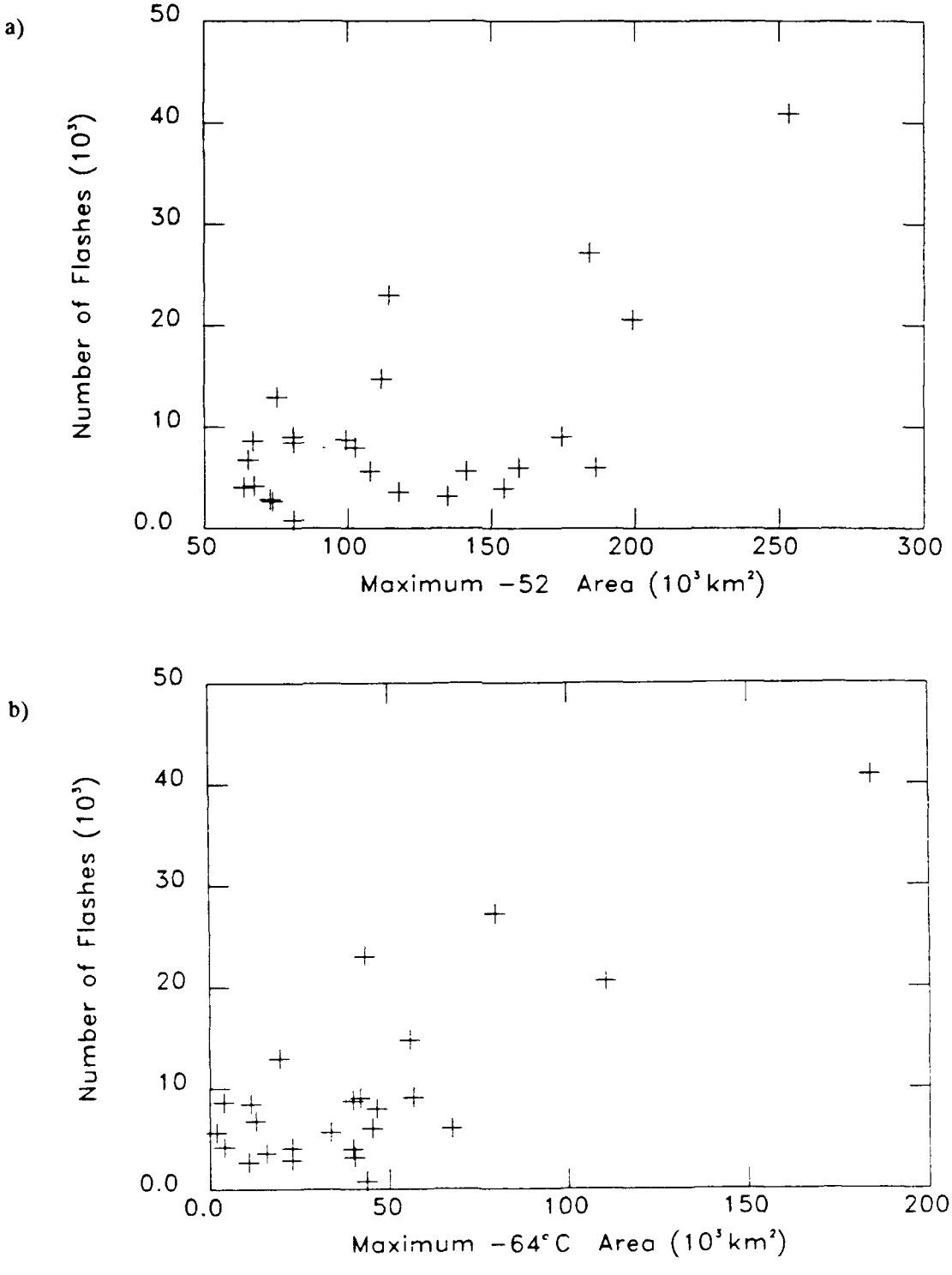

Figure 3.1. Scatterplots of the number of flashes versus a) the maximum -52°C area and b) the maximum -64°C area attained by each MCS.

(1989) for all flashes that occurred in the warm seasons (April-September) of 1985 and 1986. (The flashes of this study are a subset of the data used by Reap and MacGorman.) This suggests the ratio of positive flashes to total flashes is somewhat larger, on average, in MCSs than in other types of thunderstorms on the Great Plains.

The time series of all flashes (positive and negative) generally had a single peak in the number of flashes, with rapid growth and decay, similar to that found by Goodman and MacGorman (1986) for a composite of lightning life cycles of MCCs. The eight systems that had two or three peaks of lightning activity consisted of cloud shields with separable components, each of which had cycles of lightning strike activity with different lifetimes and phases. This does not imply that the cases with only one peak of lightning activity were simple systems consisting of only one region of lightning activity. Often a single peak of lightning activity (Figure 3.2a) occurred with a system that had more than one region of lightning activity, such as the many small components of August 26 (Figure 3.2b). Our observations of MCSs consisting of multiple components agree with observations of MCCs by McAnelly and Cotton (1986); they observed that large, meso-α-scale MCCs (200-2000 km, >6 h) had multiple meso-ß-scale (20-200 km, <6 h) components throughout their life cycles, while smaller MCCs tended to be dominated by a single meso-ß component.

Using the time in the center of the half hour interval in which the maximum peak occurred, total lightning strike activity peaked an average of 6.4 h after the first strike. The earliest peak occurred only 1.7 h after the first strike on June 23, and

a)

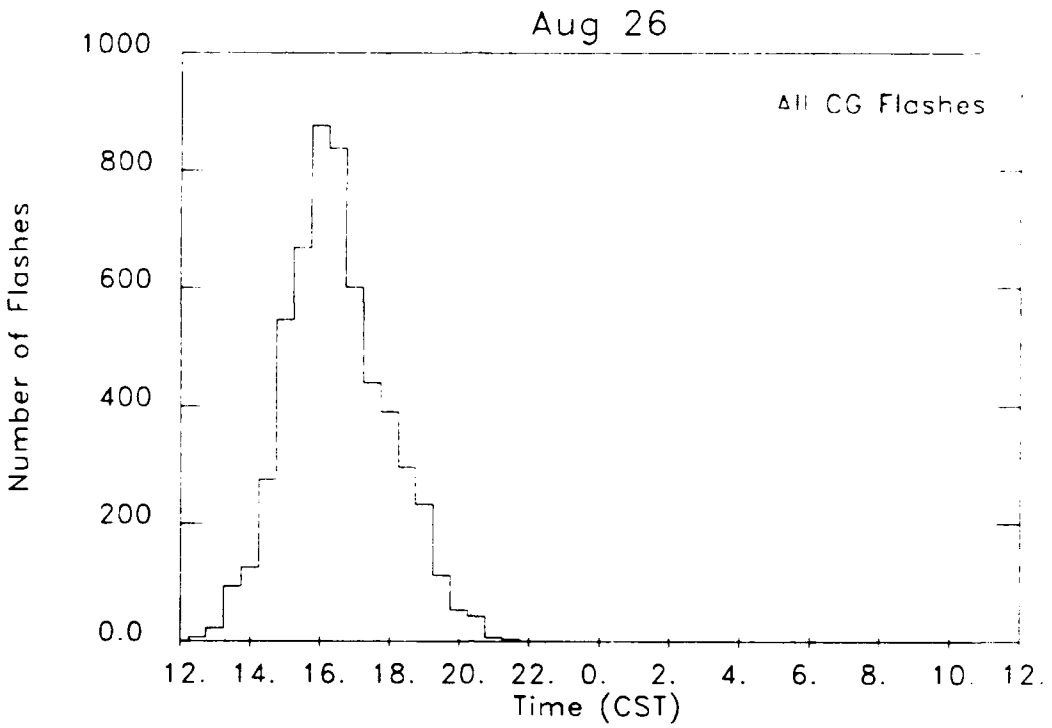

b)

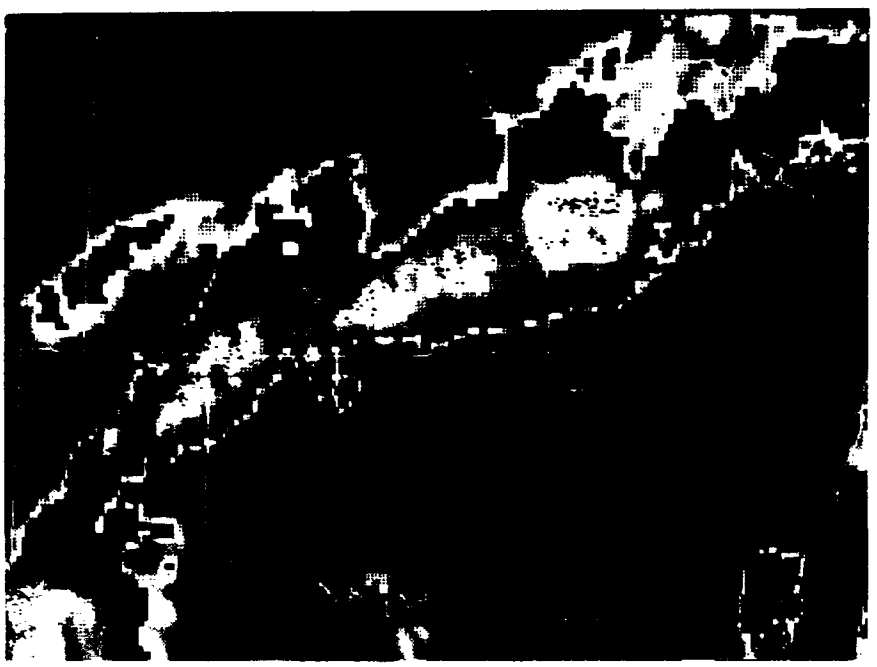

Figure 3.2. a) Time series histogram of CG flashes that shows the rapid growth and decay from the peak. Each bin of the histogram is a half hour wide. b) Satellite image for August 26 1700 CST over which is plotted the location and polarity of CG flashes for a half hour period centered on the time of the image. Negative flashes are indicated by (-) and positive flashes are indicated by (+).

the latest peak was 11.6 h after the first strike on May 8-9 (1). If these values are adjusted by using the first relative maximum rather than the absolute maximum in cases with multiple peaks, the average becomes 5.3 h after first strike. With this change, the earliest peak remained the same, but the latest peak occurred sooner, 9.4 h after the first strike for the case on August 8-9.

In their study of MCCs, Goodman and MacGorman (1986) found that lightning activity peaked an average of 7.0 h after the initial storms in an MCS began. This is slightly longer than the 6.4 h we found for the MCSs of this study. The average time to peak flash rates may be longer in Goodman and MacGorman (1986) because the duration of the MCCs they studied was longer (average duration of 14.3 h) than that of the MCSs in this study (13.4 h).

The time series plots of negative flashes usually appeared similar to plots of all ground flashes for most MCSs, because most cloud-to-ground flashes were normally negative. However, the time series plots of positive flashes were often quite different from the plots for negative flashes. The plots for positive flashes had more variability between systems, a smaller likelihood of a single peak of activity, and in some cases, short one hour periods of high positive flash rate activity. The average time to maximum peak after the first strike was 5.9 h for positive flashes, half an hour earlier than that found for negative flashes. This seems contrary to what one might expect based on the observations of Fuquay (1982), Orville et al. (1983), Rust (1986) and Rutledge and MacGorman (1988), who report a tendency for positive flashes to appear in the later stages of thunderstorm development.

However, there was also greater variability in the time to first peak for positive flashes; the earliest peak occurred 1.1 h after the first strike (August 13-14) and the latest peak occurred after 15.4 h (July 12-13). In all cases when the time to the peak for positive flashes was less than 4 h, a high percentage of positive flashes occurred early in the lifetimes of the systems, with a peak prior to that of negative flashes. The earlier average time to peak for positive flashes, therefore, was caused by an early peak in positive flash rates for several MCSs. Although the tendency for positive flashes to occur in the later stages of thunderstorms has been reported most often, there also have been observations of large numbers of positive flashes occurring early in a thunderstorm's lifetime as discussed in section 1.2. The cases we observed that had early peaks in the number of positive flashes will be discussed in more detail in sections 3.2 through 3.4.

A related lightning characteristic can be seen in time series plots of the fraction of flashes that were positive. Again, reports of a tendency for positive flashes to occur in mature and decaying thunderstorms might lead to an expectation that the fraction of positive flashes would increase toward the end of a storm's lifetime, as the negative flash rate decreases and positive flashes dominate. This was true for 17 cases, such September 28-29 (2) (Figure 3.3a) and August 14-15 (1) (Figure 3.3b). Figure 3.3c shows satellite imagery of the August 14-15 (1) case, in which the ratio of positive to total flashes increased when cloud tops fell to warmer temperatures as the storm in northwestern Oklahoma decayed. Both of these cases are good examples of positive flashes occurring in decaying thunderstorms. In both

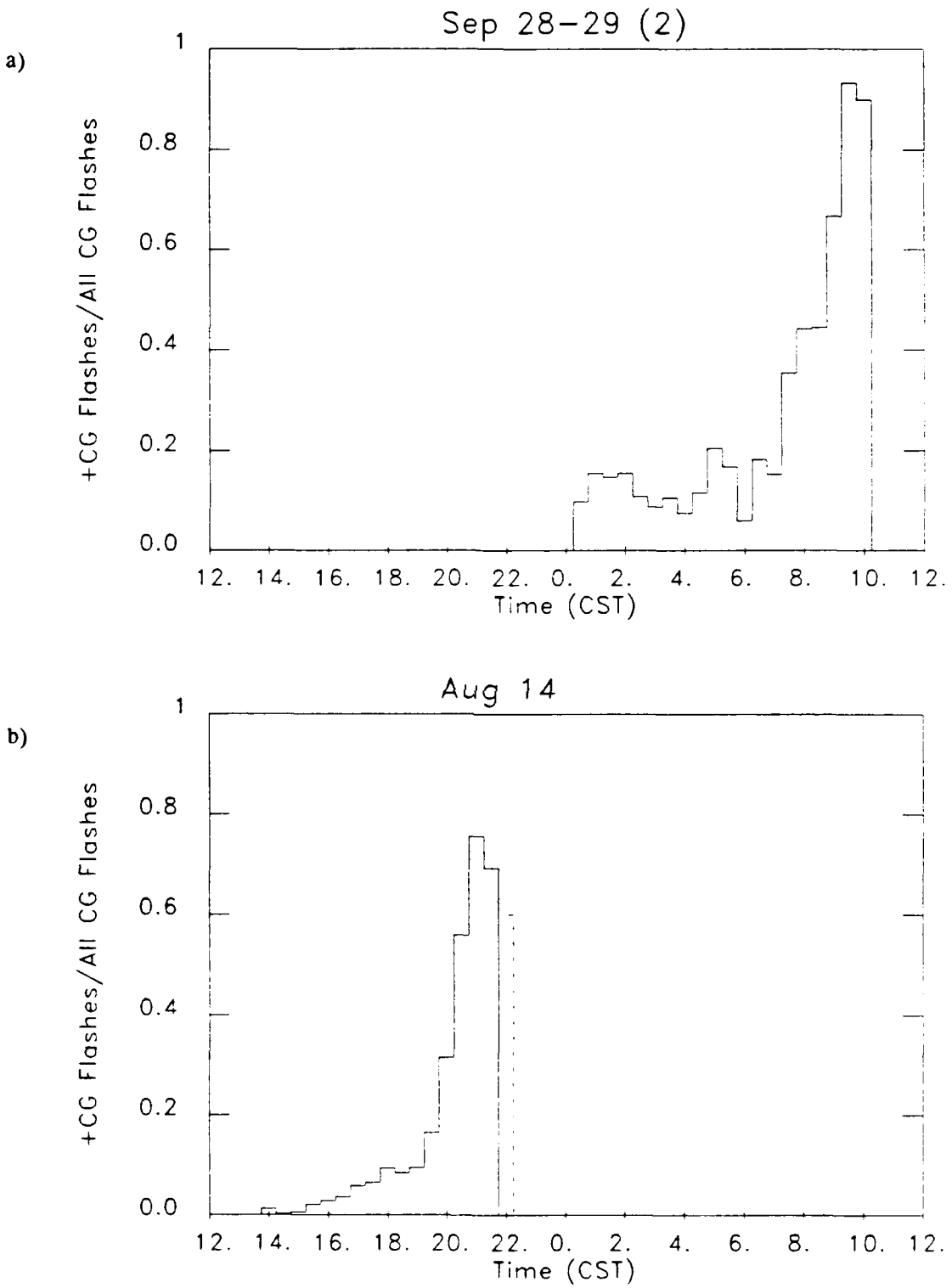

Figure 3.3. Time series histograms of the ratio of positive flashes to total flashes. Note the increasing fraction at the end of systems that occurred on a) September 28-29 (2) and b) August 14. Dashed lines indicate that five or fewer flashes occurred within that half hour bin. Shown in c) is the satellite image for August 14 2000 CST as in Figure 3.2b.

c)

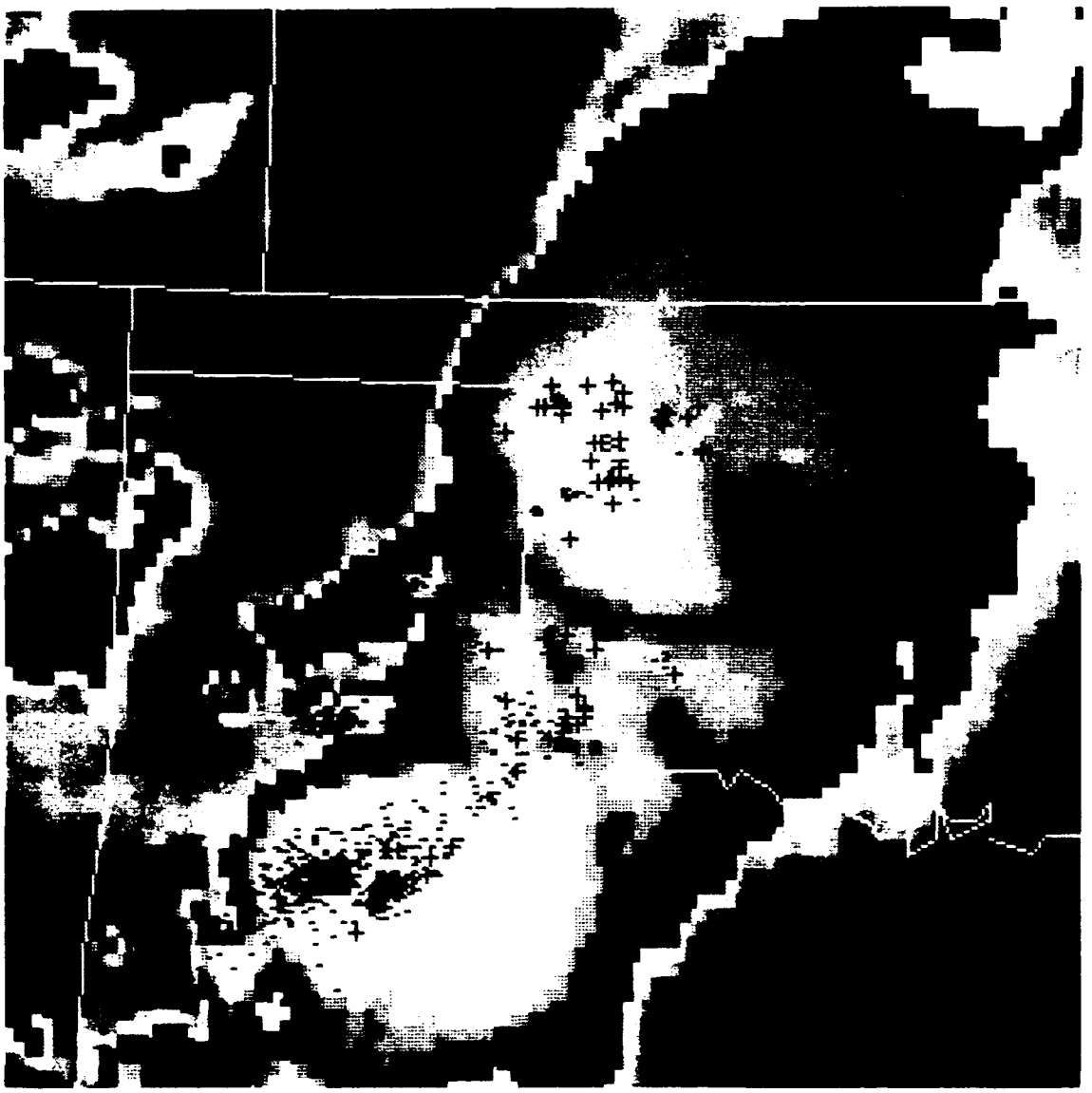

Figure 3.3. Continued.

cases, the number of flashes decreased toward the end of the storm but the number of negative flashes decreased faster than the number of positive flashes.

In some cases (three of 17), when there was a peak in the fraction of flashes that were positive at the end of a storm, there was also a higher fraction at the beginning of a storm. In all three of these cases, the fraction early in the storm exceeded the fraction at the end of the storm (for example, see Figure 3.4). The early peak in the fraction generally was caused by unusually large concentrations of positive flashes occurring before most negative flashes, not by just a few positive flashes with even fewer negative flashes, as often occurred at the end of MCSs.

Time series plots of the fraction of flashes having a single return stroke appeared to be related to time series plots of the fraction of flashes that were positive, in that peaks in the fraction of flashes having a single return stroke often occurred at the same time as peaks in the fraction of flashes that were positive (e.g. Figure 3.5). Cloud-to-ground flashes that occurred in the first half hour of a MCS were more likely to have a single return stroke (e.g., Figure 3.6). This observation is consistent with the report by Krehbiel (1986) that the first cloud-to-ground strikes tend to have fewer strokes, usually only one.

Figure 3.7 shows the number of flashes versus the number of strokes that occurred per flash for negative and positive flashes. It clearly shows that positive flashes are more likely to have only a single return stroke. For all of the flashes in the 25 MCSs of this study, 83.3% of the positive flashes had only a single return stroke, while 32.7% of the negative flashes had only a single return stroke. For all

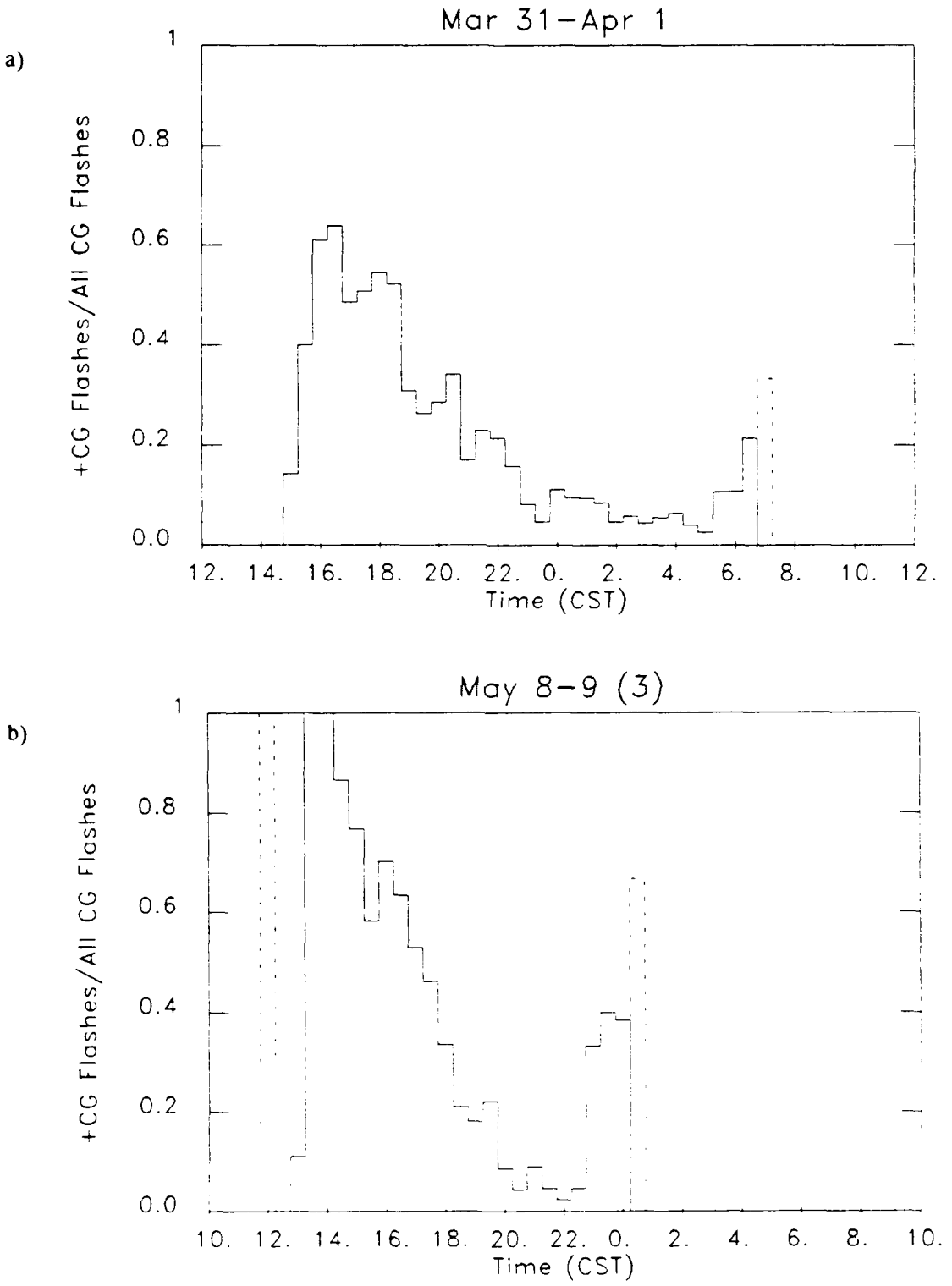

Figure 3.4. Time series histograms of the ratio of positive flashes to total flashes. Note the higher fraction at both the beginning and the end of the systems that occurred on a) March 31-April 1 and b) May 8-9 (3). Dashed lines indicate that five or fewer flashes occurred within that half hour bin.

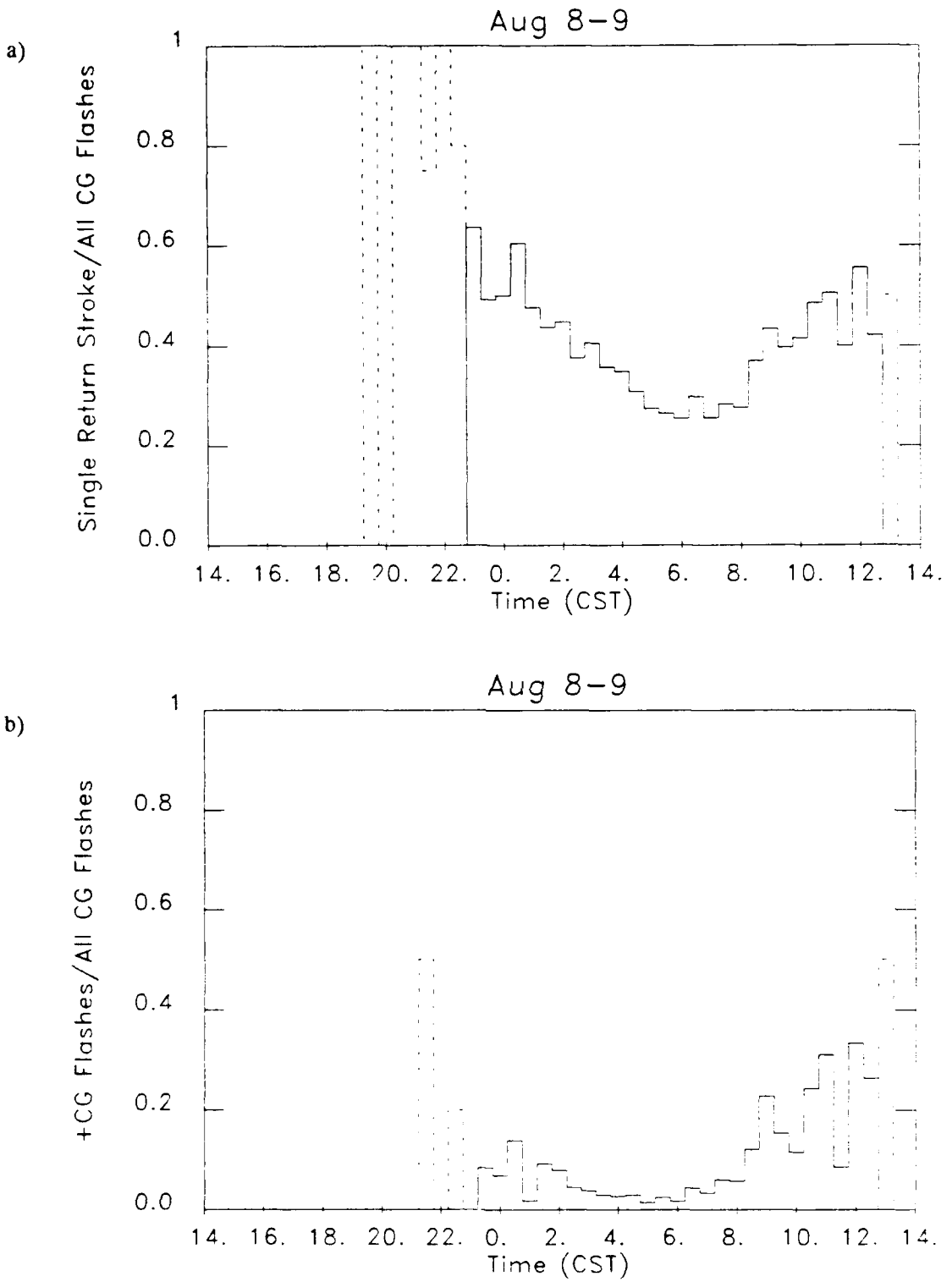

Figure 3.5. Time series histograms showing the relationships between a) the fraction of flashes that had a single return stroke and b) the ratio of positive flashes to total flashes. Dashed lines indicate that five or fewer flashes occurred in that half hour bin.

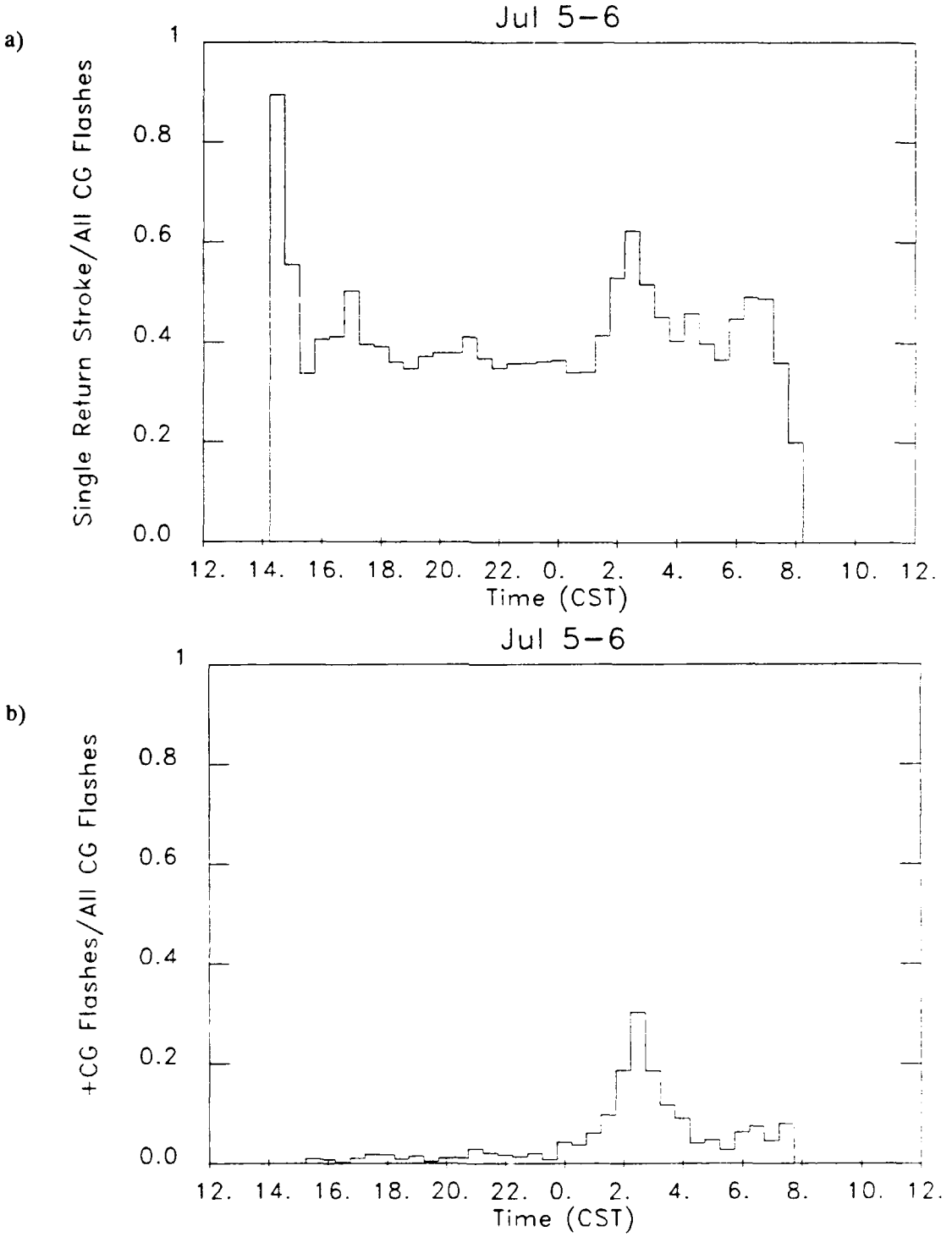

Figure 3.6. Time series histograms showing a) the fraction of flashes that had a single return stroke and b) the ratio of positive flashes to total flashes. The high fraction of flashes with a single return stroke in the first half hour of the system was not associated with a high ratio of positive flashes to total flashes.

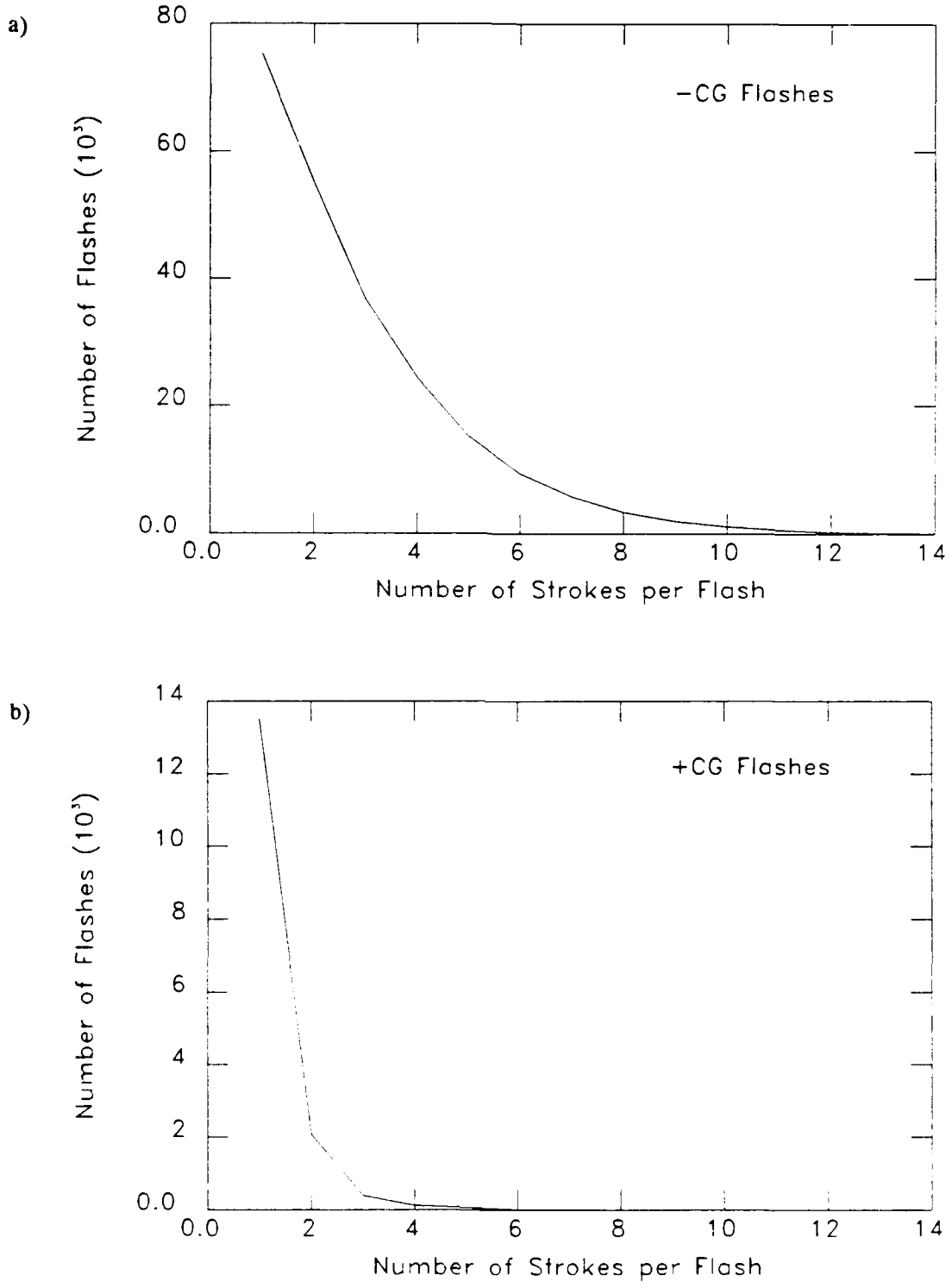

Figure 3.7. The number of flashes versus the number of strokes that occurred per flash for a) negative flashes and b) positive flashes.

storms in the warm seasons of 1985 and 1986, Reap and MacGorman (1989) report slightly lower values of 77% and 28% for positive and negative flashes, respectively.

The amplitude of the first return stroke for positive and negative flashes also showed some systematic variations. Time series plots of maximum, minimum, median and 25% and 75% quartiles show that the median amplitude for negative flashes was steady except during the beginning and end of the storm, when fewer flashes occurred and amplitude varied more. The minimum and the 25% and 75% quartiles also were relatively steady, but the maximum amplitudes varied more frequently and over a larger range. The distribution of negative amplitudes for the 230,191 negative flashes in this study are shown in Figure 3.8a. The bins have a width of 25 LLP units and the peak occurred in the fifth bin while the median value occurred in the sixth bin. This figure agrees very well with the distribution found by Orville et al. (1987) for 720,284 negative flashes, from all storms that occurred along the east coast during an entire year (Figure 3.8b). The peak and median values for his distribution also occurred in the fifth and sixth bins, respectively. We also plotted the distribution of negative amplitudes for each individual MCS. There was little variation in the shape of the curve from MCS to MCS; the peak ranged only from the fourth to the sixth bin and the median value ranged from the fourth to the eighth bin.

In contrast, most of the time series plots of amplitudes for positive flashes had extreme variability. The least and most variable time series plots of negative amplitudes are compared to the least and most variable time series plots of positive

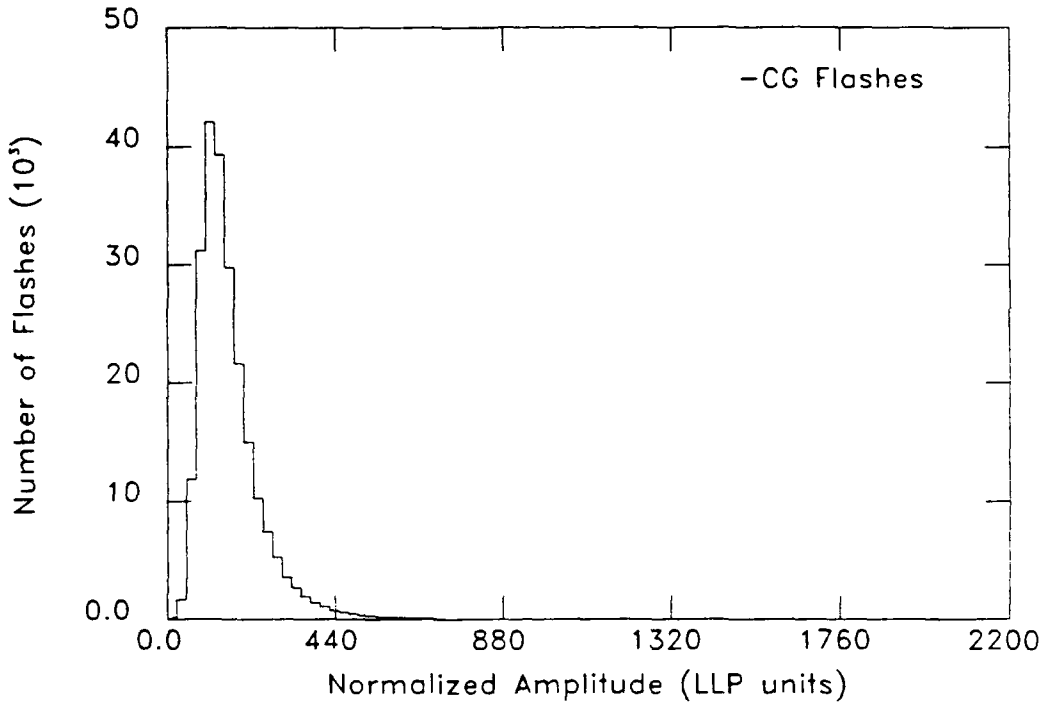

Figure 3.8a. The distibution of normalized amplitudes for 230,191 negative flashes.

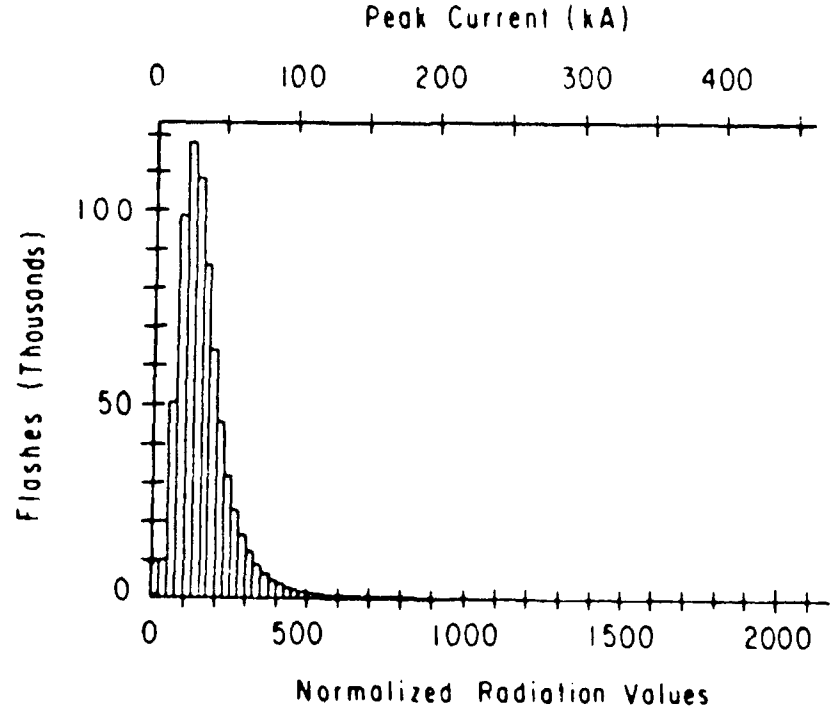

Figure 3.8b. Distribution of the peak magnetic field amplitudes and peak currents for 720,284 first return strokes lowering negative charge. (From Orville et al., 1987)

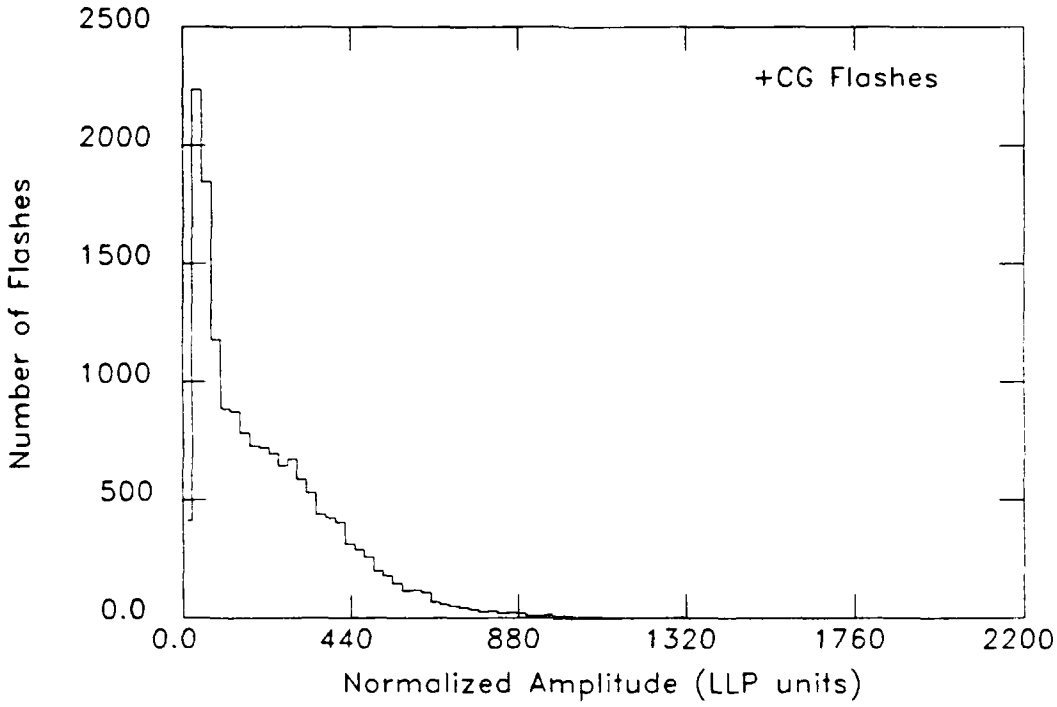

Figure 3.8c. The distribution of normalized amplitudes for 16,251 positive flashes.

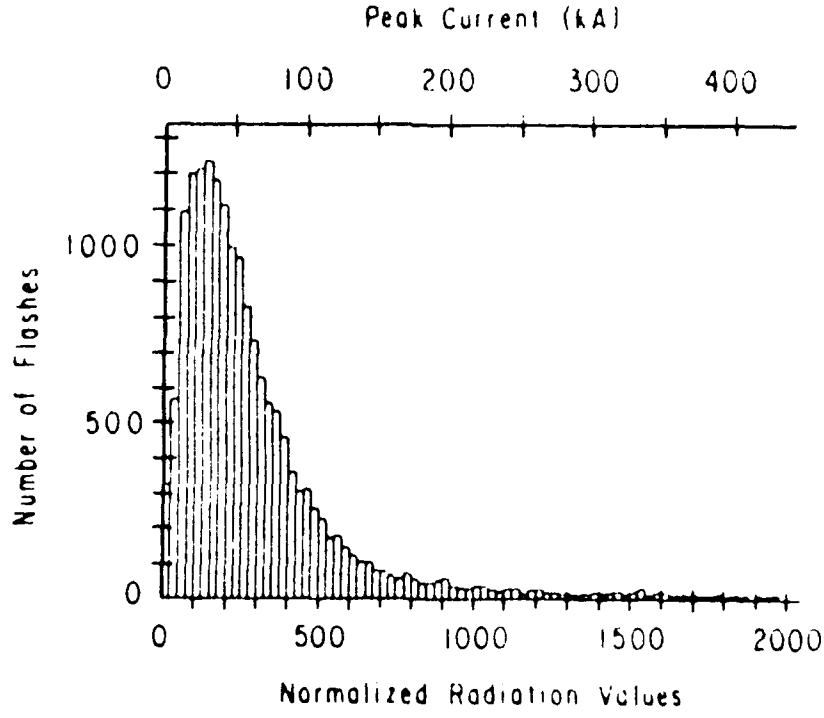

Figure 3.8d. Distribution of the peak magnetic field amplitudes and peak currents for 17,694 first return strokes lowering positive charge. (From Orville et al., 1987)

amplitudes in Figure 3.9. In some cases, the positive amplitudes decreased to extremely low values during the peak in positive flash activity, as shown in Figure 3.10, while in other cases, the amplitudes remained high during the peak in positive flash activity, as shown in Figure 3.11. In still other cases, the amplitudes did not seem to change when the number of positive flashes peaked, as shown in Figure 3.12.

The distribution of positive amplitudes for all 16,251 flashes included in this study is shown in Figure 3.8c. It is different from that found for negative flashes (Figure 3.8a) and also different from that found by Orville et al. (1987) for 17,694 positive flashes that occurred over an entire year along the east coast (Figure 3.8d). The positive flash amplitudes peak in the second bin (compared to the fifth bin for negative flashes in this study and the sixth bin for positive flashes recorded by Orville et al. (1987)) and also have a much broader distribution than negative flashes. The median value occurred in the seventh bin, compared to approximately the ninth bin for positive flashes recorded by Orville et al. The difference in the positive distribution between this study and the one conducted by Orville et al. is probably caused at least in part by the difference in the threshold for acceptance of positive flashes in the two lightning detection networks. The threshold for acceptance of positive flashes for this study was 110 to 120 mV while that used by Orville et al. was around 400 mV. Another factor that may have led to differences is that we examined only MCSs while Orville et al. examined all storms. Of course, there also may be geographical variations. Section 3.5 will discuss in more detail the variability

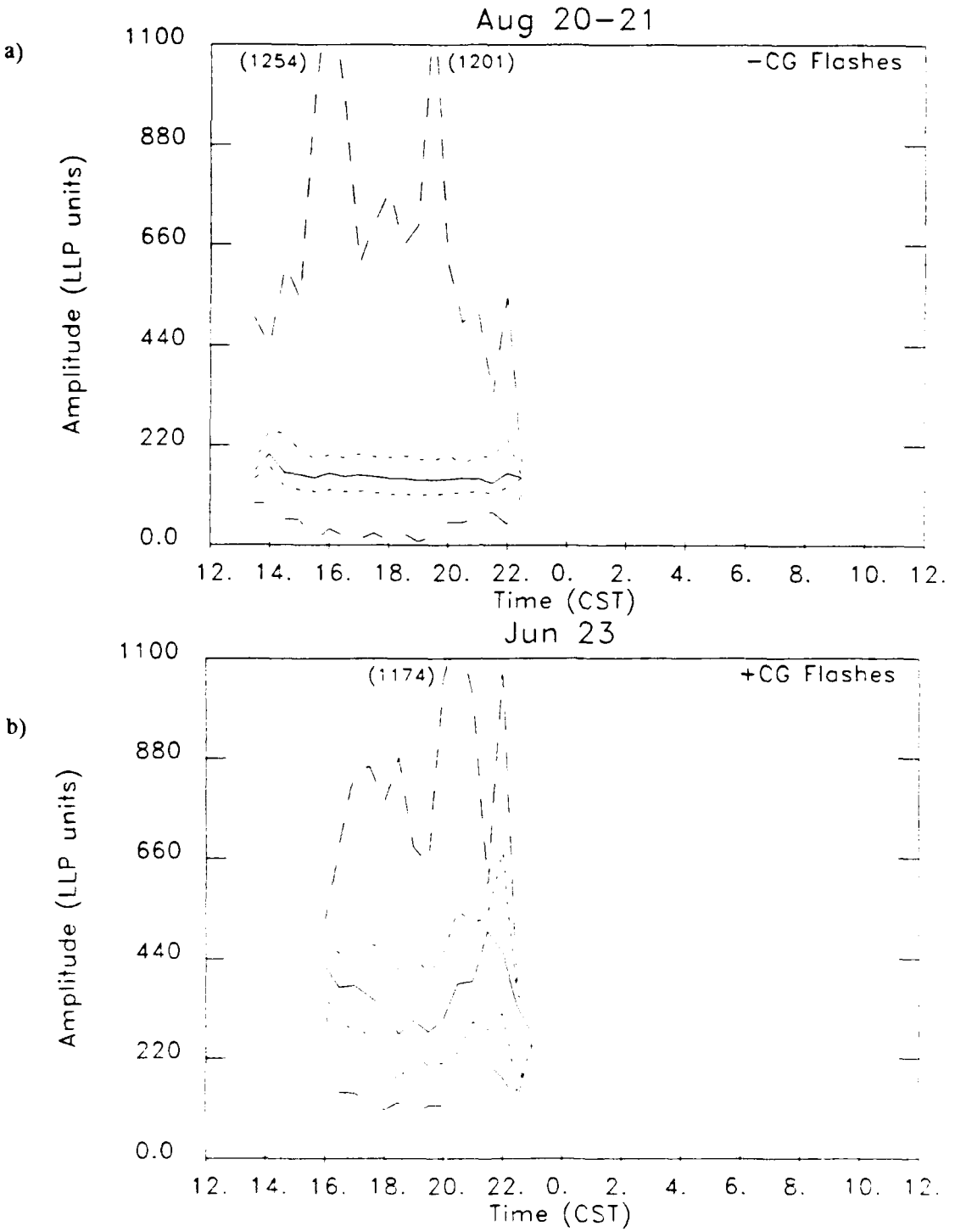

Figure 3.9. Time series of a) the least variable negative amplitudes, b) the least variable positive amplitudes, c) the most variable negative amplitudes and d) the most variable positive amplitudes. Solid lines are the median amplitude, short dash are the 25% and 75% quartiles and long dash are the maximum and minimum amplitude in a half hour period. Numbers in parenthesis indicate the value of the maximum amplitude if it is off the graph.

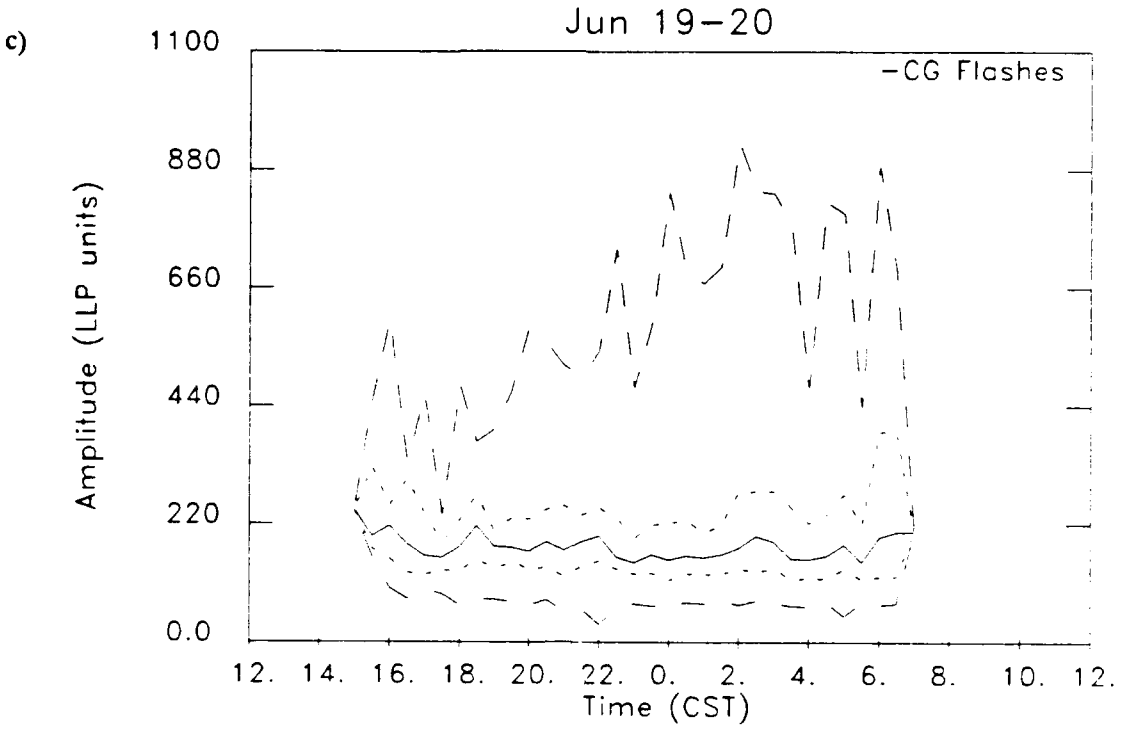

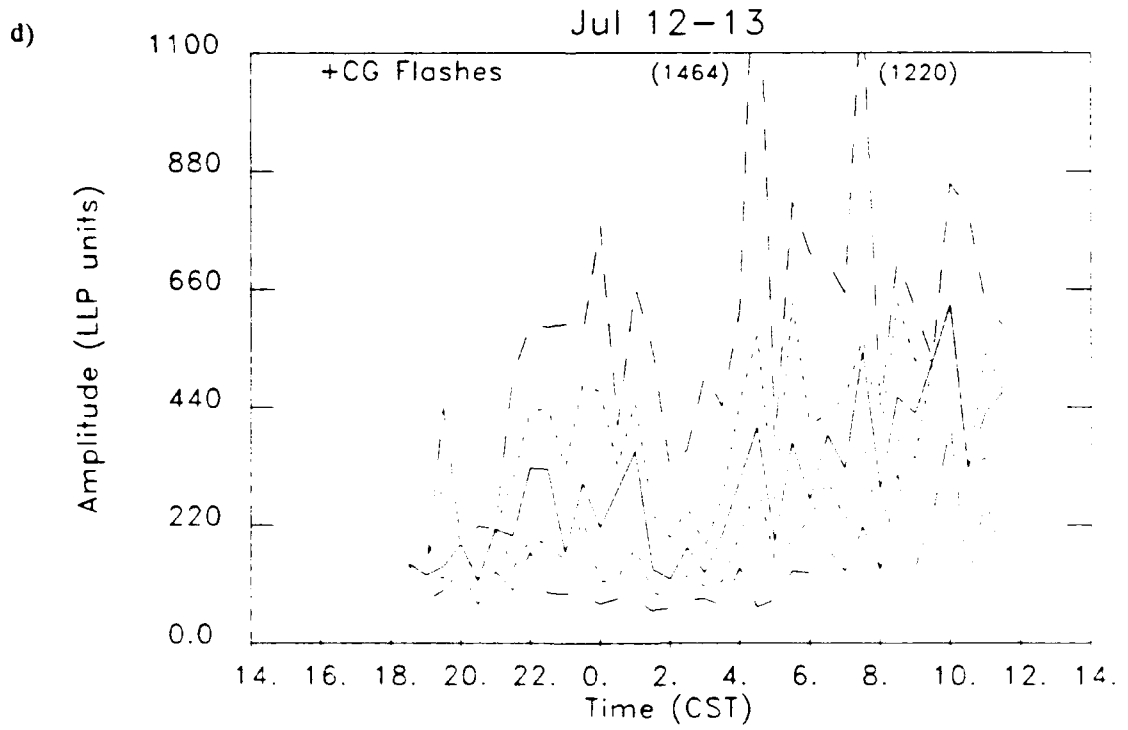

Figure 3.9. Continued.

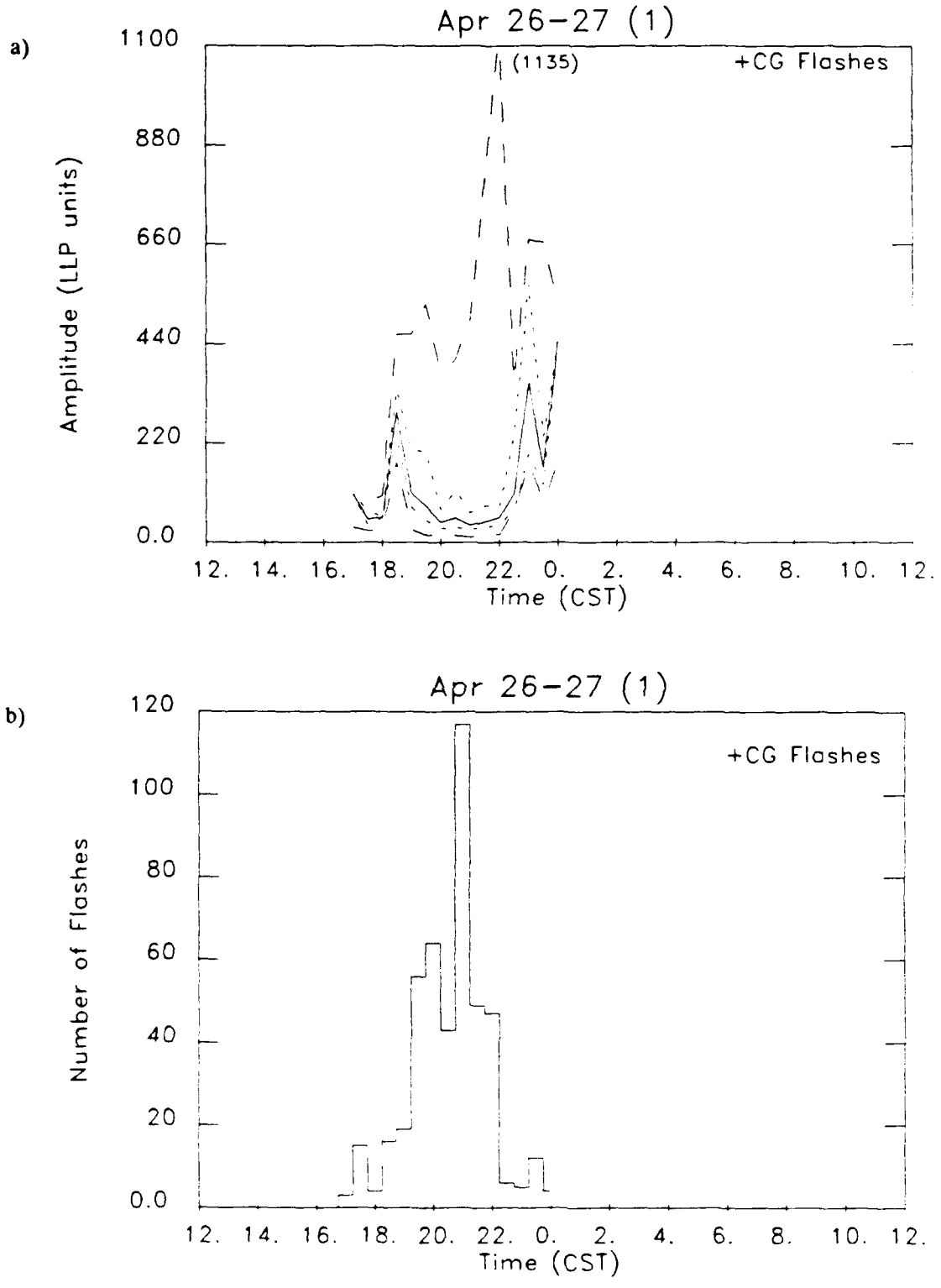

Figure 3.10. Time series of a) positive amplitudes as in Figure 3.9 and b) the number of positive flashes. The smallest median amplitude occurred when the number of flashes was the largest.

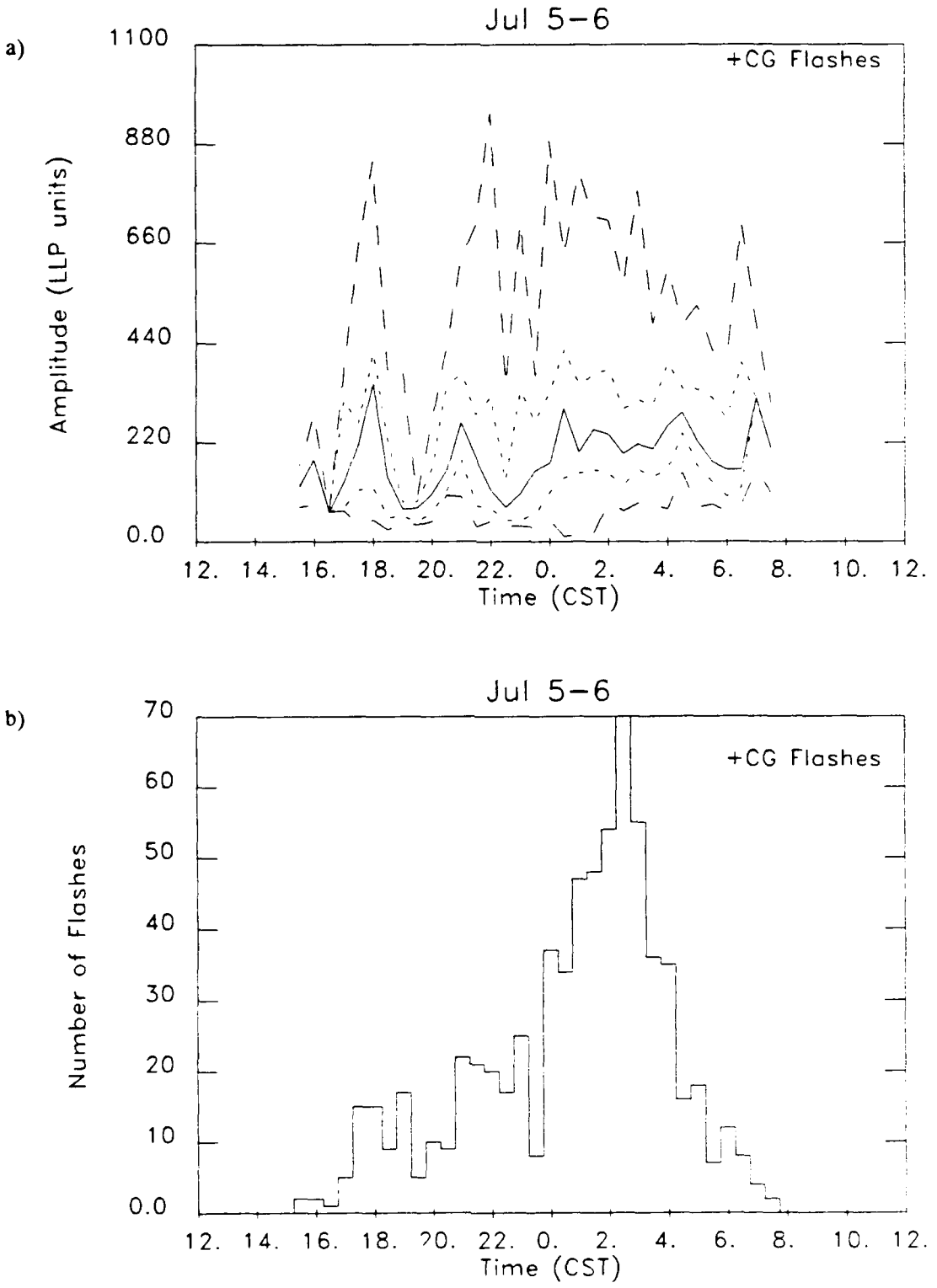

Figure 3.11. Time series of a) positive amplitudes as in Figure 3.9 and b) the number of positive flashes. Median amplitudes were large when the number of flashes was the largest.

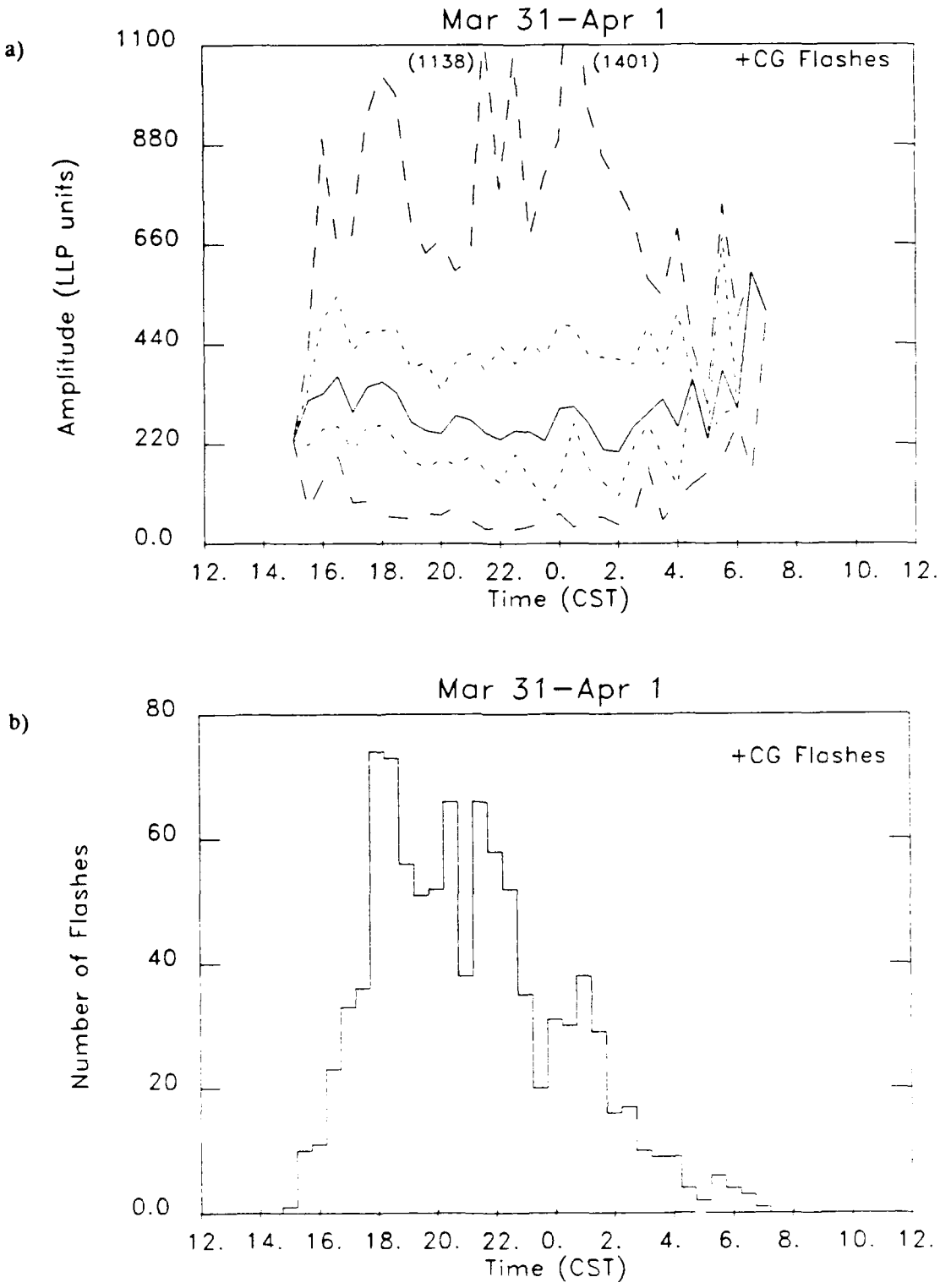

Figure 3.12. Time series of a) positive amplitudes as in Figure 3.9 and b) the number of positive flashes. Median amplitudes do not appear affected by the number of flashes.

in the amplitude distributions of positive flashes from the MCSs that we studied.

Based on the distributions of positive and negative amplitudes that they observed, Orville et al. (1987) reported that positive flashes appeared to have significantly higher peak currents than negative flashes. Although the amplitude distribution of positive flashes in the MCSs we studied was broader than the distribution for negative flashes, so that a larger fraction of positive flashes had very high amplitudes, the median amplitude for positive flashes was only 30 LLP units higher than the median amplitude for negative flashes.

3.2 Lightning Ground Strike Locations Superimposed on Satellite Imagery

The large cloud shield of an MCS often masks regions of convection occurring beneath it. Satellite imagery of different MCSs may look similar, but actually have very different patterns of convection beneath their cloud shields. Because dense clusters of lightning occur near deep convection (e.g., Lhermitte and Krehbiel, 1979; Reap and MacGorman, 1989), lightning ground strike data can greatly enhance the usefulness of satellite imagery by revealing where electrically active regions are located, thereby providing an indication of the horizontal structure of deep convection in MCSs. In the satellite image of the large MCS of June 30-July 1 (Figure 3.13a), for example, it is nearly impossible to determine where the main convection occurred within the broad structure of the cold cloud-tops. Lightning ground strike locations plotted on the image, (Figure 3.13b) however, clearly reveal where the strong convection was located. The lightning ground strike locations were

also compared to the OKC NWS radar echoes for the same time, and as expected, there is good agreement between the positions of radar echoes and the positions of clusters of lightning ground strikes (Figure 3.13c). Note that one storm indicated by lightning strikes is beyond the range of the radar.

The broader area of coverage of lightning ground strike data is especially useful for MCSs which often extend beyond the coverage of a single radar. Lightning ground strike data also can be used to detect new regions of convection that are obscured by the cloud shield of a nearby MCS. Figure 3.14 shows a sequence of two satellite images with lightning ground strike locations. The satellite imagery alone shows no indication of the growing region of convection until the MCS cloud shield begins to dissipate, but the lightning ground strike locations reveal the region at least a half hour before the satellite imagery.

Lightning ground strike locations often revealed growing convective regions before satellite imagery showed growth of cloud-tops to cold temperatures, typically detecting new convection an hour earlier than satellite IR imagery (see, for example, Figure 3.15). Goodman et al. (1988) found that trends in the flash rate of cloud-to-ground lightning provided a better indication of thunderstorm evolution than the time rate-of-change of minimum cloud-top temperatures from satellite images. Real-time radar data from volume scans are probably the best means for monitoring thunderstorm growth and development within roughly 250 km of a radar, but in the absence of a radar within this range, lightning data can be a useful forecasting tool, either alone or with satellite imagery.

a)

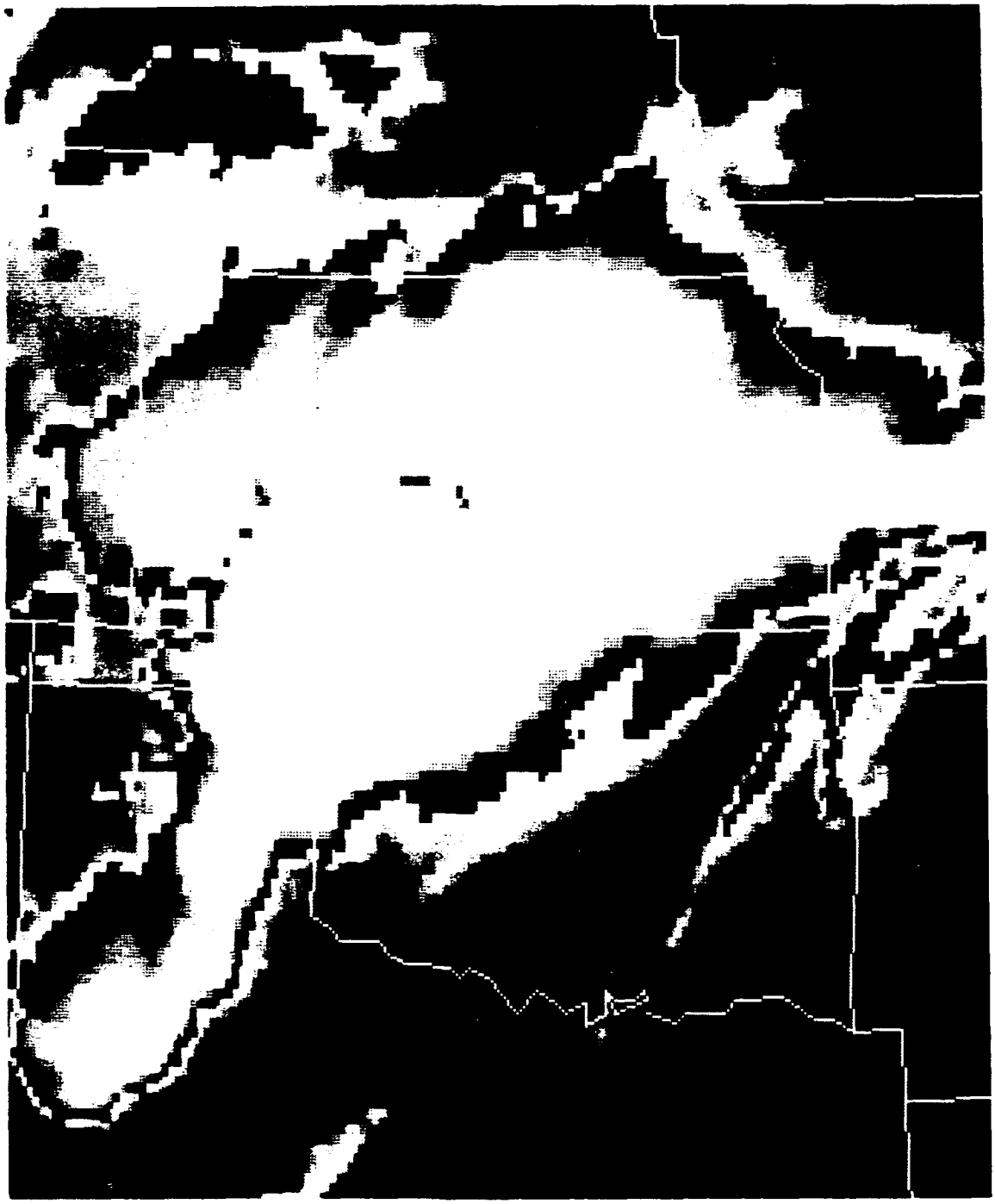

Figure 3.13. Satellite image for June 30 1900 CST a) without CG strike locations and b) with the location and polarity of CG strikes for a half hour period centered on the time of the image indicated by (-) for negative flashes and (+) for positive flashes. c) Radar reflectivity for June 30 1900 CST from Oklahoma City radar at .5° elevation.

b)

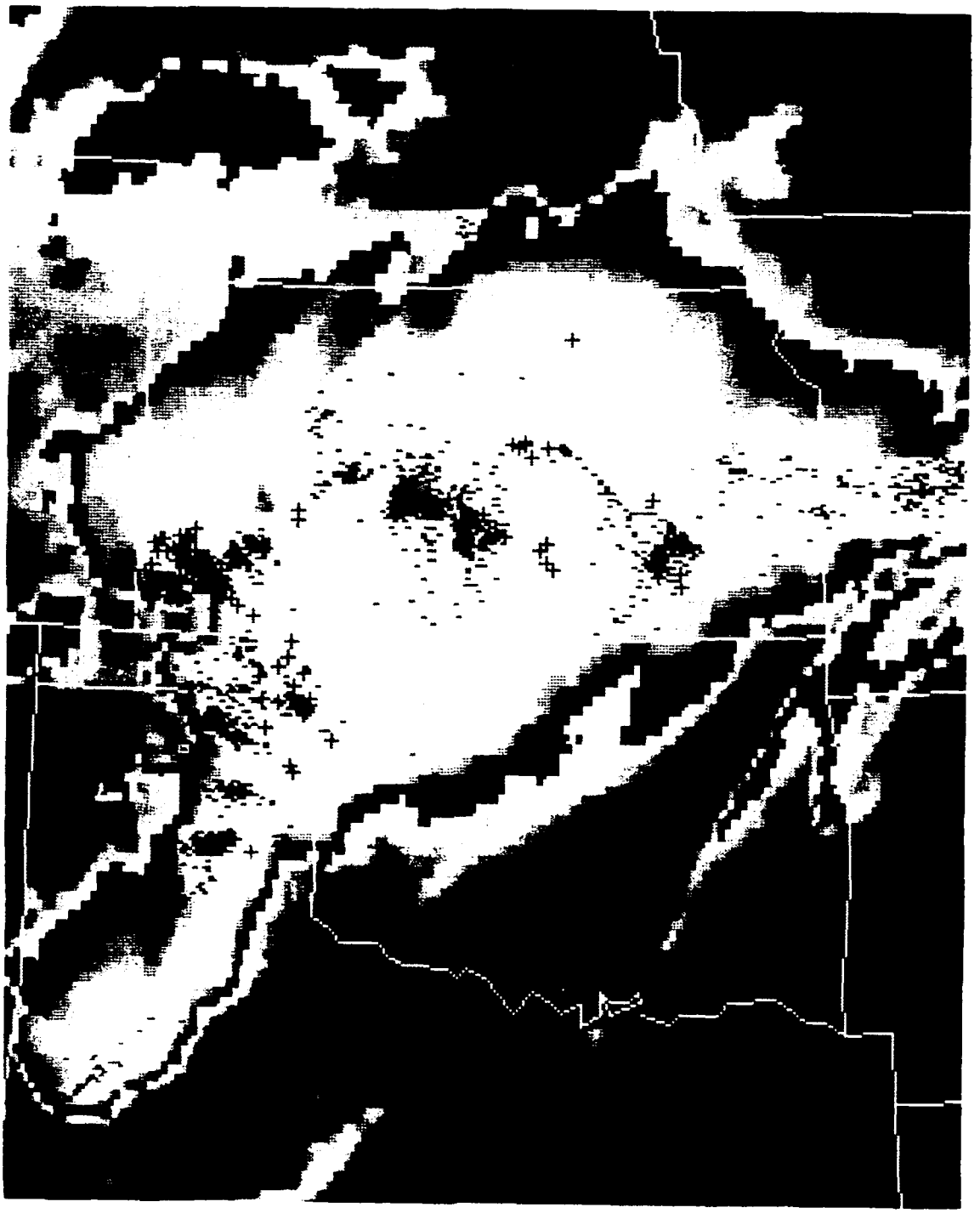

Figure 3.13. Continued.

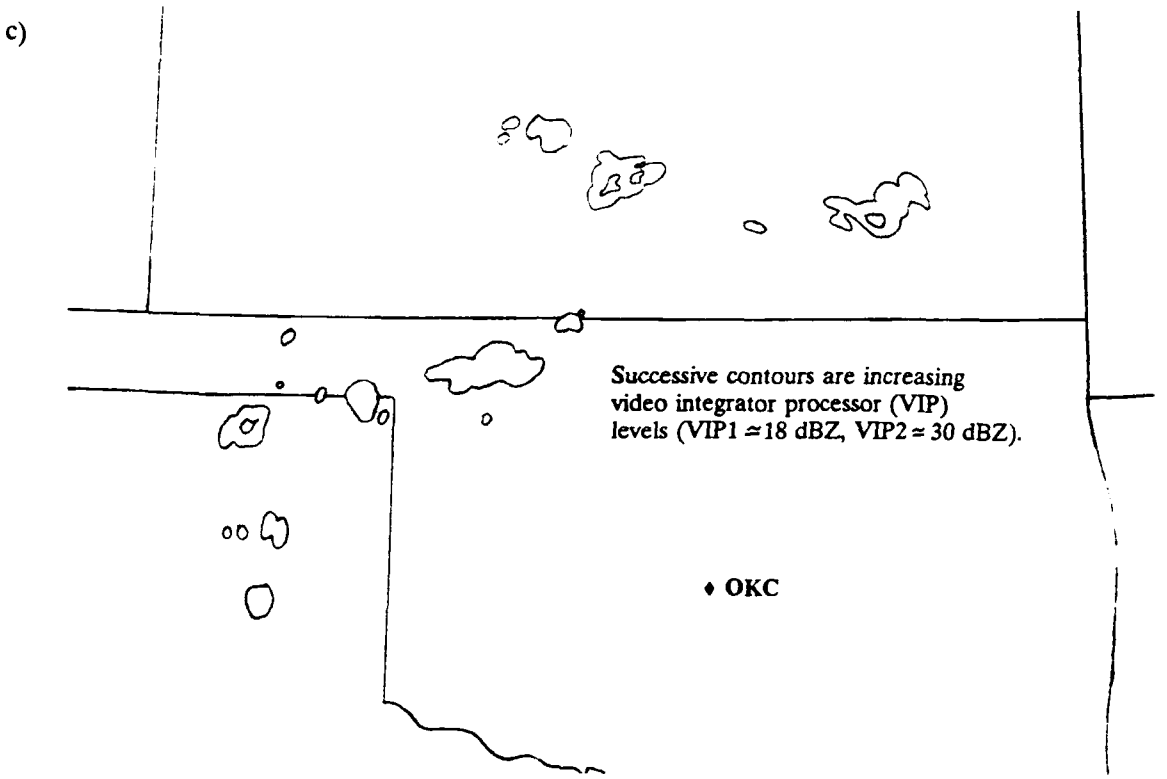

Figure 3.13. Continued.

For the MCSs in this study, lightning strike locations tended to cluster together in the earliest stages of lightning activity. Most clusters of lightning ground strike locations occurred in close proximity to the coldest cloud-tops indicated on satellite imagery through the early and mature stages of the MCSs (e.g., Figure 3.16). As an MCS began to decay, lightning strikes generally became less numerous and more diffuse, and there often was a tendency for a higher percentage of flashes to be positive (e.g., Figure 3.3c). This tendency for positive flashes in decaying thunderstorms was discussed in Section 3.1, and time series of typical examples of positive flashes dominating flash activity during the dissipating stage were shown there. Since satellite images are normally available to forecasters only every half

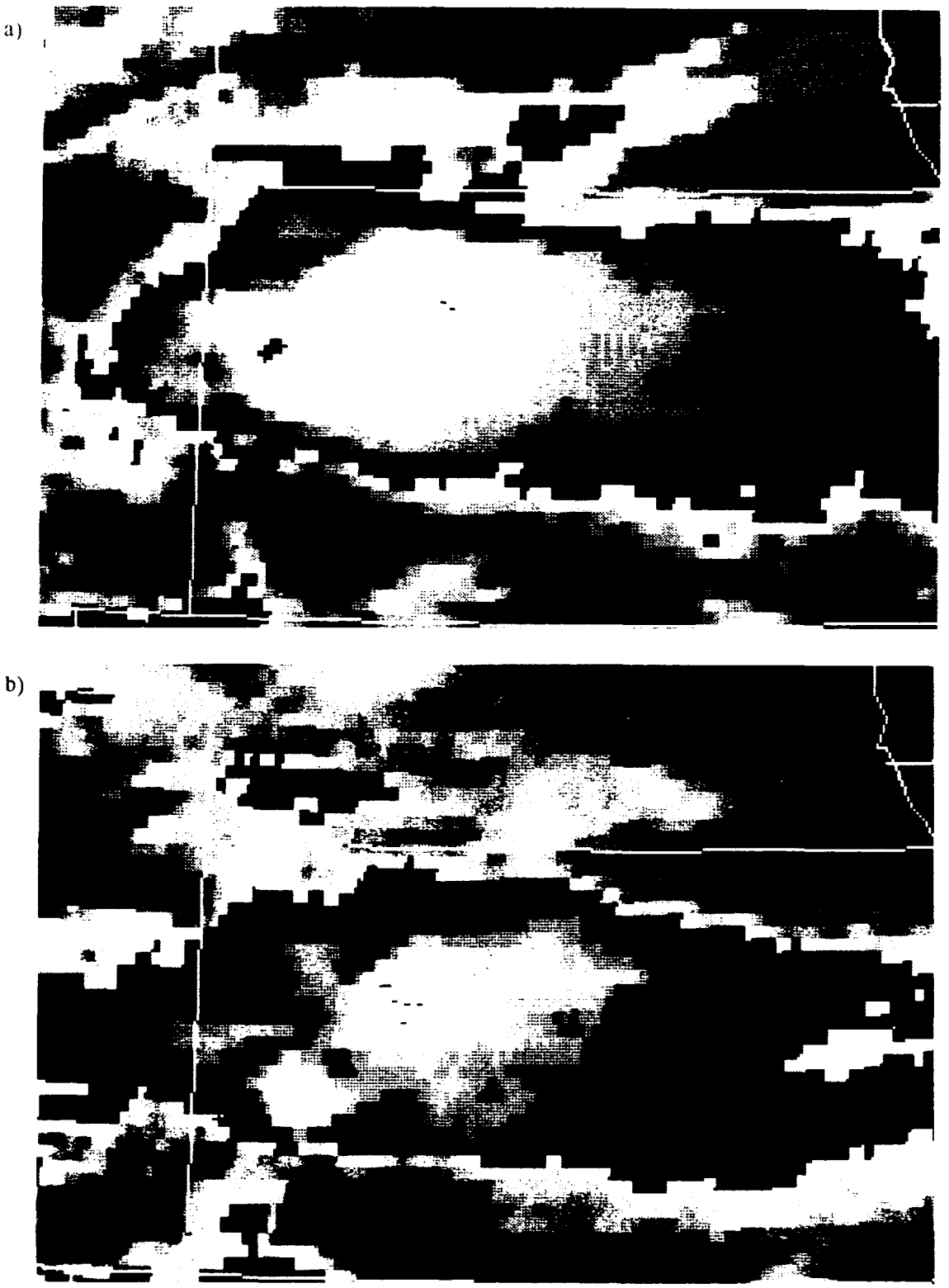

Figure 3.14. As in Figure 3.13b except for a) June 23 2200 CST and b) June 23 2300 CST.

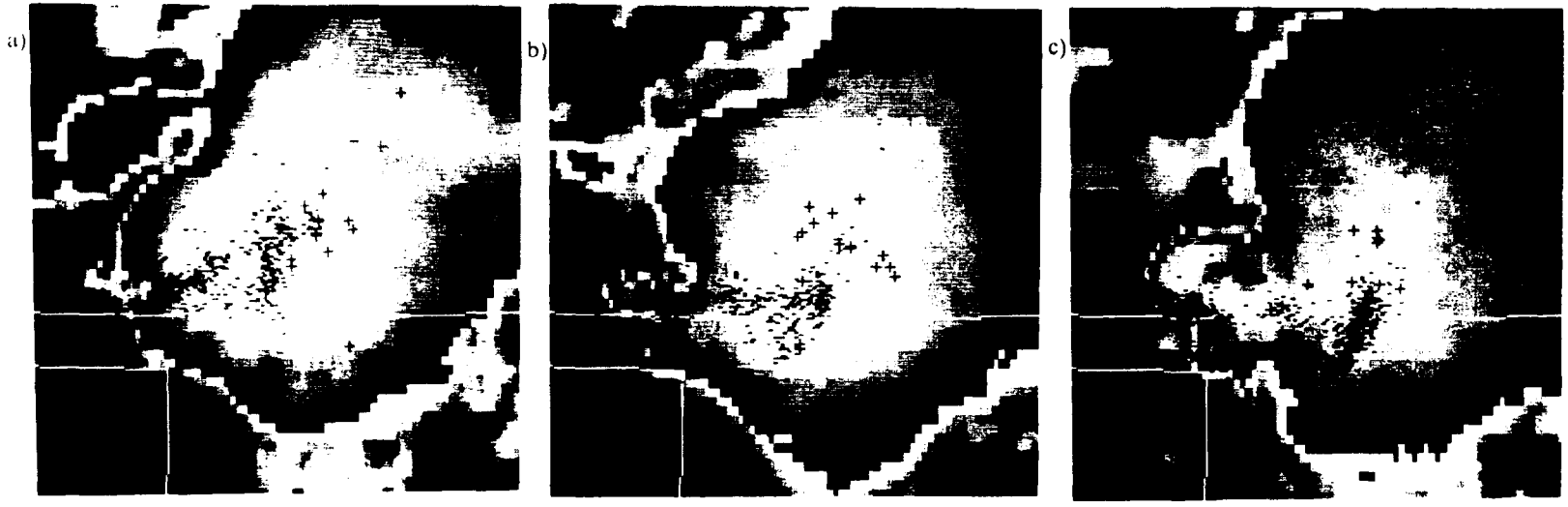

Figure 3.15 (above). As in Figure 3.13b except for a) August 13 2300 CST, b) August 14 0000 CST and c) August 14 0100 CST.

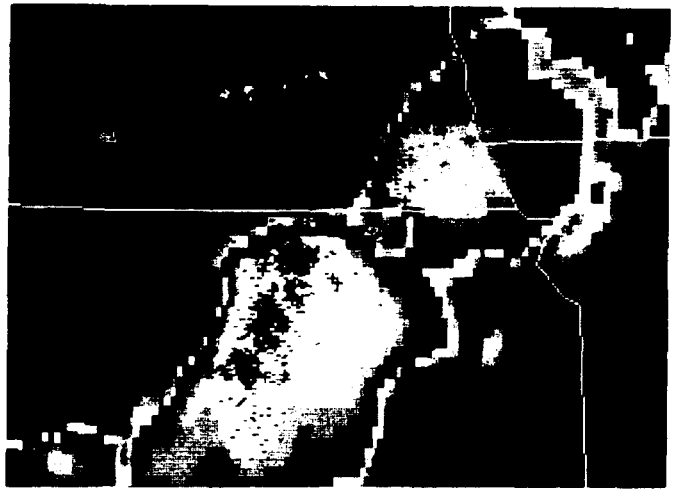

Figure 3.16. As in Figure 3.13b except for August 20 1800 CST.

hour, an increase in the ratio of positive flashes to total flashes in a mature system could often be used as an indicator that the MCSs was decaying and cloud tops soon would become warmer, as shown in Figure 3.17.

As discussed in the previous section, some MCSs had an unusually large number of positive flashes at the beginning of a storm's lifetime. These early positive flashes often dominated the flash activity in the early portion of the storm and tended to cluster near the coldest cloud-tops, like negative flashes (e.g., Figure 3.18). Normally the first strike of a storm is of negative polarity (Goodman et al., 1988), and this was true for all but two MCSs in this study. However, in nine MCSs more than 20% of the flashes that occurred during early stages of their lifetimes were positive. Further discussion of these two apparent modes of positive flashes, those that occur early in the lifetime of a system and those that occur late in the lifetime of a system, will be presented in Section 3.4.

Some of the MCSs in this study had a bipolar lightning ground strike pattern, in which regions of predominately negative flashes are spatially separated from regions of positive flashes. In some cases, the pattern was caused by two components of an MCS evolving through different stages at a given time; dissipating components of these MCSs were dominated by positive flashes, while regions of growing and mature convection usually were dominated by negative flashes. This type of system was usually oriented SW-NE, with the positive flashes occurring in the northeast (Figure 3.19a). In other cases the pattern existed within a single component of an MCS (Figure 3.19b). A simple check of the wind direction in these

a)

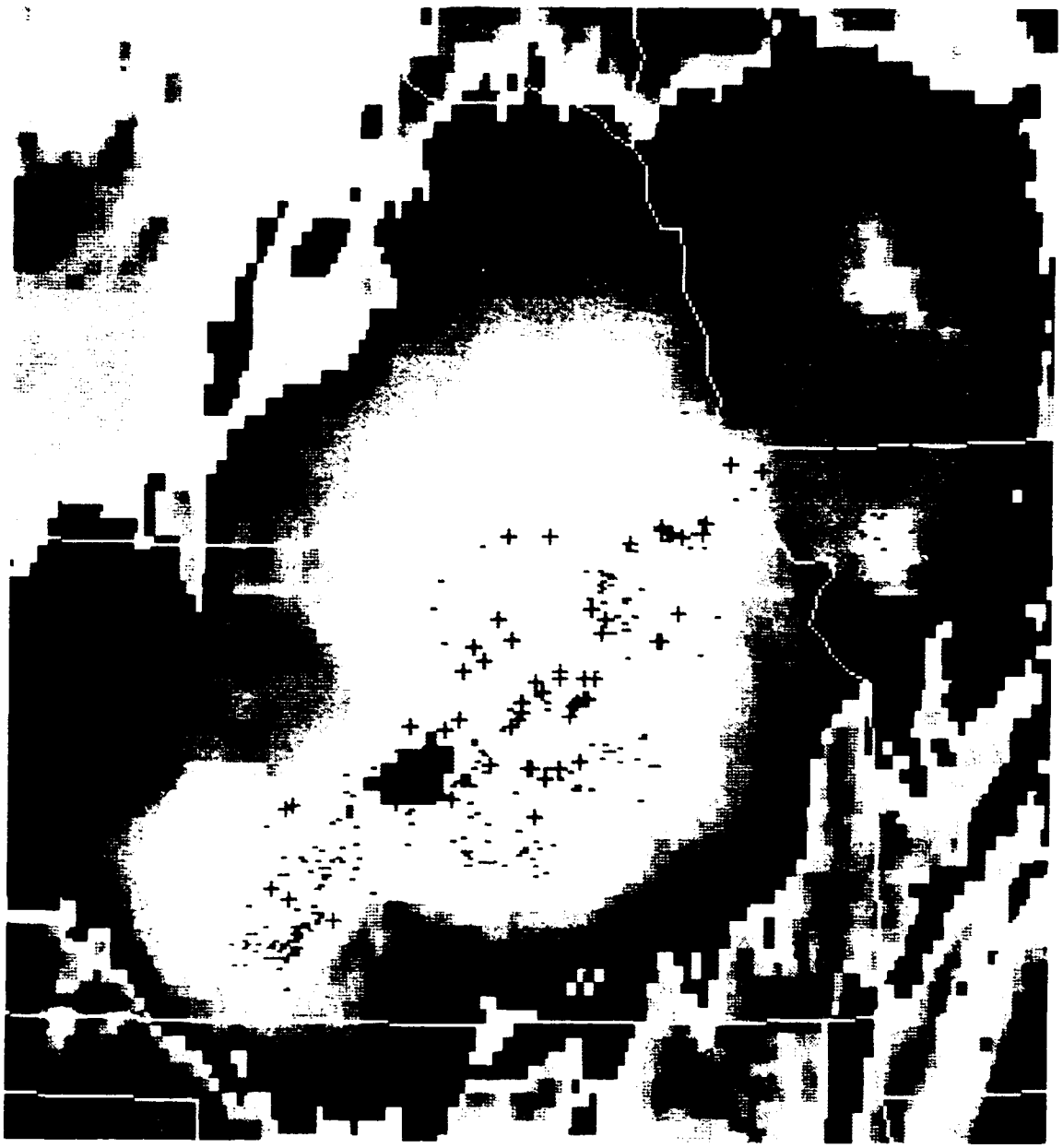

Figure 3.17. As in Figure 3.13b except for a) July 6 0200 CST, b) July 6 0300 CST and c) July 6 0400 CST.

b)

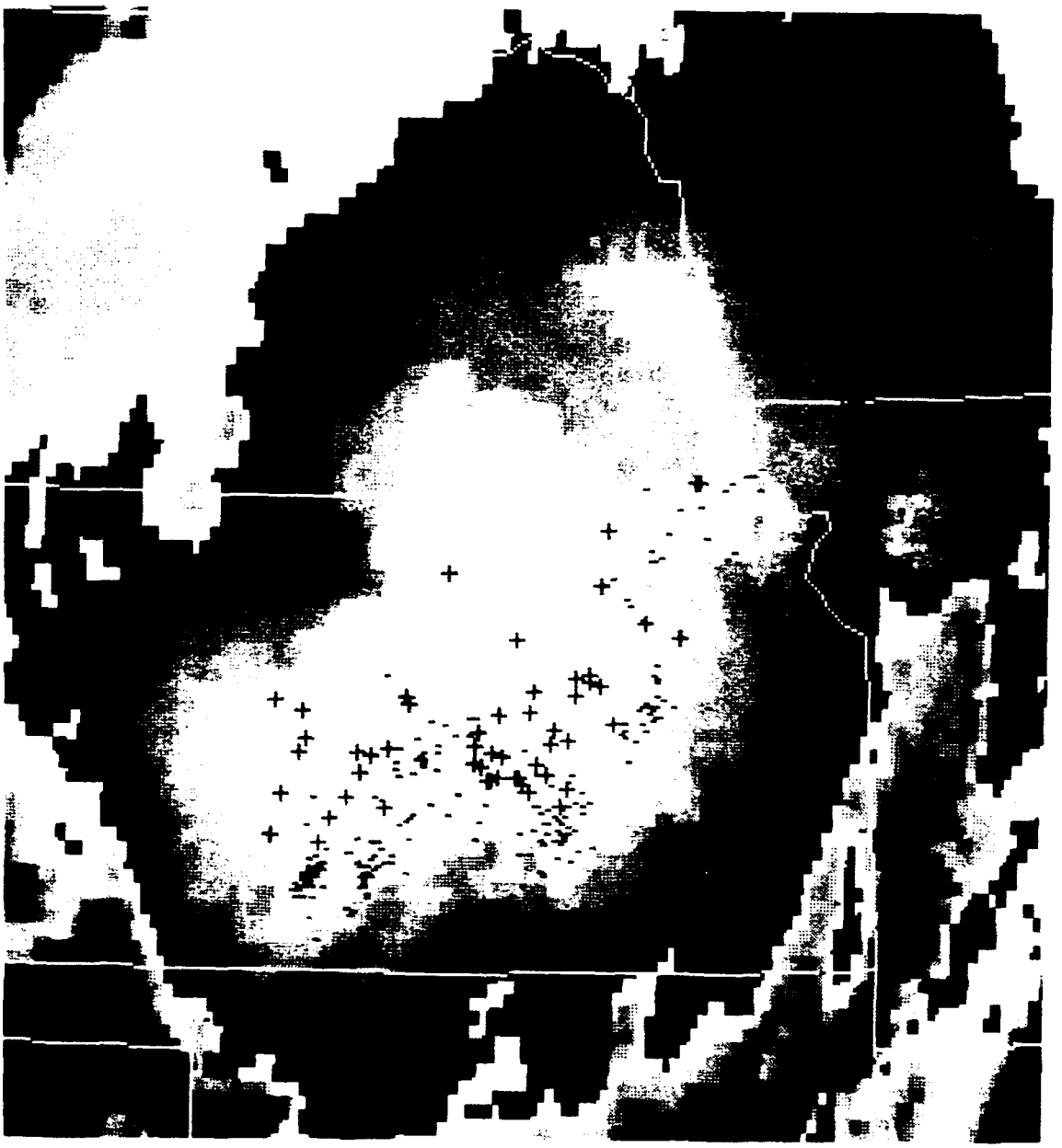

Figure 3.17. Continued.

c)

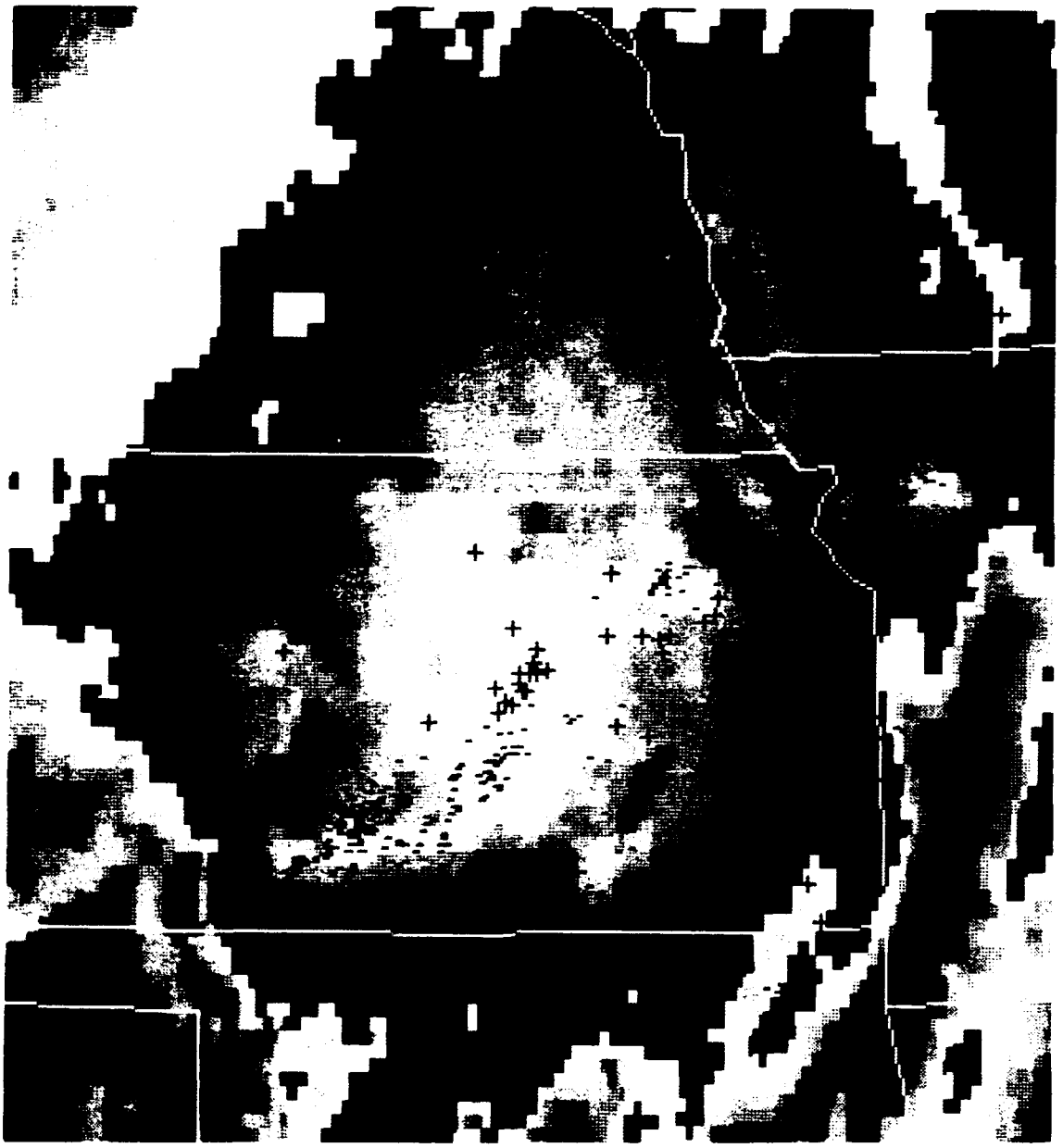

Figure 3.17. Continued.

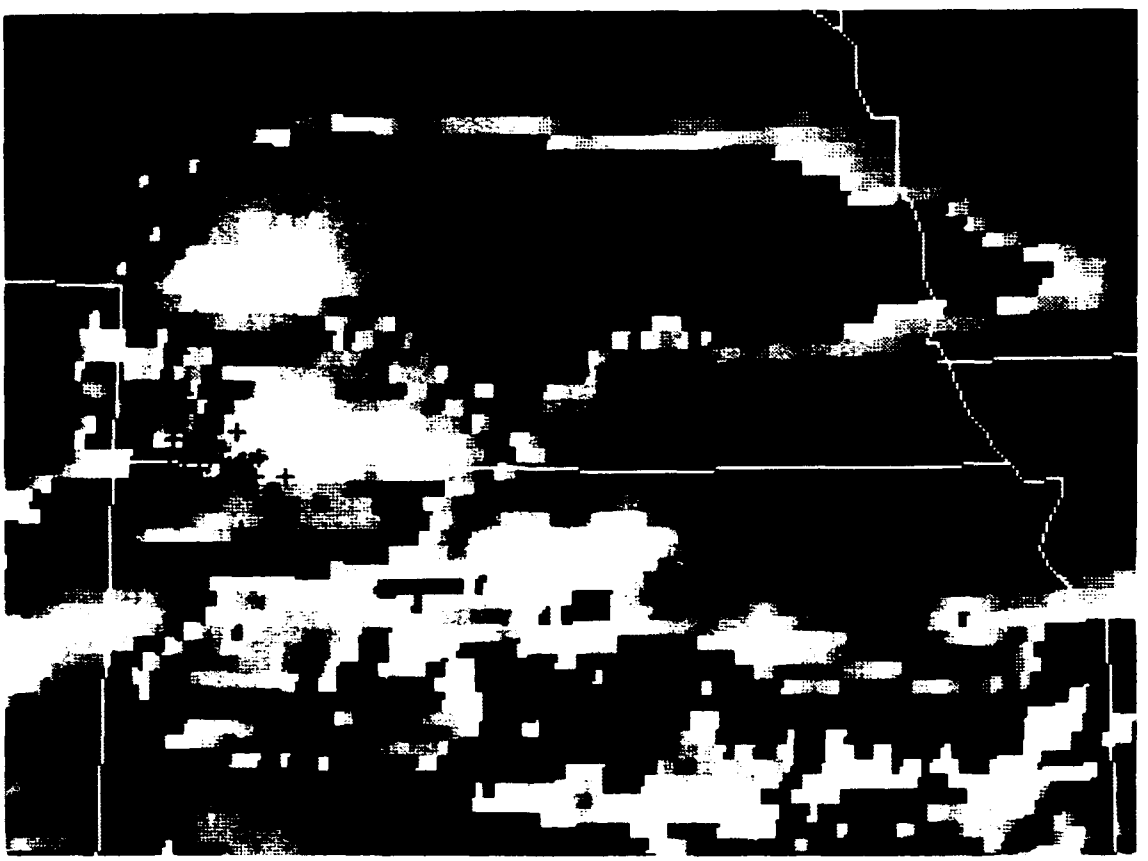

Figure 3.18. As in Figure 3.13b except for June 23 1700 CST.

cases revealed that the positive strikes were located downshear of the negative strike locations, and that the displacement from the negative strikes was oriented along the upper level geostrophic winds, in agreement with the observations of Engholm et al. (1990) and Stolzenburg (1990).

This second type of bipole pattern is consistent with the tilted storm dipole hypothesis (Brook et al., 1982; Rust et al., 1985; Orville et al., 1988). Rutledge and MacGorman (1988) and Stolzenburg (1990) hypothesized that the positive flashes were caused by positive charge that was advected by upper level winds from a source region above the main convective area into shallower stratiform clouds. Engholm et al. (1990) favored the idea that the charge causing lightning in the stratiform region was generated locally by differential particle motions. The idea of local charge generation in the stratiform region had been suggested by Orville et al. (1988) and Rutledge and MacGorman (1988) and was modelled crudely by Rutledge et al. (1990).

Another common pattern was for lightning activity to be concentrated at the southwest or southern end of a cloud shield oriented SW-NE or S-N, while the anvil to the northeast or north was relatively free of electrical activity (e.g., Figure 3.20). In these cases, the concentrated lightning activity was from new convection along the southwestern or southern flank of the MCS. This type of pattern may be related to the asymmetric pattern of a leading convective line with trailing stratiform precipitation discussed by Houze et al. (1990). The classifications in their study were based on radar reflectivities, and the asymmetric case had a convective line that was

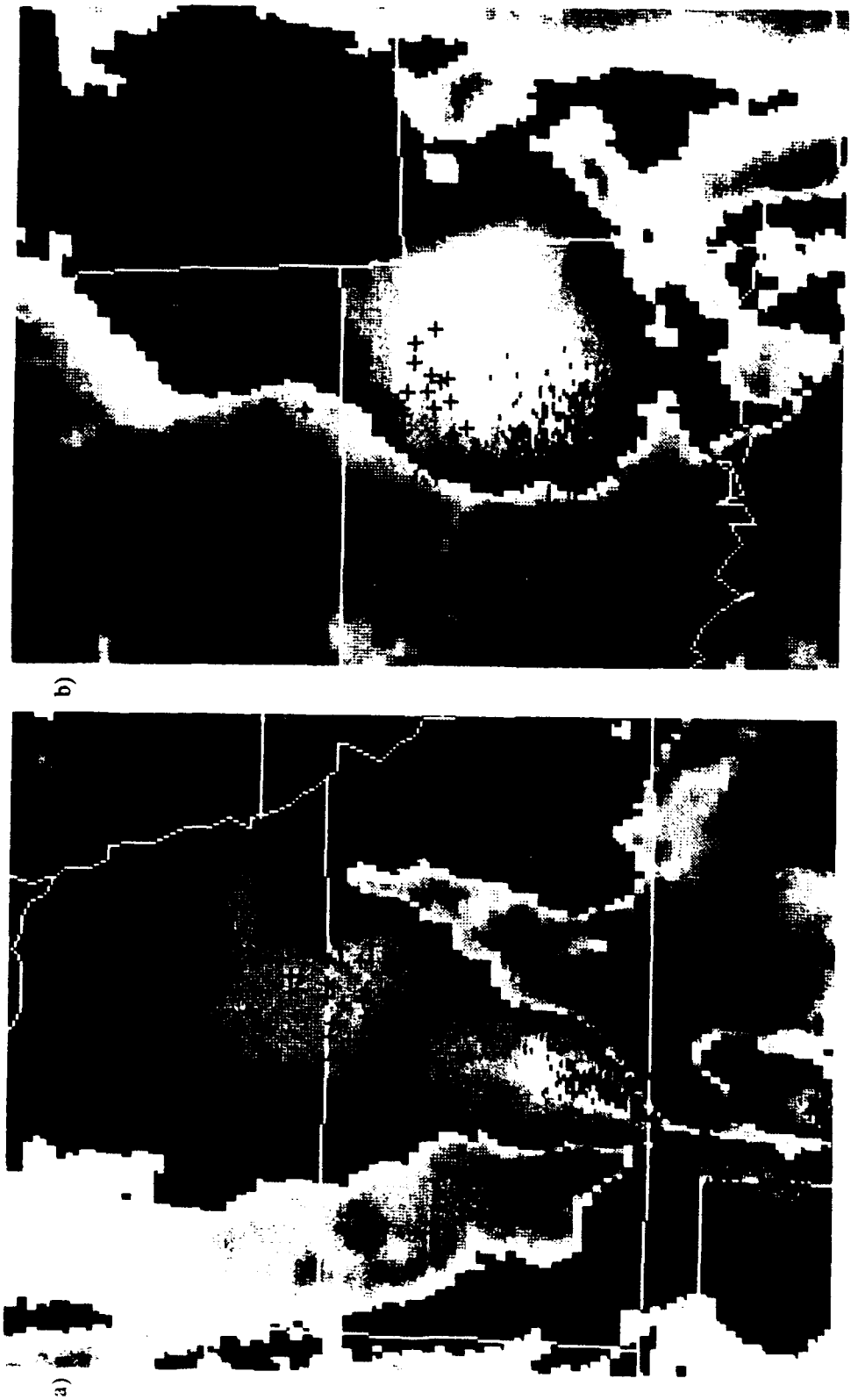

Figure 3.19. As in Figure 3.13b except for a) April 27 0300 CST and b) April 1 0300 CST with an hour period of CG strikes.

Figure 3.20. As in Figure 3.13b except for June 20 0400 CST.

strongest on the south, southwest or western end of the MCS.

Tables 1 and 2 of the previous section showed the variability of many features of the MCSs in this study. They cannot show, however, the variability of the evolution of each MCS that was found by examining hourly infrared satellite images. As stated in the methodology section of Chapter 2, the primary constraints on choosing MCS for this study concerned the duration and size of the system. There were no constraints on the complexity of the systems, unlike the study by McAnelly and Cotton (1989), which was limited to MCCs that had a single growth/decay cycle in the cloud shield. The MCSs of this study often had more than one region of frequent lightning flashes, and merging and splitting of the cloud shield and lightning regions sometimes occurred. The storms we examined ranged from relatively small to large, from unorganized to well-organized and from relatively simple to extremely complex.

One of the early goals of this project was to use satellite imagery and lightning ground strike data to classify the MCSs according to similarities in their growth and development much like MCSs that were classified using radar reflectivities, as discussed in section 1.2. However, temporal and spatial patterns in the lightning and satellite data varied considerably from one MCS to another. Variability of the internal substructure and evolution of MCCs and MCSs was also stressed in McAnelly and Cotton (1989). To categorize the MCSs in our study, it appeared necessary either to have a relatively large number of categories (20 categories for 25 MCSs) or to categorize patterns of evolution separately for different periods of

MCSs. Therefore, we did not categorize all of the MCSs of the study into a small set of classes, as we had first intended. Several systems often did appear similar for some stage of their evolution, but evolved to and from that stage differently. There was not enough time for this project to try to find a small number of categories for each stage of evolution, but it might be useful to try this in the future.

3.3 Flash Rates Compared to Satellite Data

In order to see how the temporal evolution of positive and negative flash rates compared with the temporal evolution of minimum satellite cloud-top temperatures, the number of positive and negative flashes per half hour were plotted with the hourly minimum satellite cloud-top temperature for each MCS. Data on minimum temperatures were available only at 2°C intervals from -52°C to -80°C during the time when the area of the -52°C cloud shield of the MCS was at least 5000 km^2. For example, a minimum temperature of -70°C could actually have been any temperature from -70°C to just under -72°C, and a minimum temperature of -80°C could have been any temperature equal to or colder than -80°C.

The number of negative flashes generally peaked near the same time as the minimum temperature (for example, see Figure 3.21). Figure 3.22a compares the difference in the time of the maximum number of negative flashes and the time of the maximum area of the coldest cloud-tops. (The area could be more than just a few image pixels because minimum temperature was examined only in 2°C increments.) Although there were cases when the negative flashes peaked up to 6

h before or 5 h after the maximum area of the coldest cloud-tops, 56% of the time the peak in the negative flashes was within an hour, and 76% of the time within two hours, of the time of the maximum area of the coldest cloud-tops. Similarly, Goodman and MacGorman (1986) observed that total ground flash rates, which are nearly the same as negative flash rates in most MCSs, peaked at approximately the same time as the minimum cloud-top temperature.

The relationship with positive flashes was different. In all but one of the MCSs, the maximum number of positive flashes occurred between 7.5 h before and 2.5 h after the maximum area of the coldest cloud-tops (Figure 3.22b). The times of the maximum number of positive flashes did not cluster about the times of the

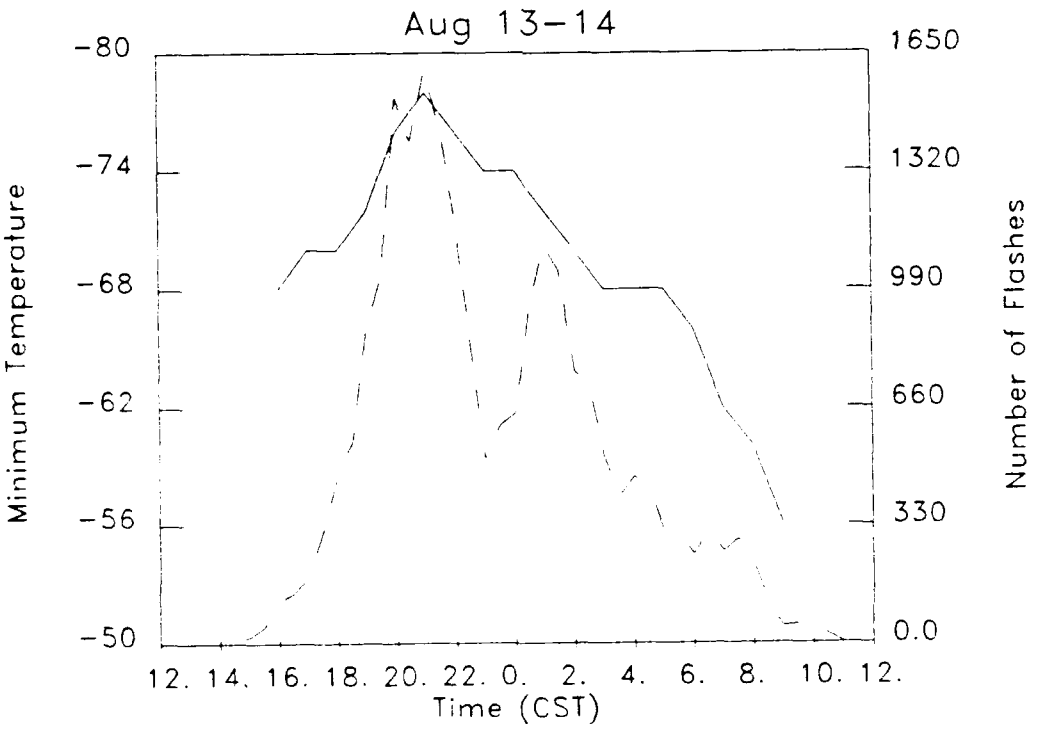

Figure 3.21. Time series of the minimum satellite cloud shield temperature in 2° increments (solid line) and the number of negative flashes (dashed line).

maximum area of the coldest tops as they did for negative flashes.

Time series of the area within as many as 15 temperature intervals were plotted for each MCS and compared to time series plots of positive and negative flashes. Often this type of comparison was confusing or misleading. This was especially true for MCSs with several small components that grew and decayed with different lifecycles or for systems whose cloud shields merged in such a way that the areas within the temperature contours masked much of the evolution of one of the systems. The comparisons that will be shown are for organized MCSs with cloud shields not significantly contaminated by other nearby systems.

Time series of negative flashes agreed best with the time series of the area within -60°C to -70°C temperature contours. The times of initial large increases and final large decreases in areas for these temperatures were similar to those for initial increases and final decreases in the number of flashes (e.g., Figure 3.23a). Figure 3.23b shows a small secondary peak in the number of negative flashes that corresponds with a secondary peak in the area within -68°C. The number of flashes usually peaked either close to the same time or earlier than the maximum area within these -60°C to -70°C contours, usually near the time of the maximum area of the coldest tops (Figure 3.23c). That negative flashes often peaked before the -60°C to -70°C areas is consistent with results shown in Figure 3.22a: negative flashes often peaked near the time of the coldest tops, which usually occurred earlier in the MCS lifetime than the maximum area within contours of somewhat warmer temperatures.

The temperature contour whose time series plot agreed best with the

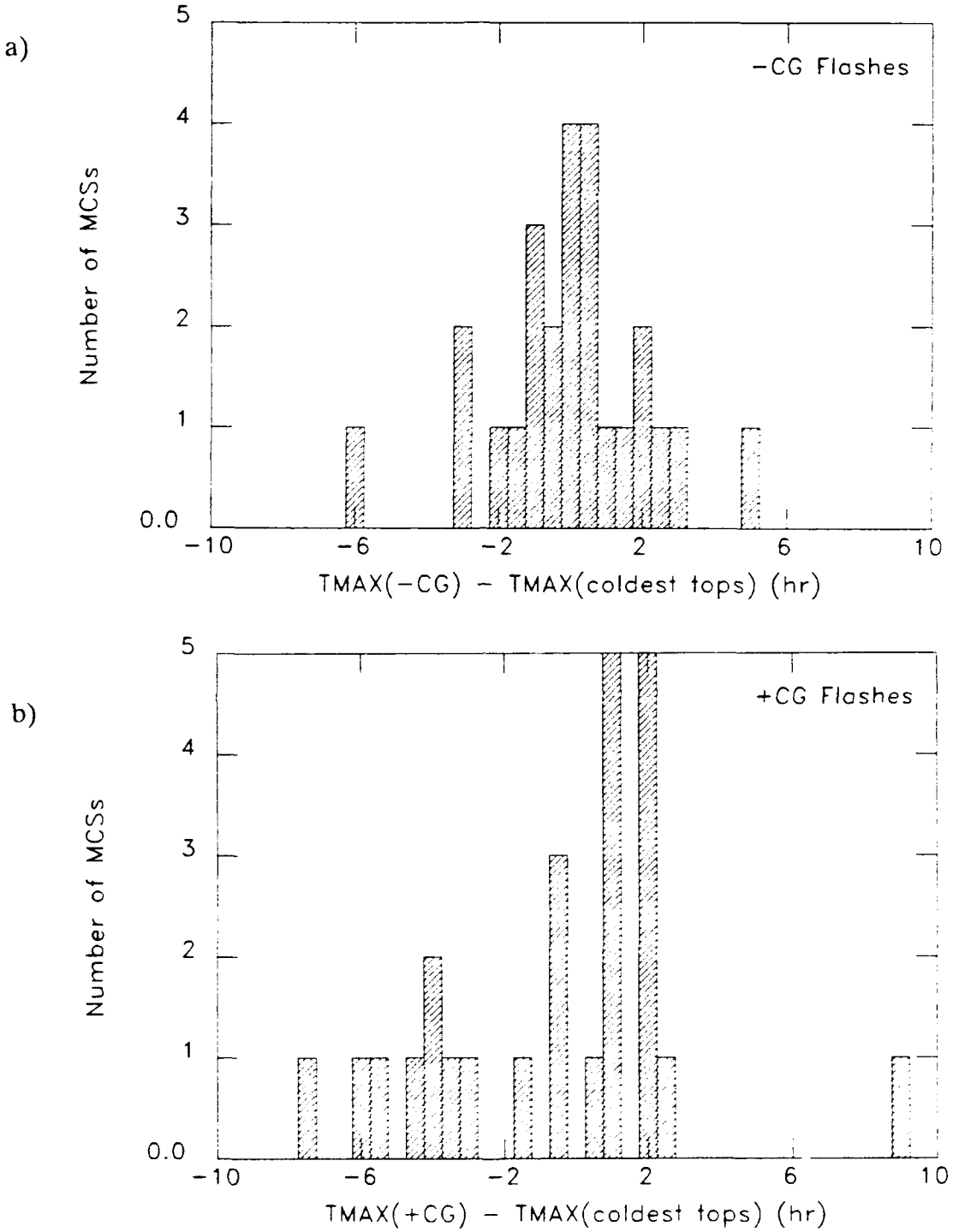

Figure 3.22. A comparison of the difference in time between the maximum area of the coldest cloud-tops and a) the maximum number of negative flashes per half hour or b) the maximum number of positive flashes per half hour. Negative values indicate that the flashes peaked prior to the maximum area of the coldest cloud-tops, positive values indicate that the flashes peaked after the maximum area of the coldest cloud-tops and a value of zero indicates that they occurred at the same time.

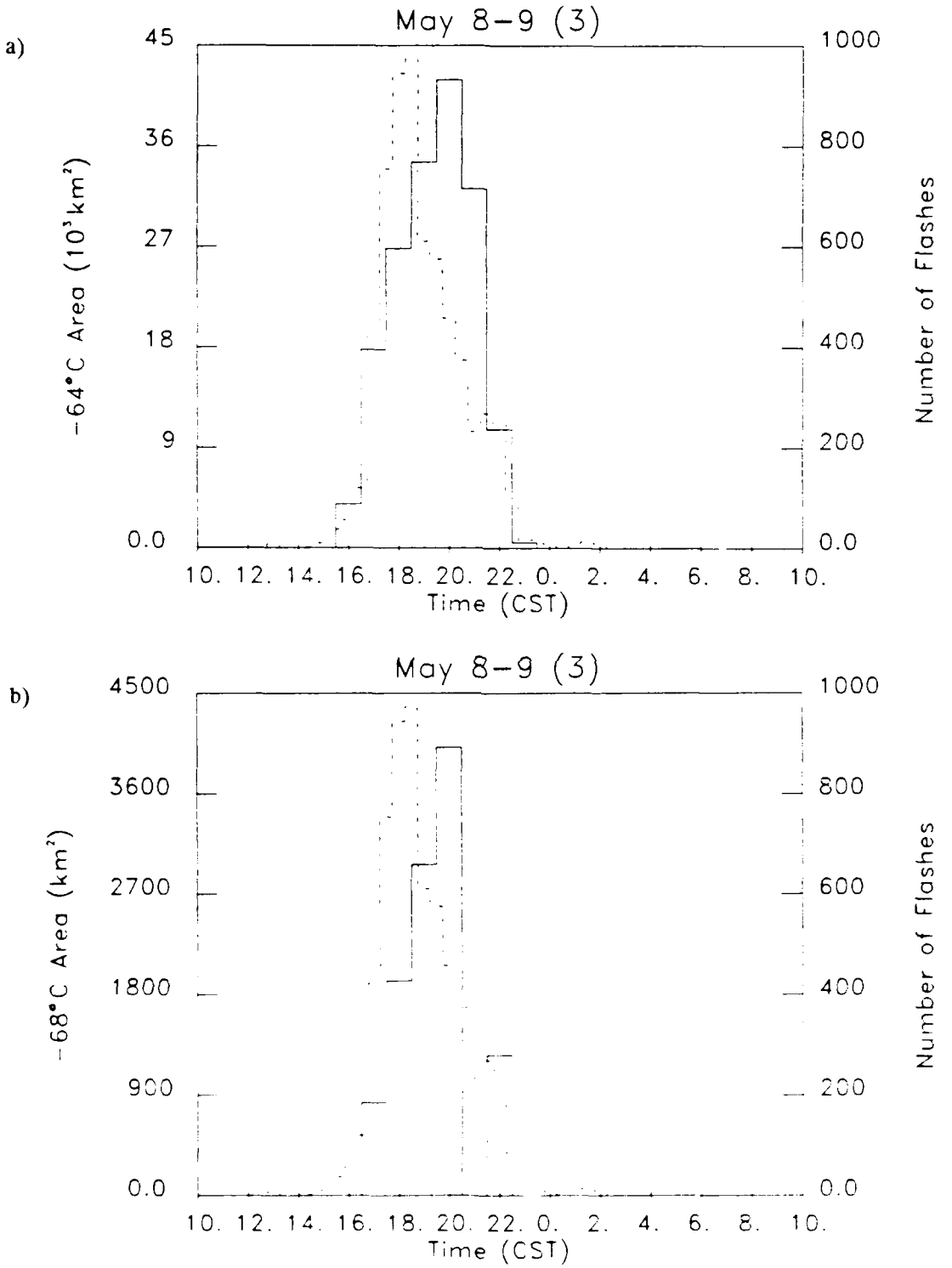

Figure 3.23. Comparison of the time series of the number of negative flashes (dashed line) with a) the area within the -64°C contour (solid line), b) the area within the -68°C contour (solid line), and c) the area within the -72°C contour (solid line).

c)

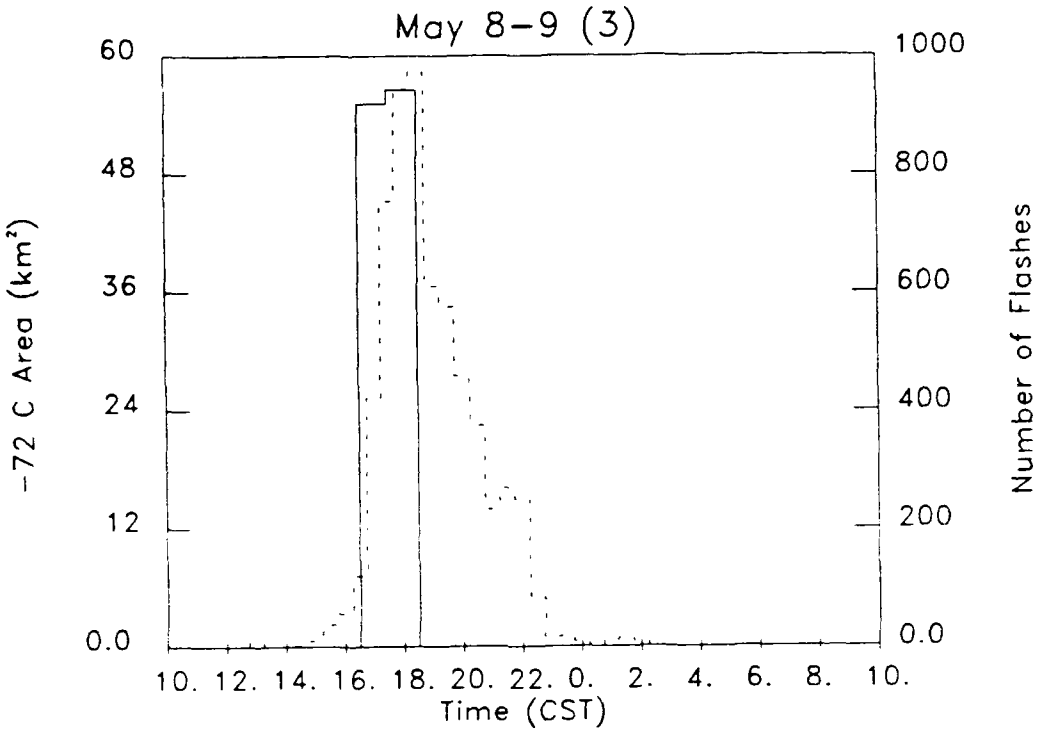

Figure 3.23. Continued.

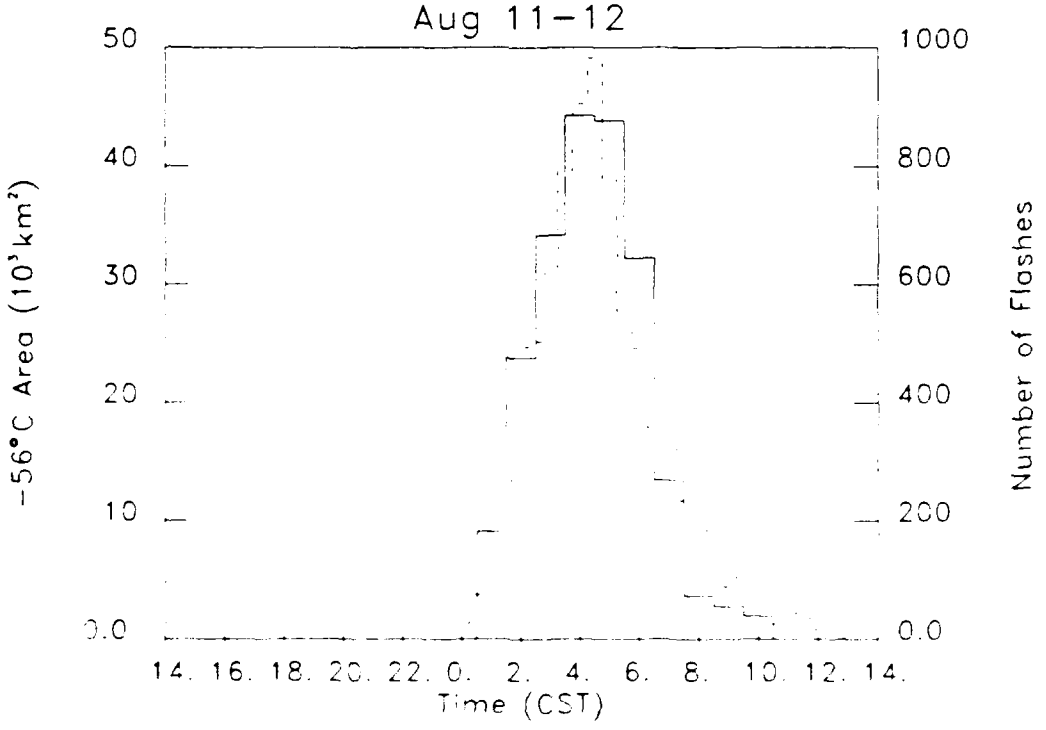

Figure 3.24. As in Figure 3.23 except the area is within the -56°C contour.

evolution of the number of negative flashes was dependent in part upon the minimum cloud-top temperature reached during the lifetime of the MCS, which in turn was dependent upon the temperature of the tropopause. (The minimum cloud-top temperature reached by an MCS was an average of 6°C less than the temperature of the tropopause). An example of this dependence is shown by the MCS on August 11-12, whose coldest cloud-top temperature was only -66°C, compared with the median coldest temperature of -72°C for all other cases. In this case, the number of negative flashes agreed best with the area within the -56°C contour, a much warmer temperature than usual (Figure 3.24). The peak in negative flash rates does not lead the area within the -56°C contour in this MCS because the maximum area of the coldest cloud tops occurs at the same time as the maximum area within the -56°C contour.

For positive flashes, the relationship with areas within temperature contours appeared to have two modes. If the maximum number of positive flashes occurred early in the system's lifetime, the peak in positive flashes agreed best with a peak in the area within the coldest cloud-tops (e.g., Figure 3.25) (This correspondence was not always with the maximum area of the coldest cloud-top temperature; recall that when positive flashes occurred early, they generally peaked earlier than the maximum area of the coldest cloud-tops). If the maximum number of positive flashes occurred late in the system's lifetime, the peak in positive flashes agreed best with the area within warmer cloud-tops, around -52°C (e.g., Figure 3.26). As for negative flashes, the temperature contour which agreed best with positive flash rates

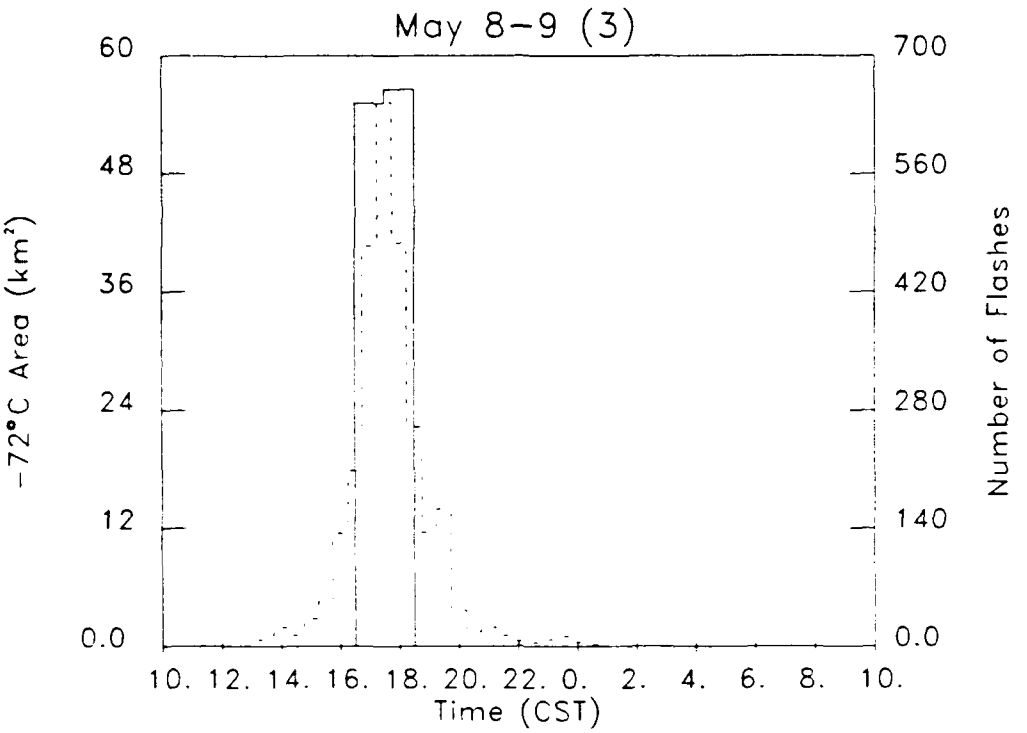

Figure 3.25. Comparison of the time series of the number of positive flashes (dashed line) with the area within the -72°C contour (solid line).

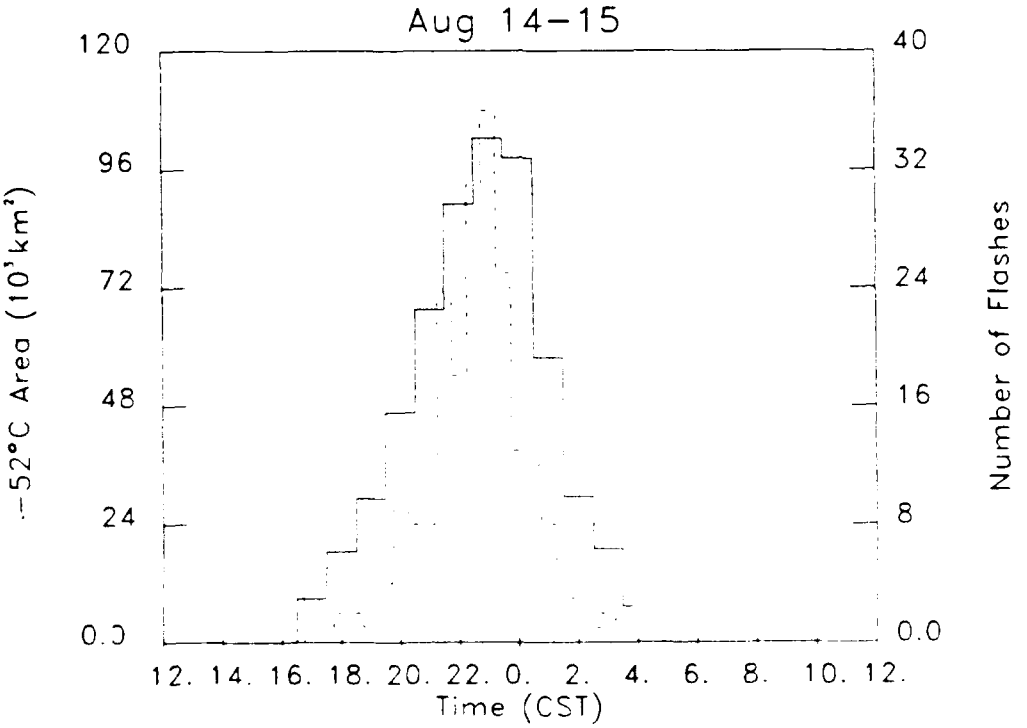

Figure 3.26. As in Figure 3.25 except the area is within the -52°C contour.

was dependent upon the minimum cloud-top temperature reached by the MCS.

Relationships between lightning rates and the areas within various satellite cloud shield temperature contours might be expected, since the area within the contours can be related to the growth of the system. Recall that strong electrification usually is not observed in storms until they grow vigorously above a height of 8 km MSL in summer, corresponding to a temperature of about -20°C (e.g., Krehbiel, 1986). Various references supporting dramatic increases in lightning rates with increasing cloud depth are listed by Engholm et al. (1990).

3.4 Positive Lightning Modes

In the previous three sections, there has been evidence that the number of positive flashes evolve in two modes. The first we call the *convective* mode, because the number of positive flashes tended to peak early in the lifetime of an MCS, when radar indicated that positive flashes were usually in a relatively dense cluster near reflectivity cores corresponding to thunderstorm cells (Figure 3.27). We saw in previous sections that the ratio of positive flashes to total flashes was larger in the early, growing stage of the MCSs in the convective mode. Therefore, to identify this mode from parameters that were readily available from our analysis, we tentatively identified the convective mode with periods early in an MCS when at least 20% of the flashes were positive. In most cases, this period agreed well with the period when positive flashes occurred in dense clusters. In one case, however, this fraction was low, due to large numbers of negative flashes in other regions of the same MCS.

a)

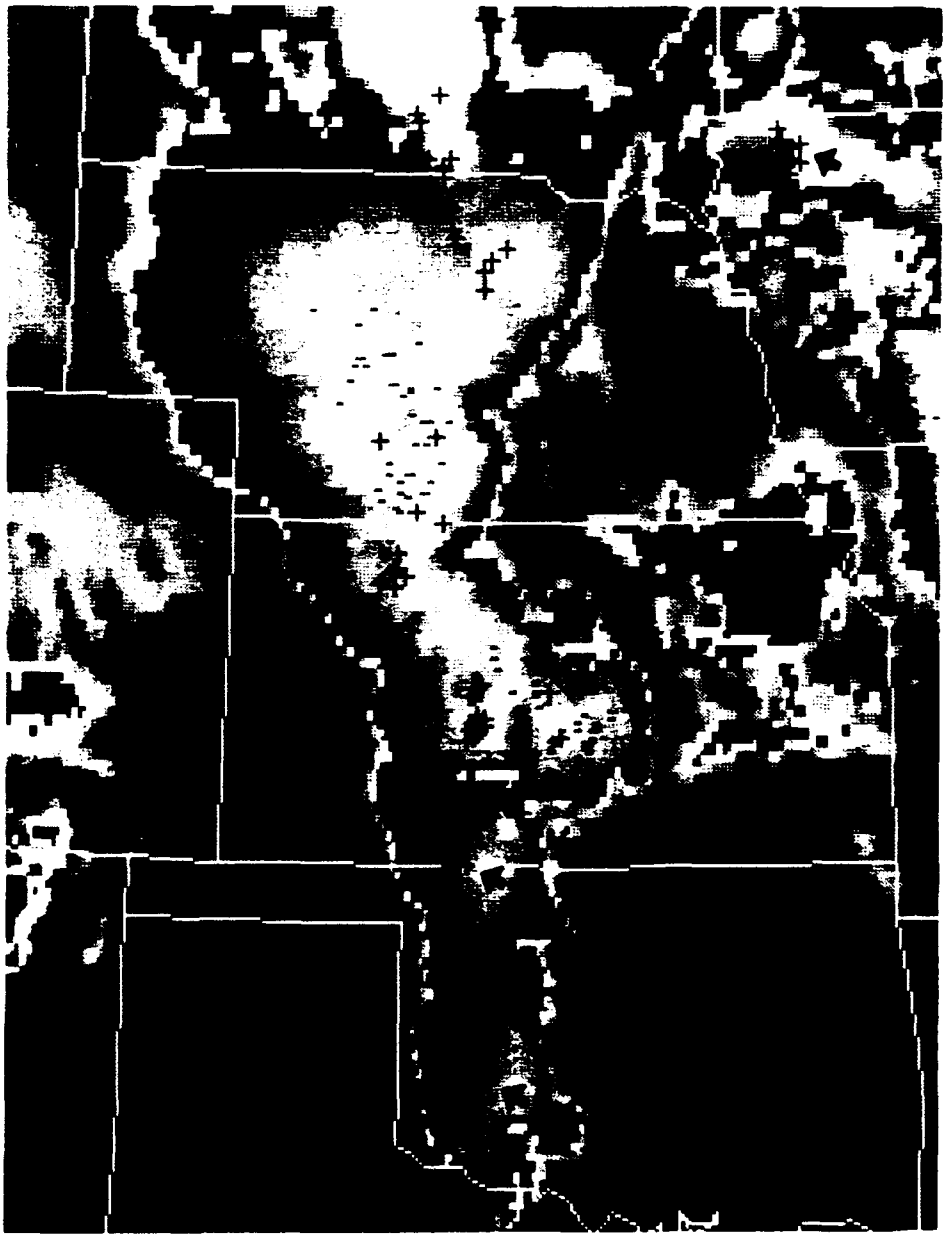

Figure 3.27. a) As in Figure 3.13b except the data are from May 8 1500 CST. Clusters of lightning strikes indicated by the arrows have between 13 and 31 positive flashes and no more than one negative flash. b) Radar reflectivity from Oklahoma City radar at .5° elevation for the same time.

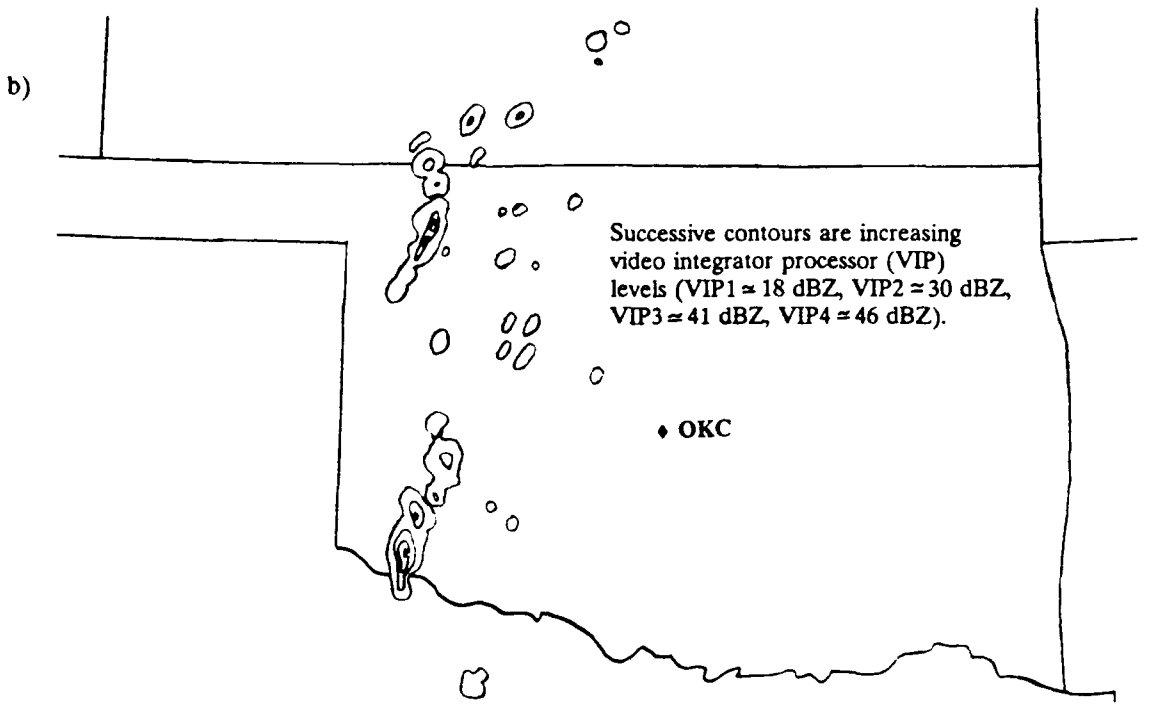

Figure 3.27. Continued.

For this case, a high density and number of positive flashes was used to define the period of the convective mode.

The convective mode of positive flashes occurred in nine (36%) of the MCSs included in this study (see Table 3). Most of these MCSs were in April, May and June. Stolzenburg (personal communication, 1991) found that this mode tended to occur also at slightly higher latitudes in June and July. A similar northern migration has been found to occur in severe thunderstorm activity, which tends to move northward with the jet stream and advancing warm moist air during the spring and summer (Davies-Jones, 1986). As discussed previously, comparisons with the minimum cloud-top temperatures show that the largest ratio of positive to total flashes occurred when the area of the MCS was growing and the cloud-top

TABLE 3 Positive Lightning Characteristics for the Convective Mode

Date (1986)	Max fraction in convective mode	Duration* (hrs)	Max fraction in stratiform/ dissipating mode	Avg # of positives/0.5 h in conv mode	Avg # of positives/0.5 h for lifetime
31 Mar-1 Apr	.64	6.5	.33	47	28
8-9 May (1)	1.00	8.0	.38	65	36
8-9 May (3)	1.00	6.5	.67	192	95
13-14 Jun	.69	3.0	-	22	19
19-20 Jun	.56	1.5	-	14	4
21-22 Jun	.44	.5	-	35	12
23 Jun**	1.00	7.5	-	102	102
30 Jun-1 Jul***	(.10)	2.0	-	139	40
13-14 Aug	.53	1.0	-	50	20

* The duration is defined as the number of hours that the fraction of flashes that were positive was at least 0.2 except for the MCS on 30 Jun-1 Jul.
** The entire lifetime of the MCS on 23 Jun had convective mode characteristics.
*** The fraction of positive flashes in the MCS on 30 Jun-1 Jul was low because the convective mode occurred in a small portion of the MCS while extremely large numbers of negative flashes occurred in other portions.

temperature was decreasing (see, for example, Figure 3.28a). The peak in positive flash counts often occurred at about the time of a peak in the area of coldest cloud-tops.

The average duration of the convective mode was 4 h. In this mode, positive flash counts peaked an average of 3.5 h after the first lightning strike and tended to peak prior to negative flash counts. Figure 3.29a presents the difference in the times of the maximum negative and positive flash rates for the nine MCSs that exhibited the convective mode. The number of positive flashes per half hour peaked from 7.5 h to 0.0 h before the number of negative flashes, averaging 3.5 h before negative flashes. The maximum ratio of positive to total flashes ranged from 0.4 to 1.0

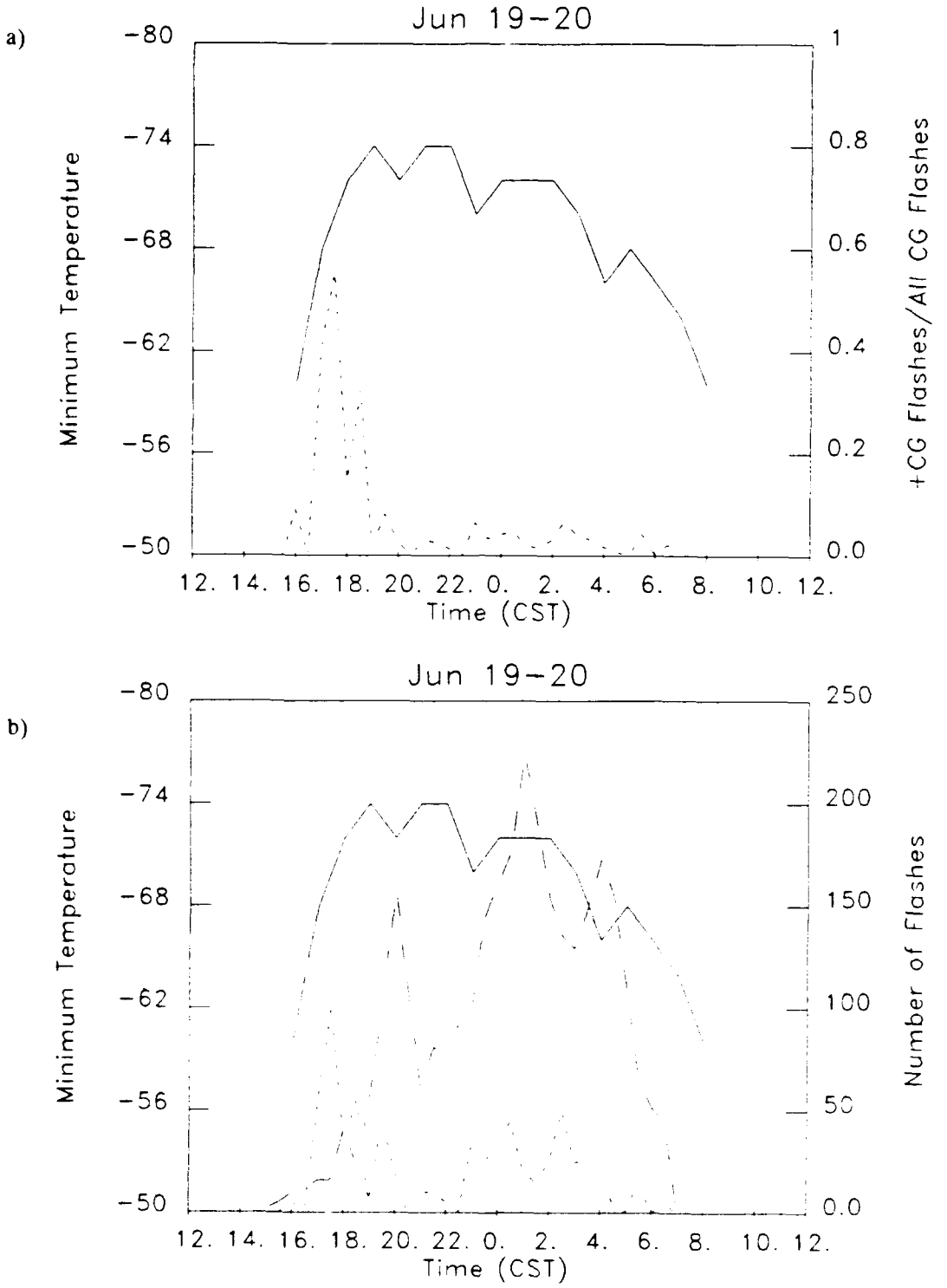

Figure 3.28. Time series of the minimum satellite cloud shield temperature at 2°C increments (solid line) with a) the ratio of positive to total flashes (short dashed line) and b) the number of negative flashes (long dashed line) and the number of positive flashes multiplied by a factor of five (short dashed line).

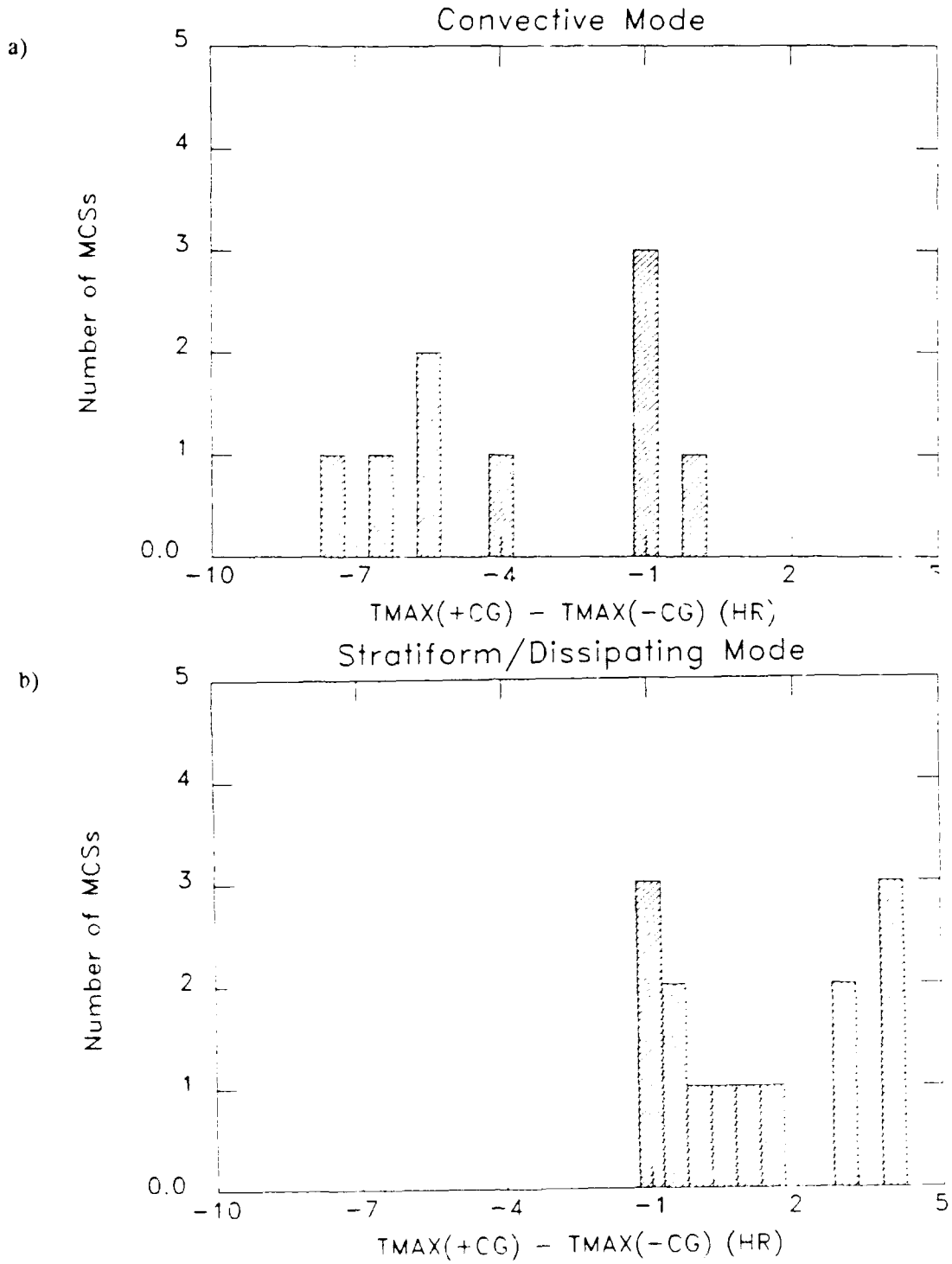

Figure 3.29. A comparison of the differences in time between the maximum number of positive flashes and the maximum number of negative flashes for a) the convective mode of positive flashes and b) the stratiform/dissipating mode of positive flashes. Negative values indicate that the positive flashes peaked prior to the negative flashes, positive values indicate that the positive flashes peaked after the negative flashes and a value of zero indicates that they occurred at the same time.

(excluding data for 30 Jun-1 Jul; see note with table). The average number of positive flashes was relatively high throughout the period of the convective mode (e.g., Figure 3.28b). In all cases, the average number of positive flashes per half hour during the convective mode met or exceeded the average for the lifetime of the MCS. The previously studied characteristics of the thunderstorms discussed in section 1.2, which had positive flashes early in their lifetimes, appear to have characteristics similar to those of the MCSs in this study that exhibit the convective mode.

We called the second mode the *stratiform/dissipating* mode, because positive flashes tended to occur late in a system's lifetime, when radar indicated that positive strikes usually were located either in stratiform precipitation or in dissipating convective cells (Compare Figure 3.3c with Figure 3.30). In the MCSs that were beyond the range of the Oklahoma City radar data used in this study, it was not known whether positive flashes occurred within stratiform regions or within dissipating convective cells. However, the appearance of plots of positive flashes appear similar in the two cases, so we do not consider the stratiform and dissipating cases separately.

We found in previous sections that positive flashes in this mode have a low density (Figure 3.3c), and the maximum in the ratio of positive flashes to total flashes occurred at the end of the system's lifetime. The stratiform/dissipating mode occurred in 17 (68%) of the MCSs in this study (see Table 4). These 17 cases occurred throughout the entire warm season.

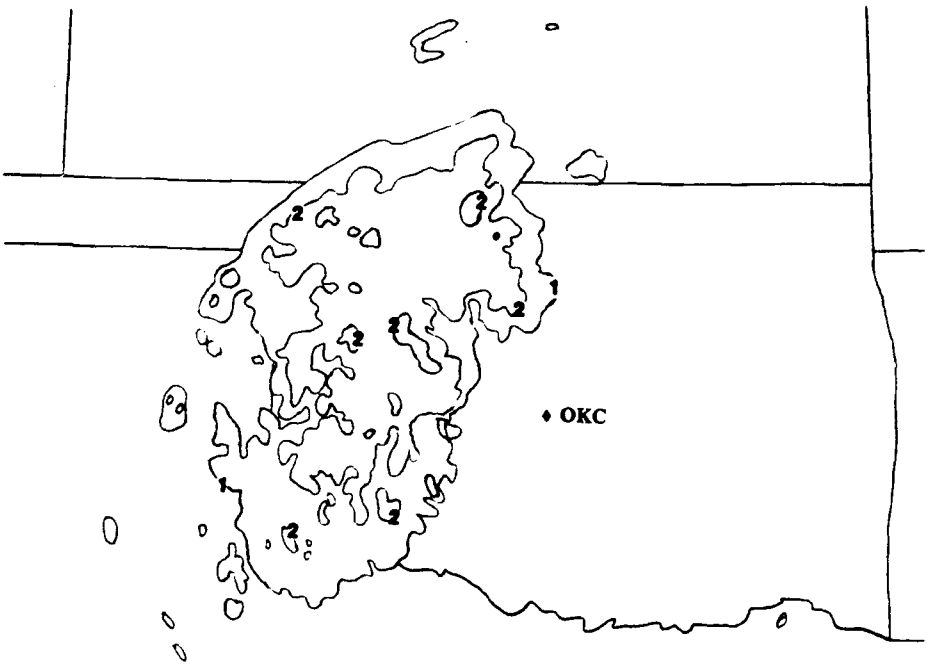

Figure 3.30. Radar reflectivity from Oklahoma City radar at 0.5° elevation for August 14 2000 CST. Contours are marked by video integrator processor (VIP) levels. There are no contours higher than VIP2 (VIP1 ≃ 18 dBZ, VIP2 ≃ 30 dBZ). Compare with the satellite image for the same time in Figure 3.3c.

The stratiform/dissipating and convective modes of positive flashes can occur separately, together or not at all. Table 3 shows that the stratiform/dissipating mode occurred with the convective mode in three of the 17 cases. Stolzenburg (1990) also reported that the ratio of positive flashes to total flashes was highest at the beginning and end of storms, possibly indicative of the convective and stratiform/dissipating modes occurring together. When both modes occurred, the convective mode dominated the production of positive flashes, and the maximum number of flashes and largest fraction of flashes that were positive occurred early in the system's lifetime. Two (8%) of the MCSs had low ratios of positive to total flashes throughout their lifetimes and did not show characteristics of either of the two

TABLE 4 Positive Lightning Characteristics for the Stratiform/Dissipating Mode

Date (1986)	Max fraction in st/d mode	Duration* (hrs)	Avg # of positives/0.5 h in st/d mode	Avg # of positives/0.5 h for lifetime
26-27 Apr (1)	.40	.5	12	23
26-27 Apr (2)	.22	.5	5	8
26-27 Apr (3)	.88	.5	7	19
8-9 May (2)	1.00	3.0	7	10
5-6 Jul	.30	.5	70	20
6-7 Jul	.56	2.5	9	27
12-13 Jul	.20	.5	3	9
8-9 Aug	.50	3.0	22	14
14 Aug	.76	2.5	32	28
14-15 Aug	1.00	1.5	2	9
20-21 Aug	1.00	1.5	4	23
26 Aug	1.00	2.0	8	12
28-29 Sep (1	1.00	1.5	7	33
28-29 Sep (2)	1.00	4.0	11	31

* The duration is defined as the number of hours that the fraction of flashes that were positive was at least 0.2.

modes of positive flashes.

Because positive flash rates were much higher in the convective mode and so dominated time series plots of positive flashes, the three cases in which both modes occurred were omitted from our analysis of the stratiform/dissipating mode. In the 14 remaining MCSs with the stratiform/dissipating mode, positive flash counts tended to peak near or after negative flash counts. The maximum number of positive flashes per half hour peaked between 1.0 h before and 4.0 h after the maximum number of negative flashes (Figure 3.29b), averaging 1.2 h after the peak

in negative flashes. The average period during which at least 0.20 of the flashes were positive was 1.7 h, 2.3 h less than the average duration of the convective mode. The maximum ratio of positive to total flashes for each of the 14 MCSs ranged from 0.2 to 1.0. Positive flashes peaked an average of 7.5 h after first strike and the average number of positive flashes occurring during the stratiform/dissipating mode was small in most cases (see Figure 3.31a; positive flashes have been multiplied by a factor of five in this figure). In all but three cases, the average during the period of the stratiform/dissipating mode was smaller than the average number of positive flashes occurring throughout the lifetime of the MCS.

The evolution of the number of positive flashes agrees well with the evolution of the area within warmer cloud-top temperatures (around -52°C) for the stratiform/dissipating mode. Comparisons with the minimum cloud-top temperature showed that the maximum in the ratio of positive flashes to total flashes occurred as the MCS was decaying and the cloud-tops were warming (Figure 3.31b).

Positive flashes have been observed in mature and decaying thunderstorms by Fuquay (1982), Orville et al. (1983) and Rust (1986). Rutledge and MacGorman (1988) observed positive flashes in the trailing stratiform region of a squall line. In Orville et al. (1983), the fraction of flashes that were positive was highest at the end of a storm when a small number of flashes occurred.

Recall that most published observations of positive flashes in MCSs discuss what we have named the stratiform/dissipating mode of positive flashes. Our results indicate that the convective mode of positive flashes may not be uncommon (nine

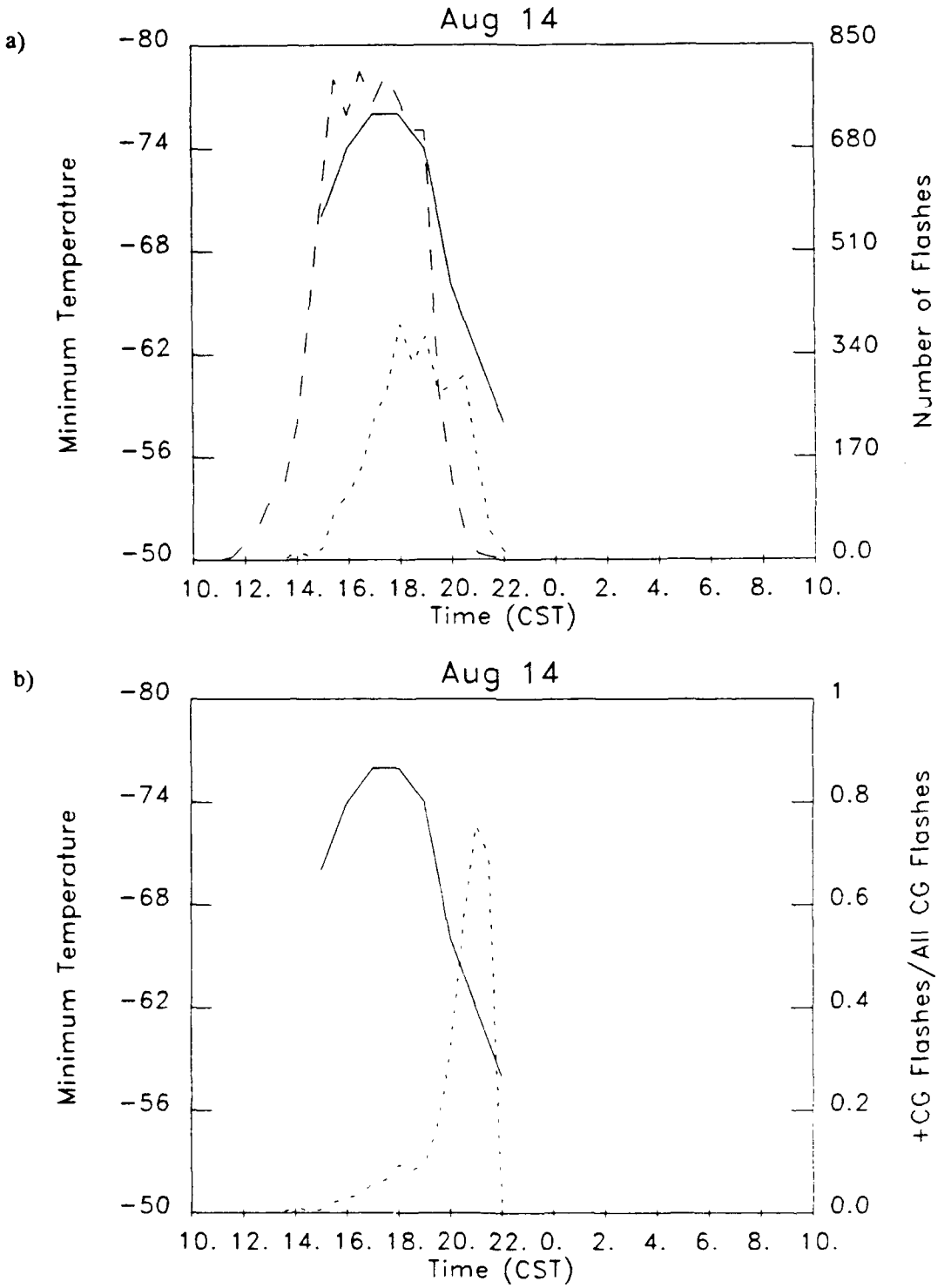

Figure 3.31. Time series of the minimum satellite cloud shield temperature at 2°C increments (solid line) with a) the number of negative flashes (long dashed line) and the number of positive flashes multiplied by a factor of five (short dashed line) and b) the fraction of positive flashes (short dashed line).

of 25 cases). Table 5 summarizes characteristics of these two modes.

Once we identified the convective mode, we compared the synoptic environments when this mode occurred to the synoptic environments when this mode did not occur. We quickly examined soundings and surface, 850, 700, 500 and 300 mb charts to look for features that could explain why the convective mode of positive flashes occurred in some cases. Unfortunately, this cursory examination did not reveal any obviously unique features. Part of the reason an explanation was not uncovered is that the positive flashes in the convective mode occurred on scales much smaller than the synoptic scale. This difficulty was compounded because clusters of positive flashes indicative of the convective mode sometimes occurred near clusters of negative flashes (Figure 3.27a), so determination of the synoptic

TABLE 5 Characteristics of the two modes of positive flashes

Convective	Stratiform/Dissipating
Occurs in the early, formation stage	Occurs in the mature & dissipating stages
Occurs within strong convective cells	Occurs within the stratiform region or within dissipating convective cells
High density of flashes	Low density of flashes
Positive flashes peak before negative	Positive flashes peak near or after negative
Large number of positive flashes when the ratio of positive to total flashes is large	Small number of positive flashes when the ratio of positive to total flashes is large
Occurs most often in spring and early summer	Occurs all warm season

conditions favorable to the production of positive flashes in the convective mode was difficult. Furthermore, the duration of the convective mode was only a few hours, so it was difficult to sample the environment of the storm when the mode was occurring. (The period when at least 0.2 of the flashes were positive averaged 4 h and was no longer than 8 h.)

Rust et al. (1985) examined the synoptic conditions that existed when several storms produced large numbers of positive flashes in a convective mode on May 13, 1983. They found that the magnitude of the vertical wind shear was above the value hypothesized by Brook et al. (1982) to be necessary for the production of positive flashes. Reap and MacGorman (1989) and Curran and Rust (1991) have suggested that a relatively large vertical wind shear may be a necessary but not a sufficient condition for the occurrence of positive flashes. A study by Stolzenburg (personal communication, 1991) hypothesized a link between high positive flash rates and the early, rapid vertical growth stage of storms.

3.5 First Return Stroke Amplitudes

In Section 3.1, we discussed how the median amplitude of the first stroke of positive flashes, which is proportional to the median peak current, varied with time for individual MCSs. There were also variations in the overall distribution of amplitudes from one MCS to another. Distributions of the amplitudes of positive and negative flashes have been plotted for a large number of flashes, but this is the first time distributions for separate MCSs have been plotted. We found that these

amplitude distributions could be grouped into three categories:

(1) In the low amplitude category, most flashes had low amplitudes; there was a sharp decrease in the number of flashes at moderate to large amplitudes. A composite of the six MCSs in the first category is shown in Figure 3.32a.

(2) The amplitudes in the middle category still peaked at low values, as for the low amplitude category, but the number of flashes decreased much less rapidly with increasing amplitude. A composite of the nine MCSs in the middle category is shown in Figure 3.32b.

(3) The amplitudes in the high category peaked at much higher values and had relatively few flashes at the lowest amplitudes. A composite of the ten MCSs in the high amplitude category is shown in Figure 3.32c.

Although we assigned all 25 MCSs to a category, some characteristics of the amplitude distributions of five of the MCSs were not described very well by the typical distributions in any one category. For example, the distribution might fall off too rapidly to match most of the distributions in the middle category, but too slowly to match distributions in the low amplitude category.

After examining each of the MCSs, we noticed that all of the MCSs in the low amplitude category were near direction finder stations for a large portion of their lifetimes, so we were concerned that the observations might be an artifact of the instrumentation. Low amplitude flashes will be detected more easily if they occur near direction finders, so we considered the possibility that MCSs may have low amplitude positive flashes that are only being detected if the MCSs are close to the

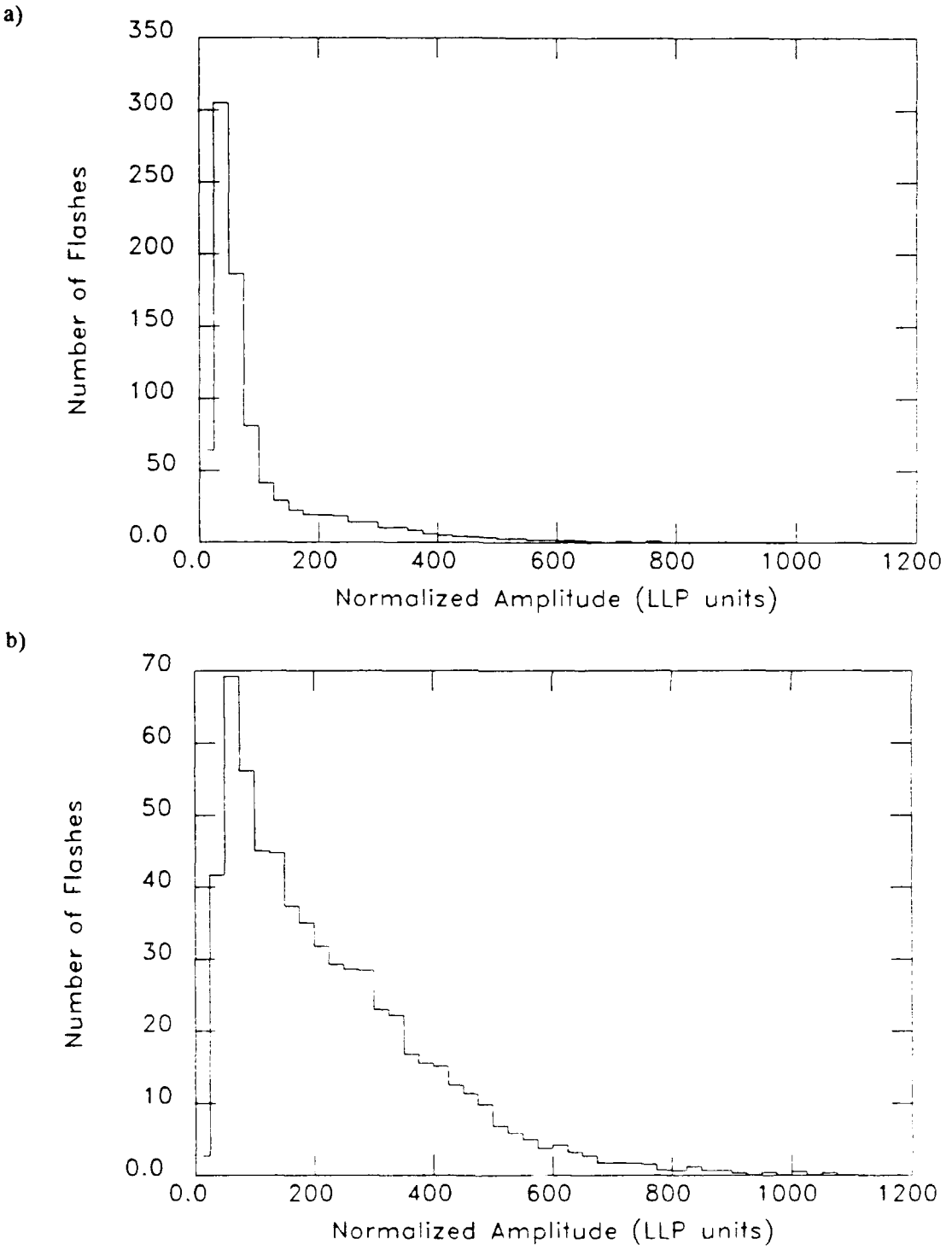

Figure 3.32. The distribution of normalized amplitudes for the positive flashes in a) the six MCSs in the low amplitude category, b) the nine MCSs in the middle amplitude category and c) the ten MCSs in the high amplitude category.

c)

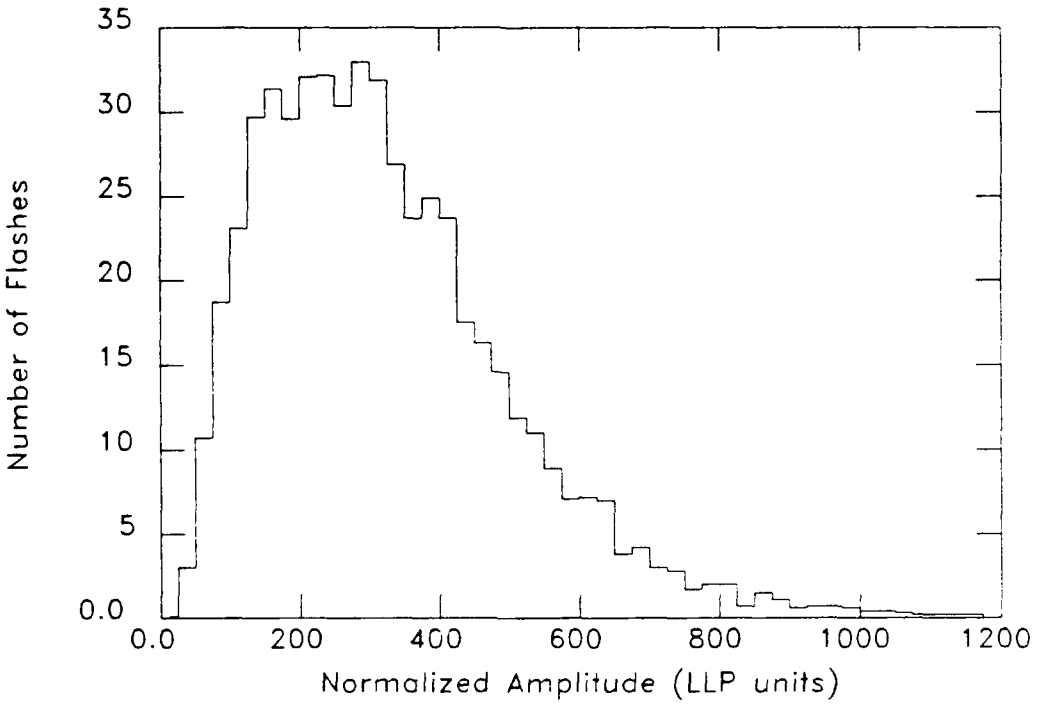

Figure 3.32. Continued.

direction finders. However, other MCSs were near the direction finders, but did not have a large number of low amplitude flashes, so it appears that not all MCSs have a large number of low amplitude flashes.

Another possible effect of instrumentation is that intracloud flashes were mistakenly identified as positive cloud-to-ground flashes by the lightning strike mapping system. However, according to the results of MacGorman and Taylor (1989), who looked at false detection of low amplitude positive flashes, false detection is negligible when the range-normalized amplitude is at least 50 LLP units. When range-normalized amplitudes are less than 50 LLP units, no more than approximately 15% are likely to be false detections. Even if we remove 15% of the

flashes with amplitudes less than 50 LLP units, our amplitude distributions remain basically unchanged. Therefore, it seems likely that the low amplitude category is valid and that different MCSs can have different categories of amplitude distributions.

Table 6 summarizes the modal and quartile values of the positive and negative amplitudes in LLP units for the three categories. There was little change from one category to another in the medians and quartiles of the amplitude distributions for negative flashes. The modal amplitude of positive flashes changed little from the low to the middle category but had a significant increase from the middle to the high category. The largest difference in the three categories were the

TABLE 6 Characteristics of Distributions in the Positive Amplitude Categories

Positive Amplitude Category	Mode	25% Quartile	Median Amplitude	75% Quartile
Positive flashes:				
Low	25-50	37	57	115
Middle	50-75	93	183	317
High	275-300	189	295	420
Negative flashes:				
Low	100-125	94	131	182
Middle	100-125	107	138	185
High	125-150	116	155	213

values of the 25% and 75% quartiles and the median amplitudes. The median increased by more than 100 LLP units from the low to the middle category and by more than another 100 LLP units from the middle to the high category.

The number of low amplitude positive flashes that occurred at the peak of the composite of the low amplitude category was much larger than the number of flashes that occurred at the peak in the composites of the other two amplitude categories, but the composite was also affected by the extremely high number of flashes with low amplitudes that occurred in the May 8-9 (3) MCS. When this MCS is excluded from the composite, the number of flashes in the peak for the low amplitude category is considerably smaller, though still higher than the other two categories (Figure 3.33).

The time series of median amplitudes for positive flashes of MCSs in the low amplitude category sometimes had the smallest median amplitudes when the largest number of positive flashes were occurring (Figures 3.10 and 3.34). A scatterplot of the median amplitude versus the number of flashes for each half hour of four MCSs most representative of the low amplitude category is shown in Figure 3.35a. In all but one of the cases in which the number of flashes in 30 minutes exceeded 70, the median amplitude was small. This result is similar to the prediction of Williams (1985) that the charge transfer per flash will be smaller for storms with large flash rates. However, a more accurate description of our result is that the median amplitude could be anywhere in the range of possible values when the number of flashes in a 30 minute period was small, but the median amplitude tended to be

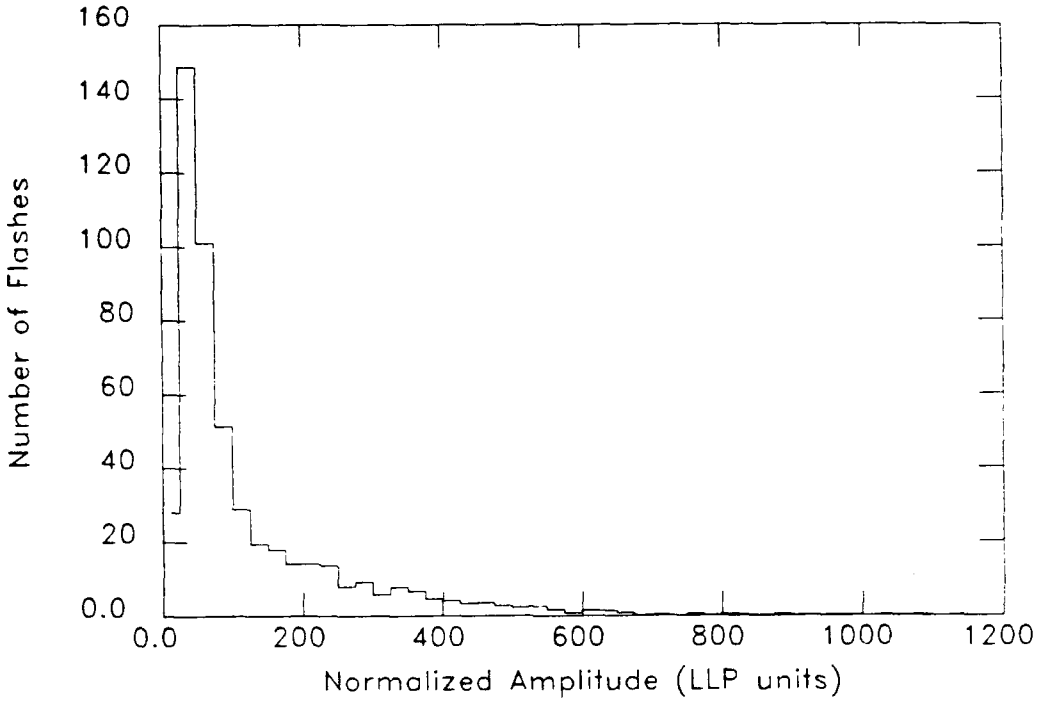

Figure 3.33. The distribution of normalized amplitudes for the positive flashes in five of the MCSs of the low amplitude category. The MCS on May 8-9 (3) was excluded.

small when flash rates were high.

Similar scatterplots for four MCSs most representative of each of the other two amplitude categories are shown in Figures 3.35b and 3.35c. In these two categories, however, the median amplitude was relatively high when the largest number of flashes occurred in a 30 minute period. This is different from the low amplitude category and contradicts the prediction of Williams (1985), stated above.

The same type of scatterplot for positive flashes of all the MCSs in this study is shown in Figure 3.36a. There are two peaks in the number of flashes, one with low median amplitudes and one with high median amplitudes, as might be expected from the above discussion. Figure 3.36b shows the corresponding scatterplot for

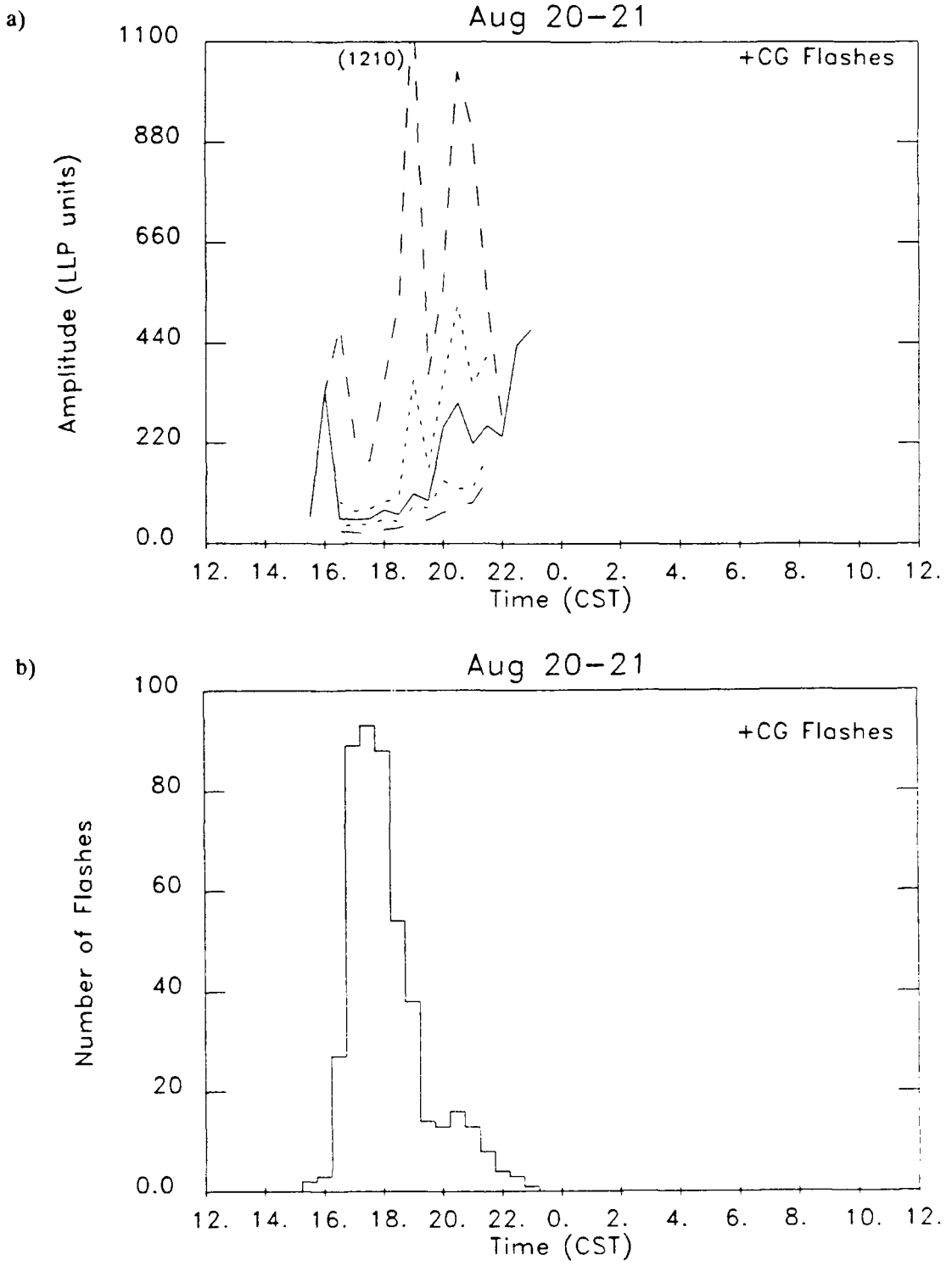

Figure 3.34. Time series of a) positive amplitudes as in Figure 3.9 and b) the number of positive flashes.

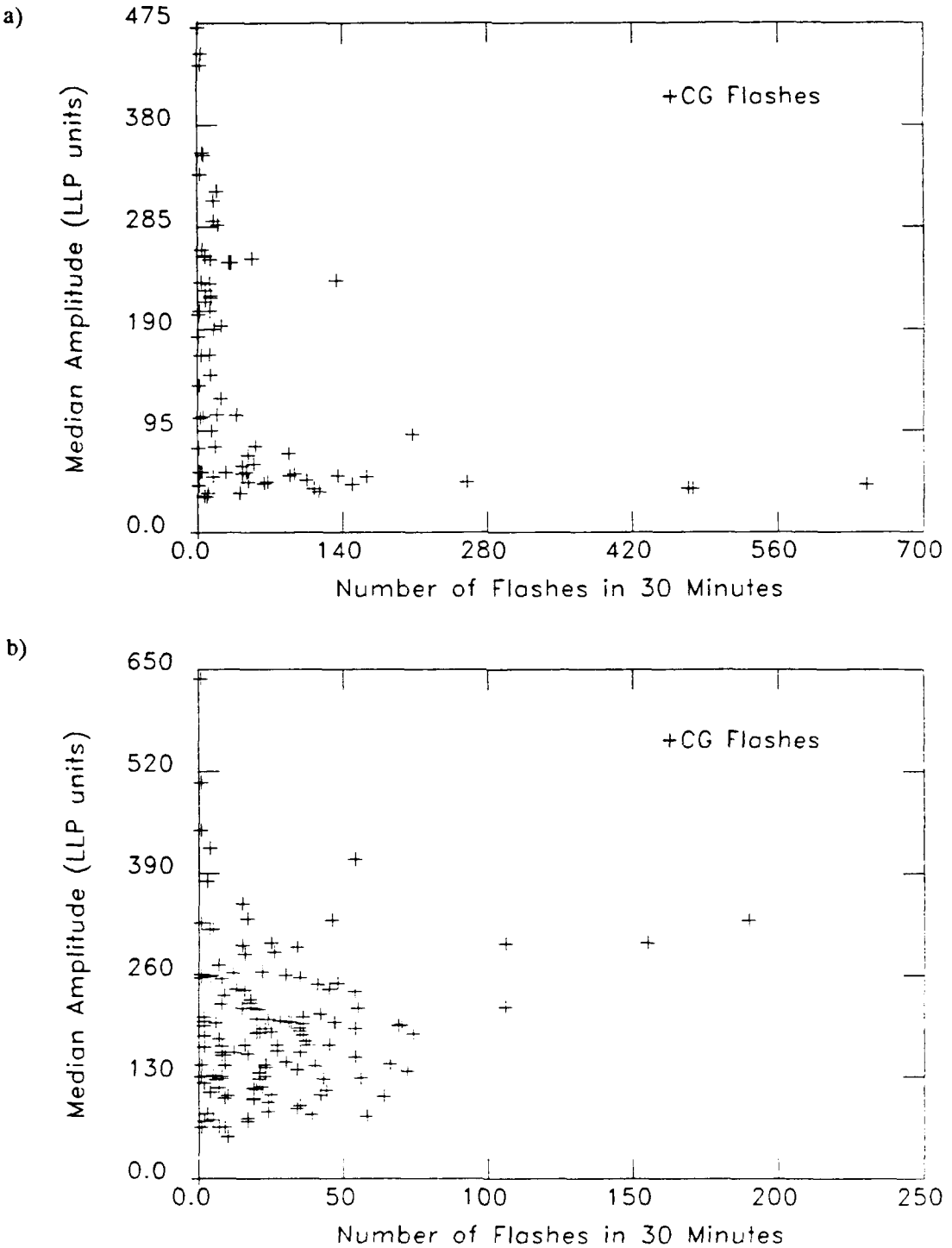

Figure 3.35. Scatterplot of the median amplitude versus the number of positive flashes occurring in a half hour period for the four most representative MCSs in a) the low positive amplitude category, b) the middle positive amplitude category and c) the high positive amplitude category.

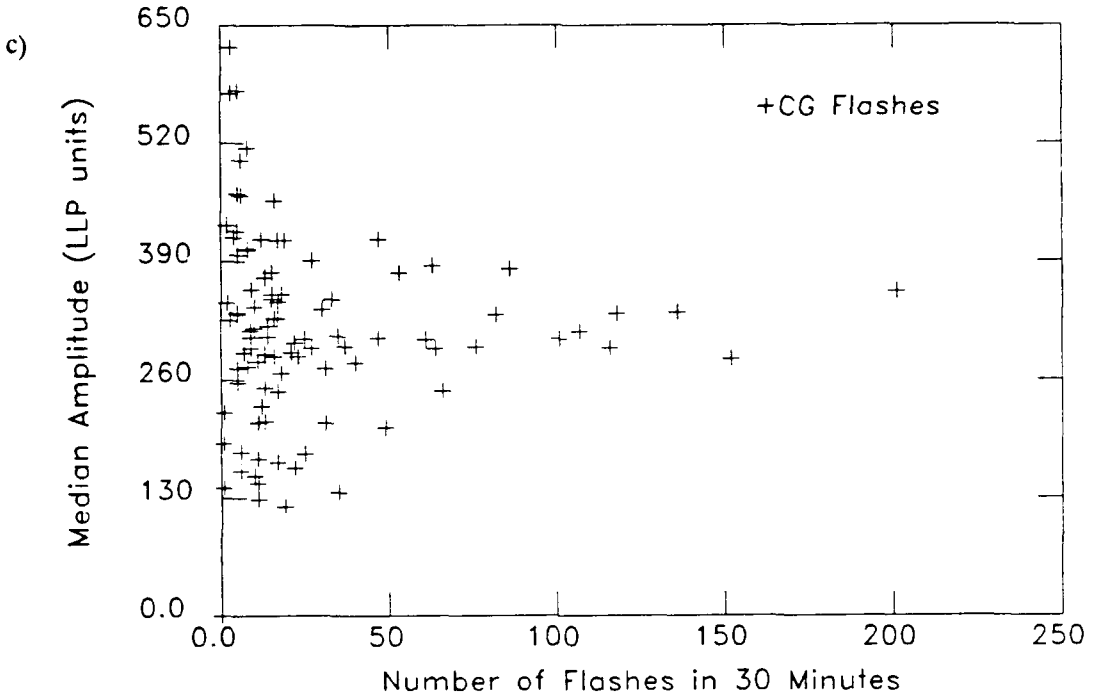

Figure 3.35. Continued.

negative flashes for all of the MCSs of this study. The distribution of median amplitudes for negative flashes is much narrower than the distribution for positive flashes, particularly at lower flash rates. The median amplitude remains close to 150 LLP units, no matter how many flashes occur in a 30 minute period. Again, this seems to be contradictory to the prediction by Williams (1985).

MCSs that had positive flashes in the convective mode were most likely to be in the high amplitude category (five of nine) and least likely to be in the low amplitude category (one of nine). MCSs having positive flashes in the stratiform/dissipating mode were almost equally distributed among the three categories of amplitudes. Table 7 summarizes the convective mode and

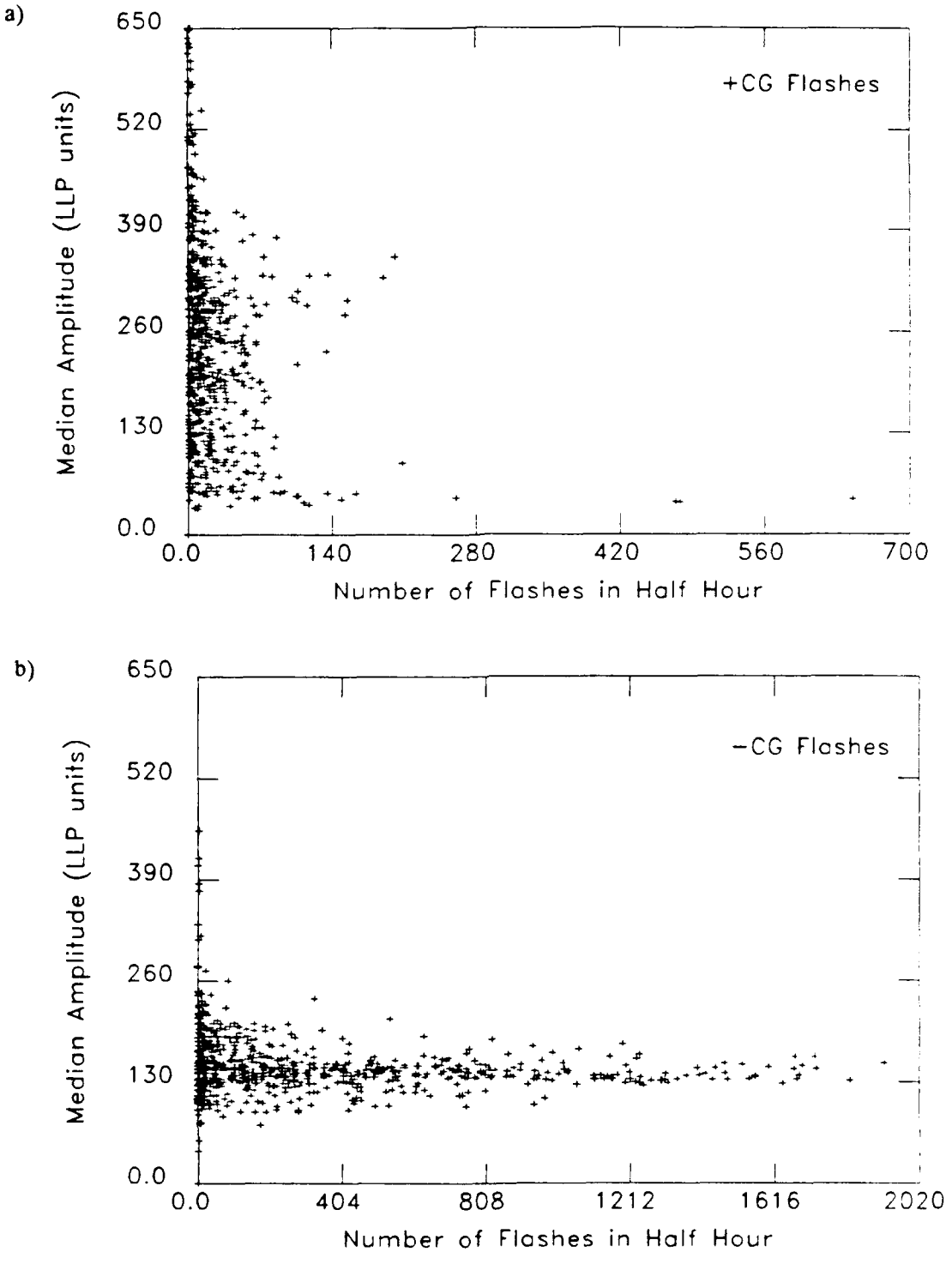

Figure 3.36. Scatterplot of the median amplitude versus a) the number of positive flashes occurring in a half hour period and b) the number of negative flashes occurring in a half hour period for all of the MCSs of this study.

TABLE 7 Positive Amplitude Categories

Low	Middle	High
Total MCSs (6)	Total MCSs (9)	Total MCSs (10)
Apr, May and Sep	Mid-Jun through Aug	All warm season
Conv (1)	Conv (3)	Conv (5)
Strat/Diss (5)	Strat/Diss (5)	Strat/Diss (4)
Unclass (0)	Unclass (1)	Unclass(1)

stratiform/dissipating mode cases within each of the amplitude categories. Severe weather was reported with almost every MCS in this study, and there was no obviousrelationship between types of severe weather and the three categories of positive amplitudes.

The probability that the amplitude distribution of positive flashes would be in each of the three categories appeared to vary seasonally. The low amplitude category tended to occur in the cooler months of the warm season, April, May and September; the middle amplitude category tended to occur in the hot months of the warm season, mid-June through August; and the high amplitude category occurred during all months of the warm season. Because of the seasonal variation, we expected there to be a difference in the temperature profile of the atmosphere for each of the categories. Table 8 shows the average and range of the altitude of various temperature levels for the four most representative MCSs within each of the three categories. As expected, the low amplitude category had cooler atmospheric temperatures than the middle amplitude category (i.e., the same temperature levels

TABLE 8 Altitudes of Various Temperature Levels for Amplitude Categories

Positive Amplitude Category	Avg level of 0°C (mb)	Range of 0°C level (mb)	Avg level of -15°C (mb)	Range of -15°C level (mb)	Avg level of -30°C (mb)	Range of -30°C level (mb)
Low	617	570.5-654	447	425-463.5	341	316.5-361
Middle	561	549.5-576	411.5	405-426	310.5	300.5-320
High	604.5	580-617.5	466.5	443-482.5	355.5	343-368

occurred at lower altitudes). Even though the high amplitude category occurred throughout the warm season, it also had relatively cool atmospheric temperatures.

Sounding analyses of the four archetypical MCSs within each of the categoriesrevealed that there were smaller amounts of precipitable water for the high and low amplitude categories than for the middle amplitude category, almost certainly related to the seasonal differences between the categories. The soundings appeared to have greater instability in the high amplitude category. Average lapse rates between 700 mb and 500 mb for the low, middle and high categories were -6.29, -6.74 and -7.97 deg/km, respectively.

Although all the tendencies discussed above are suggestive, our analysis didnot reveal a definite explanation for different amplitude distributions of positive flashes. To determine the differences among the three categories with enough certainty to develop an explanation, analysis of additional cases in more detail is required.

CHAPTER IV

SUMMARY AND RECOMMENDATIONS

4.1 Summary of Results

Many of the cloud-to-ground lightning characteristics in the 25 mesoscale convective systems of this study have been reported previously. For example, the first cloud-to-ground flashes were usually negative flashes and were more likely to have a single return stroke than later flashes. The percentage of flashes that were positive varied considerably, but was generally below 16%, with an average of only 6.6%. Positive flashes were much more likely to have a single return stroke than negative flashes (83.3% of positive flashes were single return stroke versus 32.7% for negative flashes). Total flash rates increased rapidly to a peak and also decreased rapidly from the peak unless the MCS consisted of separable components with different lifecycles.

Although we tried to categorize the MCSs by the relationship of lightning to other MCS characteristics, we were unable to, because the relationships varied considerably. However, the combination of lightning ground strike locations superimposed on satellite imagery was a better indicator of regions of thunderstorm activity than satellite imagery alone, especially when the cloud shield of an MCS

obscured the convection beneath it. Lightning strike data can be useful for monitoring the location and movement of deep convection corresponding to electrically active regions when radar data are unavailable. Negative flashes usually clustered near the coldest cloud-tops on satellite imagery in the early and mature stages of the MCS.

An interesting observation was the occurrence of two modes in which positive cloud-to-ground flashes occur. We named these two modes the *convective* mode and the *stratiform/dissipating* mode. In the convective mode, positive strike locations were relatively dense and occurred within growing regions of deep convection early in the lifetime of the MCS. In this mode, a high fraction of flashes were positive early in the MCS and was associated with a relatively high number of positive flashes. The maximum number of positive flashes per 30 minute interval in this mode always occurred either before or at the same time as the maximum number of negative flashes. The convective mode was most common during the months of April, May and June and occurred in nine of the 25 MCSs that we studied.

In contrast, during the stratiform/dissipating mode, positive flashes had low densities and occurred within either the stratiform region during the MCS's mature stage or within dissipating convective cells late in the lifetime of the MCS. The highest fraction of positive flashes occurred late in the lifetime of the MCS, but the number of flashes was generally small when the fraction was large. In this mode, the maximum number of positive flashes per 30 minute interval occurred at about the same time or after the maximum number of negative flashes. This mode occurred

throughout the warm season, in 14 MCSs without the convective mode and in three MCSs in which the convective mode also occurred.

The relationship between positive flash counts and the area within temperature contours on satellite imagery depended on the mode of positive flashes that occurred. In the convective mode, the evolution of positive flash counts was most similar to the evolution of the area within the coldest cloud-top temperatures, while in the stratiform/dissipating mode, the evolution of positive flash counts was most similar to the evolution of the area within warmer cloud-top temperatures (around -52°C). Negative flash counts appeared most similar to the area within temperature contours of -60°C and -70°C on satellite imagery. The temperature giving best agreement for a particular storm depended in part on the temperature of the tropopause, with colder temperatures giving the best agreement when the tropopause was colder.

The distribution of signal amplitudes for all positive ground flashes in an MCS tended to occur in one of three separate categories. In the low amplitude category, there were a large number of flashes with low amplitudes and a sharp decrease in the number of flashes with higher amplitudes. This category occurred least often in 1986 (six of 25 MCSs) and tended to occur during the cooler months of the warm season, April, May and September. The middle amplitude category also had a large number of flashes with low amplitudes but had a gradual decrease in the number of flashes with higher amplitudes. This category occurred in nine of 25 MCSs and tended to occur during the warmest months of the warm season, mid-June through

August. The high amplitude category had the largest number of flashes with high amplitudes and had very few low amplitude flashes. It occurred in ten of the 25 MCSs and occurred during almost every month of the warm season. Sounding analyses of four of the most representative MCSs in each of the three categories showed that the low and high amplitude categories tended to occur when the atmospheric temperatures were relatively cooler and resulting calculations of precipitable water were lower than in the middle amplitude category. The lapse rate of the high amplitude category appeared to be the most unstable of the three categories.

4.2 Recommendations for Future Work

Only MCSs that occurred during the warm season of 1986 were examined in this study. To determine if the patterns observed in the small sample of MCSs from this one year are common, MCSs that occurred in the warm seasons of additional years need to be examined.

We would like to determine if positive flashes in other years occurred in the two modes we found, the convective mode and the stratiform/dissipating mode. If so, the characteristics of these two modes in other years should be compared to the characteristics we observed for these two modes in 1986. It also would be interesting to determine if the amplitude distributions of positive flashes in MCSs from additional warm seasons fit into the three categories of distributions that occurred in 1986, and if the same seasonal differences exist between the categories.

We found no obvious pattern in the synoptic environment accompanying the convective mode of positive flashes versus the synoptic environment when the convective mode did not occur, but a more detailed examination may be able to find clues as to why high densities of positive flashes occur early in the lifetime of some MCSs. The relationship between intense convective growth and high densities of positive flashes hypothesized by Stolzenburg (1991, personal communication) should be studied in more detail. Comparisons of the values of CAPE for MCSs exhibiting the convective mode versus those that do not may show evidence to support this hypothesis. Soundings closer in time and space to systems exhibiting the convective mode may be needed. Doppler radar data may be helpful for determining updraft strengths and other characteristics of the convective mode and may be useful for comparing differences between MCS elements that were close together, but exhibited different modes of positive flashes.

A detailed examination of the synoptic environment occurring with the three categories of amplitude distributions of positive flashes is also required to test the differences we noted and to determine if there are other differences between these categories. It would be interesting to plot the positive amplitude distributions for each of the components of an MCS to see if they differ significantly from the distribution for the entire MCS.

Closer examination of low amplitude positive flashes may be needed to ensure that there are no biases from the instrumentation, especially since the MCSs in this category all occur near direction finder stations.

Although we were unable to classify the entire lifetime of the MCSs according to similarities in the evolution of their lightning, it may be possible to divide the MCSs into a small number of categories for each stage of evolution, as discussed in section 3.2. If the stages can be classified separately, it would be helpful to see if there were corresponding differences in relationships with the synoptic environment.

We visually examined how lightning flash rates compared to the areas within various temperature contours on satellite imagery. It may be useful to do cross-correlations between lightning flash rates and the areas within various temperature contours on satellite imagery for each MCS to quantify these relationships better. It appears from our analysis that the temperature level whose area correlates best with flash rates depends on the temperature of the tropopause. This seems reasonable since the minimum cloud-top temperature of an MCS depends on the temperature of the tropopause, but this dependence on the temperature of the tropopause needs to be examined more closely.

BIBLIOGRAPHY

Augustine, J. A., 1985: An automated method for the documentation of cloud-top characteristics of mesoscale convective systems. NOAA Tech. Memo. ERL ESG-10, Dept. of Commerce, Boulder, CO, 121 pp.

-----, E. I. Tollerud and B. D. Jamison, 1988: Distributions and other general characteristics of mesoscale convective systems during 1986 as determined from GOES infrared imagery. Preprints, *12th Conf. on Weather Analysis and Forecasting*, Monterey, Amer. Meteor. Soc., 437-442.

----- and K. W. Howard: Mesoscale convective complexes over the United States during 1985. *Mon. Wea. Rev.*, **116**, 685-701.

Bartels, D. L., J. M. Skradski and R. D. Menard, 1984: Mesoscale convective systems: A satellite-data-based climatology. NOAA Tech. Memo. ERL ESG-8, Dept. of Commerce, Boulder, CO, 58 pp.

Beasley, W. H., 1985: Positive cloud-to-ground lightning observations. *J. Geophys. Res.*, **90**, 6131-6138.

Blanchard, D. O., 1990: Mesoscale convective patterns of the southern high plains. *Bull. Amer. Meteor. Soc.*, **71**, 994-1005.

Brook, M., M. Nakano, P. Krehbiel and T. Takeuti, 1982: The electrical structure of the Hokuriku winter thunderstorms. *J. Geophys. Res.*, **87**, 1207-1215.

-----, R. W. Henderson and R. B. Pyle, 1989: Positive lightning strokes to ground. *J. Geophys. Res.*, **94**, 13,295-13,303.

Curran, E. B. and W. D. Rust, 1991: Observations of positive ground flashes produced by low precipitation thunderstorms in Oklahoma on 26 April 1984. *Mon. Wea. Rev.*, submitted.

Davies-Jones, R. P., 1986: Tornado Dynamics. *Thunderstorm Morphology and Dynamics, 2nd ed.*, The University of Oklahoma Press, 197-236.

Deetz, C. H. and O. S. Adams, 1945: *Elements of Map Projection with Applications to Map and Chart Construction. 5th ed. revised*, Washington: United States Government Printing Office, 226 pp.

Engholm, C. D., E. R. Williams and R. M. Dole, 1990: Meteorological and electrical conditions associated with positive cloud-to-ground lightning. *Mon. Wea. Rev.*,

118, 470-487.

Fuquay, D. M., 1982: Positive cloud-to-ground lightning in summer thunderstorms. *J. Geophys. Res.*, **87**, 7131-7140.

Goodman, S. J., and D. R. MacGorman, 1986: Cloud-to-ground lightning in mesoscale convective complexes. *Mon. Wea. Rev.*, **114**, 2320-2328.

-----, D. E. Buechler and P. J. Meyer, 1988: Convective tendency images derived from a combination of lightning and satellite data. *Wea. Forecasting*, **3**, 173-188.

Houze, R. A. Jr., B. F. Smull and P. Dodge, 1990: Mesoscale organization of springtime rainstorms in Oklahoma. *Mon. Wea. Rev.*, **118**, 613-654.

Kane, R. J., C. R. Chelius and J. M. Fritsch, 1987: Precipitation characteristics of mesoscale convective weather systems. *J. Climate Appl. Meteor.*, **26**, 1345-1357.

Krehbiel, P. R., 1986: The electrical structure of thunderstorms. *The Earth's Electrical Environment*, National Academy Press, 90-113.

Krider, E. P., 1986: Physics of lightning. *The Earth's Electrical Environment*, National Academy Press, 30-40.

-----, R. C. Noggle and M. A. Uman, 1976: A gated, wideband magnetic direction finder for lightning return strokes. *J. Appl. Meteor.*, **15**, 301-306.

-----, -----, A. E. Pifer and D. L. Vance, 1980: Lightning direction finding systems for forest fire detection. *Bull. Amer. Meteor. Soc.*, **61**, 980-986.

Lhermitte, R. and P. R. Krehbiel, 1979: Doppler radar and radio observations of thunderstorms. *IEEE Trans. Geosci. Electron.*, **GE-17**, 162-171.

Lopez, R. E. and R. M. Passi, 1991: Simulation experiments in site error estimation for direction finders. *J. Geophys. Res.*, submitted.

MacGorman, D. R. and W. D. Rust, 1988: An evaluation of two lightning ground strike locating systems. Final Rep. to Office of Federal Coordinator for Meteorological Services and Supporting Research, 76 pp.

----- and W. L. Taylor, 1989: Positive cloud-to-ground lightning detection by a direction-finder network. *J. Geophys. Res.*, **94**, 13,313-13,318.

----- and K. E. Nielsen, 1991: Cloud-to-ground lightning in a tornadic storm on 8

May 1986. *Mon. Wea. Rev.*, submitted.

Mach, D. M., D. R. MacGorman, W. D. Rust and R. T. Arnold, 1986: Site errors and detection efficiency in a magnetic direction-finder network for locating lightning strikes to ground. *J. Atmos. Oceanic Technol.*, **3**, 67-74.

Maddox, R. A., 1980: Mesoscale convective complexes. *Bull. Amer. Meteor. Soc.*, **61**, 1374-1387.

McAnelly, R. L. and W. R. Cotton, 1986: Meso-ß-scale characteristics of an episode of meso-α-scale convective complexes. *Mon. Wea. Rev.*, **114**, 1740-1770.

----- and -----, 1989: The precipitation life cycle of mesoscale convective complexes over the central United States. *Mon. Wea. Rev.*, **117**, 784-808.

Orville, R. E., R. W. Henderson and L. F. Bosart, 1983: An east coast lightning detection network. *Bull. Amer. Meteor. Soc.*, **64**, 1029-1037.

-----, R. A. Weisman, R. B. Pyle, R. W. Henderson and R. E. Orville, Jr., 1987: Cloud-to-ground lightning flash characteristics from June 1984 through May 1985. *J. Geophys. Res.*, **92**, 5640-5644.

-----, R. W. Henderson and L. F. Bosart, 1988: Bipole patterns revealed by lightning locations in mesoscale storm systems. *Geophys. Res. Lett.*, **15**, 129-132.

Reap, R. M. and D. R. MacGorman, 1989: Cloud-to-ground lightning: Climatological characterisitics and relationships to model fields, radar observations and severe local storms. *Mon. Wea. Rev.*, **117**, 518-535.

Rust, W. D., 1986: Positive cloud-to-ground lightning. *The Earth's Electrical Environment*, National Academy Press, 41-45.

-----, D. R. MacGorman and R. T. Arnold, 1981a: Positive cloud-to-ground lightning flashes in severe storms. *Geophys. Res. Lett.*, **8**, 791-794.

-----, W. L. Taylor, D. R. MacGorman and R. T. Arnold, 1981b: Research on electrical properties of severe thunderstorms in the Great Plains. *Bull. Amer. Meteor. Soc.*, **62**, 1286-1293.

-----, D. R. MacGorman and S. J. Goodman, 1985: Unusual positive cloud-to-ground lightning in Oklahoma storms on 13 May 1983. Preprints, *14th Conf. on Severe Local Storms*, Indianapolis, Amer. Meteor. Soc., 372-375.

Rutledge, S. A. and D. R. MacGorman, 1988: Cloud-to-ground lightning activity in the 10-11 June 1985 mesoscale convective system observed during the Oklahoma-Kansas PRE-STORM Project. *Mon. Wea. Rev.*, **116**, 1393-1408.

-----, C. Lu and D. R. MacGorman, 1990: Positive cloud-to-ground lightning in mesoscale convective systems. *J. Atmos. Sci.*, **47**, 2085-2100.

Stolzenburg, M., 1990: Characteristics of the bipolar patterns of lightning locations observed in 1988. *Bull. Amer. Meteor. Soc.*, **71**, 1331-1338.

Watson, A. I., J. G. Meitin and J. B. Cunning, 1988: Evolution of the kinematic structure and precipitation characteristics of a mesoscale convective system on 20 May 1979. *Mon. Wea. Rev.*, **116**, 1555-1567.

Williams, E. R., 1985: Large-scale charge separation in thunderclouds. *J. Geophys. Res.*, **90**, 6013-6025.

-----, 1989: The tripole structure of thunderstorms. *J. Geophys. Res.*, **94**, 13,151-13,167.